THE ASTRONOMICAL JOURNAL

PUBLISHED BY THE AMERICAN INSTITUTE OF PHYSICS
FOR THE AMERICAN ASTRONOMICAL SOCIETY

VOLUME 66 1961 October ~ No. 1293 *NUMBER 8*

SYMPOSIUM ON COMETS

Sponsored By
The American Astronomical Society
and
The Maria Mitchell Observatory
with the support of
The National Science Foundation
June 20, 1961
Nantucket, Massachusetts

For the 108th Meeting of the American Astronomical Society, at the Maria Mitchell Observatory, the subject of comets was selected as the symposium topic. Reasons for this choice included the historic discovery of a comet which first brought Maria Mitchell to the attention of the scientific world, the current energetic research on comets which has not recently been given prominent presentation, and the growing prospect of direct space probes for which the instrumentation must be guided by present knowledge.

Arrangements for the Symposium were largely made by Dr. Dorrit Hoffleit, Nantucket hostess, with the active cooperation of Dr. Herzberg, who also acted as moderator. To the originally scheduled set of five subjects, the Council at Nantucket added a brief presentation by Dr. Rosen of some very recent work.

Topics and participants were:

Presiding, **Gerhard Herzberg,** National Research Council, Ottawa, Canada
"Structure and Development of the Gas Tails of Comets," **K. Wurm,** Hamburg-Bergedorf Observatory
"Astrometric Observations and Orbits of Comets," **Elizabeth Roemer,** U. S. Naval Observatory, Flagstaff Station
"Photoelectric Photometry of Comets," **William Liller,** Harvard College Observatory
"Problems of the Cometary Nucleus," **Fred L. Whipple,** Smithsonian Astrophysical Observatory and Harvard College Observatory
"The Survival of Comets and Cometary Material," **Ernst J. Öpik,** University of Maryland
"New Investigations on the C_3 Spectrum at 4050 A," **B. Rosen,** Astrophysical Institute of the University of Liége and National Research Council, Ottawa, Canada

Discussion following the papers was not entirely audible on the tape records; B. Marsden kindly helped to recover and edit these remarks.

Support by the National Science Foundation, of publication as well as of the Symposium itself, is gratefully acknowledged.

Structure and Development of the Gas Tails of Comets

K. Wurm
Hamburg-Bergedorf Observatory

I. INTRODUCTION

It is well known that in treating atmospheric constituents of comets we have to distinguish between two different types of tails: those consisting of ionized gases and those consisting of dust. When we are able to look nearly perpendicular to the orbit, we see that the two types of tails, when existing, are well separated by a different curvature. The dust tail is strongly curved, while the gas tail is curved barely at all. A strong curvature indicates that the particles suffer a small repulsive force; straight tails originate from high repulsive forces, high with respect to the value of solar gravitation at the position of the comet. The main constituent of the gas tails is always the singly ionized carbon monoxide molecule.

Twenty to thirty years ago, most of us believed that no serious difficulty remained in understanding the appearance of such tails, although we realized, of course, that all details of their structure had not yet been explained. It had been established that the ions of the tails shine by fluorescence, excited by solar light. With the absorption of solar radiation the particles must suffer repulsion by light pressure. It seemed logical, then, to assume that light pressure was responsible for the acceleration of the tail ions. We know now that this explanation is impossible because of the low f value in the tail band system of the carbon monoxide ion.

Since we may be certain that light pressure plays no role, we must look for another force. In addition, the tails exhibit a number of peculiar phenomena which have yet to find an explanation. We are certainly still far from a theory of the tails, and no attempt will be made in the present paper to offer such a theory. Rather I have tried to prepare a critical representation of the main observational facts and in this way to lay the groundwork for the planning of new observations.

From many recent publications on comets one might get the impression that a satisfactory explanation for the most striking observational facts is easily obtained by postulating high-density solar corpuscle streams and by considering the collisional interaction of these streams with the cometary particles. Although ther seems to exist a rather general inclination to accep this view, I believe this situation has arisen only because the current conceptions concerning the observational facts are too indefinite.

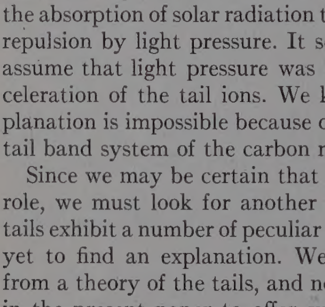

Fig. 1. Schematic distribution of particle emission from a comet.

I have selected for a closer discussion three question connected with observation which appear to me to b of particular importance with regard to a foundatio and test of a physical theory.

(1) The rate of ionization within the heads of th comets.
(2) The orbits of the tail ions with respect to th nucleus and the prolonged radius vector.
(3) The range of the repulsive forces exerted on th ions.

I plan to touch only briefly on the third question since I have nothing to add beyond what I stated in recent paper, published in the last *Liége Symposiu Proceedings* (1961). In my opinion, at the present phas of cometary physics questions 1 and 2 deserve particula attention.

II. IONIZATION WITHIN THE HEADS

Certain explanations must be made concerning th monochromatic shapes of comets since these shape have an important bearing on question 1. Monochro matic refers here to the band emission of the differen molecules observed. Our information about mono chromatic shapes is gleaned by spectrograms, in par ticular those with objective prisms. The situation rather simple (see Fig. 1). One group of molecules fil only the heads of comets; they do not appear withi the tails proper. Most representative of this first grou are the diatomic cyanogen molecule and the diatomi carbon molecule, both of which generally appear wit a high emission intensity. A second group comprise exclusively ions; their zone of emission is indicated i the drawing of Fig. 1 by the shadowed area. There some overlapping of the regions of group I and group I Some uncertainty exists with regard to classifying th two ions near the end of group I: CH^+ and OH^+ Because of their faintness they are observable with the bands only in the vicinity of the nucleus, but very prob ably they should be moved into group II. We know tha all these particles, ion as well as neutral, start the expansion into space from the vicinity of the nucleu But how close to the nucleus the ions first appear is n precisely known. From pictures of the recent Come Burnham 1959 *k*, which I note later in another conne tion, I found that the CO^+ ions were already certainl present at a distance of 5000 to 6000 km from th nucleus.

The expansion of the neutral molecules proceeds from e nucleus region more or less symmetrically in all rections, filling their space continuously. If we identify e head of a comet, as I will do later, with the extension d space of the neutral particles, we may say that the ad is approximately a sphere with the nucleus in the nter. An informative paper on the expansion velocies of the head particles was published more than 30 ars ago by Bobrovnikoff (1931) in his important study Halley's comet. For a time after perihelion this comet owed brief discontinuous outbreaks of matter from the ucleus which resulted in expanding halo formations. y comparing plates from different observatories over e world, Bobrovnikoff was able to study the expansion nd lifetimes of these halos. He found the expansion elocities rather small: They averaged below 1 km er second. The average lifetime was about two days, ter which they lost definite boundaries because of their intness, having reached radii of 130 000 to 150 000 m. The comet's position at this time was about 1 a.u. om the sun.

The radii of the cyanogen and carbon heads of comets re generally given from photographs as 150 000 to 00 000 km. We are well aware that no sharply defined adius exists. What we should investigate are the inensity gradients within the monochromatic images for larger number of comets, and derive from them the w of density distribution for a regular expulsion of atter from the nucleus. This density distribution hould depend on two factors. If ρ designates the disance from the nucleus, the first factor is ρ^{-2} because f the expansion of the gases from the nucleus in all irections; the second factor $e^{-\rho/\rho_0}$ enters since there ust be a decay of the particles. ρ_0 is defined by $\rho_0 = v\tau$, v is the expansion velocity and τ the average lifetime f the molecule.

A careful study of the density distribution should llow us to find the average lifetimes of the molecules, iving the rates for ionization plus dissociation. Studies f monochromatic intensity gradients have not yet een numerous enough to provide accurate values of he average lifetimes τ. Isophotic contours or intensity radients for CN and C_2 have been published by Yoss 1953), Miller and Liller (1956), Miller (1957), and Vorontsov-Velyaminov (1961). From the material which is available at present, one can conclude at least hat up to a distance $\rho = 200\,000$ km the influence of he decay factor is not yet very strong. It lowers the density perhaps by a factor of 2 or 3, but certainly not more.

Hence, we may conclude that the constant $\rho_0 \geq 200\,000$ km. If we adopt an expansion velocity of 1 km/sec, a ittle larger than the average measured by Bobrovnikoff, we find for the lifetime $\tau \geq 10^{5.3}$ sec. This figure is appropriate for the molecules CN and C_2 and for heliocentric distances equal to about 1 a.u. From the intensity gradients along the band lines of the molecules OH and NH it follows that the same lifetime is also valid for these molecules. This figure, $10^{5.3}$, is not far from the one which is given by Nicolet (1961) as the average lifetime of the neutral oxygen molecules in the uppermost levels of the earth's atmosphere, Nicolet's value being 10^6 sec. Thus the behavior of the observed neutral particles in the atmospheres of comets points to a rather low ionization rate for particles with ionization energies of, say, 14 ev.

A striking contradiction will appear when we analyze the behavior of the ions and derive from them, insofar as possible, the lifetimes of their parent molecules which are, of course, identical with the neutral molecules. To be sure, the comparison of the behavior of the ions and that of the neutral molecules is somewhat complicated because we are not in a position to observe the emission of the same molecule in its neutral and ionized state. Although the band emission of the neutral particles mentioned earlier is strong, the particles do not appear with a sufficiently strong emission in their ionized state, and those with a strong emission in their ionized state do not show a sufficiently strong emission in their neutral state. However, no particular difficulty exists in analyzing the behavior of the ions with respect to the ionization of their parent molecules. We do limit our considerations to the CO molecule, since the general situation with regard to it is clearest.

Some years ago I gave (Wurm 1947) a figure for the ionization rate of the parent molecule of the CO^+. The average lifetime of the neutral CO was estimated at $\tau_{CO} = 10^{3.5}$ sec. This estimate was derived from two different observations. First, since we observe CO^+ emission already close to the nucleus, ionization must take place before the neutral molecules are able to travel far from the nucleus. According to this, the lifetime can be at most a few hours. The second and even more conclusive observation concerns the fluctuations in the stream of CO^+ ions moving from the region near the nucleus into the tail. Suppose we have a cloud of CO, in which by any process ionization is occuring with a probability $\lambda = 1/\tau_{CO}$; suppose further we are observing the created ions streaming away from the cloud. A stationary state can be reached if first there exists a source which keeps the total mass of the CO cloud constant, and second if this constancy has persisted for a time $t \gg \tau_{CO}$. Fluctuations in the streams may appear either by fluctuations in the available mass of the CO or by fluctuations in λ. It can easily be shown from the differential equations of the process that, if we observe a fluctuation in the ion stream within a time interval Δt, then $\tau_{CO} < \Delta t$. It has long been known that fluctuations in the CO^+ stream of the tails become perceptible in less than an hour. This means that the average lifetime of the parent molecule of the CO^+ must be smaller than $10^{3.5}$ sec.

When we compare this figure with that which we derived for the typical head particles, there seems to exist an obvious contradiction. The head molecules CN, C_2, OH, NH have approximately the same ionization energy

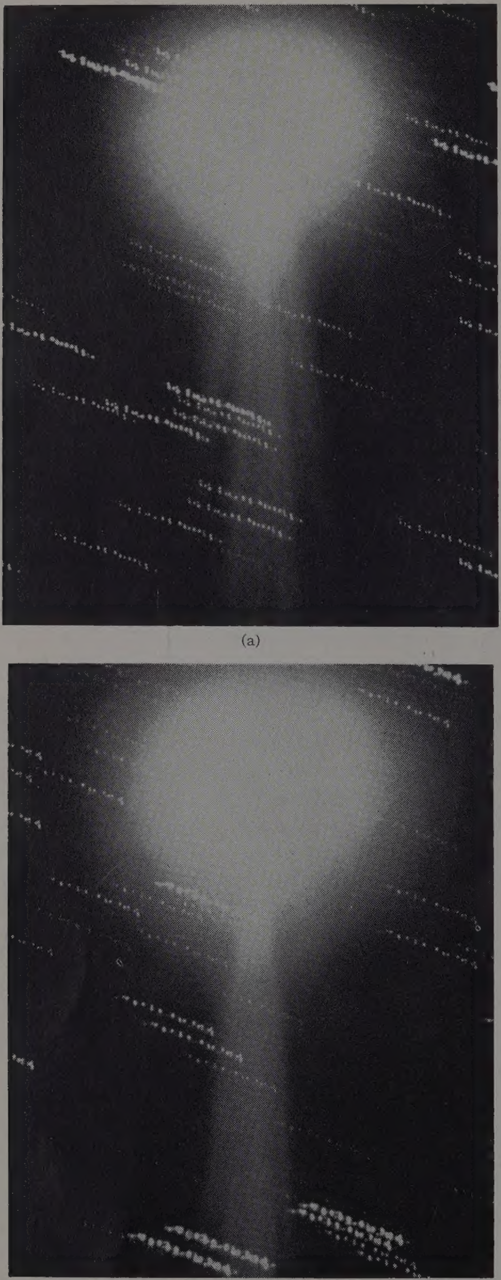

(a)

(b)

Fig. 2. (a) Comet Burnham 1959, photographed April 25–26 with 48-inch Asiago reflector. Exposure 15 minutes. (b) Same comet, 70 minutes later.

as *CO*, but we find a difference for the ionization rates which amounts to two powers of 10. Since it had long been the prevalent belief that the high rate factor found from the carbon monoxide ion was the true one, not much weight was given to the existence of neutral particles; they were regarded simply as a residue which had not yet suffered ionization. According to what have explained, this conception is certainly not tenable For a time I thought that a misinterpretation of observation was possibly connected with the low rate factor however, I no longer hold this opinion. The situatio now appears to me perfectly clear with the neutra particles, far more so than with the ions, for which reason I believe we shall have to look to them for the removal of the discrepancy. Since either derivation seem reliable enough (excluding a drastic change of th figures), I suspect we must face the conclusion that th discrepancy arises from two different processes of ioni zation, one for the comet at large originating from a external radiation (light and corpuscles), which thu far has been the only one considered, second an interna process of ionization, limited to the vicinity of th nucleus, with a high rate but with an incomplet efficiency. I can only, considering the whole situation make such a suggestion; I am not in a position to develop a picture of this internal source of ionization

III. ORBITS OF THE TAIL IONS

Coming now to the tails proper, I should summariz briefly the most striking differences in the behavio of the ions and the neutral particles. In the first plac are the much higher repulsive forces exerted on th ions. The real range of the repulsive forces is only ap proximately known; certainly values 50 to 100 time the gravitational attraction of the sun are reached Much higher values mentioned often in the literature such as a thousand to ten thousand times the solar a traction, remain very questionable. At least statisti cally they cannot be important (Wurm 1961). Secondly regarding the peculiar behavior of the ions, I woul mention their strong tendency to form rays an streamers. Normally they do not fill their space con tinuously; they arrange themselves in rays with diam eters, as far as can be measured, equal to or below 200 km. When beginning to form, the rays have an angl exceeding 45 deg to the tail axis and are convex agains the sun. While growing in length [see Fig. 3(c)] th angle decreases; the ray lies finally along the tail ax and dies out. An essential difference between the ion and the neutral particles concerns the initial velocitie which in the case of the ions are much higher than i the case of the neutral molecules. But we must make restriction here with regard to the phase in the formatio of the rays. The initial velocities are high at the be ginning of the formation but small at the end of it.

Figure 2 shows particularly clearly the turning of ta rays to the tail axis. The photographs are of the recen Comet Burnham 1959 obtained on the night Apr 25–26 by Dr. Maffei and myself with the 48-inch Asiag reflector. The comet was difficult to guide since it ha no clear nucleus. The two outermost rays of the bundl formed, on the first exposure, an angle of 19° 40′; 7 minutes later they had decreased to 11° 30′. Furthe re, on the last picture the two rays mentioned have ome somewhat less diffuse than on the first one. It ms rather evident that the cause is to be found in a rease of the angular velocity of the turning. The ee or four innermost rays are all less diffuse and rper than the outer ones. They are either already rly at rest or are moving in a plane which contains line of sight.

We can conclude directly from certain tail configura- ns that the initial velocities of the ions within the l rays are large at the beginning of the ray formation d small at the end of it. The configurations in question nsist of very long rays which have accumulated along tail axis (or radius vector, which is approximately ntical with the tail axis) having lengths of 10 to 20 llion km, and very short rays with lengths of the order the head radius (100 000 to 200 000 km). A good ample of this kind of tail was found in Comet Hassel 39 at the end of April 1939. For heliocentric distances tween 0.5 and 1.0 a.u., and assuming reasonable pulsive forces $[(1-\mu)=50$ to $100]$ we can easily mpute that the ions at the ends of these long rays t the nucleus 50 to 100 hr earlier than when these otographs were taken. From the widths of such long y complexes it follows that the ions have distances m the tail axis less than the radius of the head (say 0 000 km). Hence, their velocity normal to the radius ctor must have been on the average less than 1 km/sec. the other hand, the ions at the tips of the short rays ve already reached this distance (about 200 000 n) within time intervals of the order of one hour! This ugh picture suggests initial velocities normal to the il axis of 50 to 100 km/sec at the beginning of the ray rmation and of 1 km/sec or less at the end of the rmation. Whether the initial velocity has only a com- nent normal to the tail axis is not yet clear. From is explanation it follows conclusively that the turning the tail rays to the tail axis is kinematically connected ith and dependent on a decrease in time of the velocity mponent normal to the tail axis. Within each ray is component is, on the average, smaller the later an n leaves the region of the nucleus. It remains uncertain hether this velocity can always be identified, over the tal orbit of an ion, with its initial velocity when leav- g the nucleus region.

Stumpff (1959), in treating the kinematics and dy- amics of tail ions, concluded that the turning of the il rays can be understood quite simply by the action repulsive forces alone. His idea becomes clear with e aid of the diagram of Fig. 3(a). The straight line represents a ray at a certain time t_1 and the straight ne B the same ray at a later time t_2. The author con- ders essentially only the problem of transferring A to B by remaining in accord with the time scale of e whole turning of the ray. He neglects as outside is problem the early phases of the rays when their imensions are comparable with the diameter of the ead, and he also ignores the final fate of the rays. For his restricted problem he finds a solution if he postulates a repulsive force which is a function of the distance y from the tail axis. The numerical values are about $(1-\mu)=10$ along the tail axis and $(1-\mu)$ between 10^3 and 10^4 at distances $y>200\,000$ km. I believe it is unnecessary to explain that Stumpff's conception is not tenable.

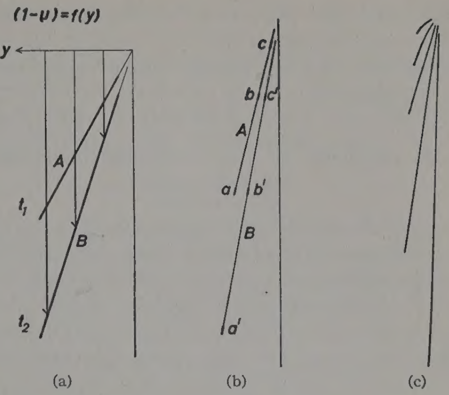

FIG. 3. Turning of the tail rays of a comet.

In a short note several years ago (Wurm 1953) I pointed out that the turning of the rays can be understood kinematically, at least to a large extent, by a constant repulsive force including a steady decrease of the velocity of expulsion. Figure 3(b) shows qualitatively for these conditions the movement of the individual particle: Point a goes over into point a′, b into b′, and c into c′. All points move away from the tail axis, but each tail ray as a whole turns toward the radius vector. This suggestion was only intended to emphasize that the turning of the rays depends on a decrease of the velocity component v_y.

At first sight, it might seem easy to investigate the orbits of the tail particles—one could simply observe shifts in time of well-defined condensations within the tail rays. The obstacle is that no well-suited material exists for this purpose. The time interval between two photographs which one can compare is for the most part too short to reveal a clear shift of a condensation. I have studied carefully any suitable pairs of photographs which I found, but very few of them gave any information. While the available material is insufficient to give a clear picture of the movement of individual particles, there is some indication that the velocity component normal to the tail axis is not identical over the whole orbit of the ion with its initial velocity v_y. It is rather probable that a new force appears which accelerates the ion in the direction toward the radius vector, diminishing in this way the initial velocity v_y. At first sight, the appearance of such a force would seem to cast doubt on our reasoning concerning the high initial velocities of the ions at the beginning of the ray formation and their low velocities at the end of the formation. However, it can be shown that the ions within the long tail rays have low velocities from the beginning. The situation is not so simple that I can explain the reasons for this opinion in a few phrases. I intend soon to publish a note on this point.

IV. CRITICISM OF THE CORPUSCULAR CAUSE OF THE TAILS

The subjects touched in this paper have not, of course, exhausted our total knowledge about the tails, but the points mentioned are certainly of prime importance with regard to the foundation of a physical theory. I do not intend to deal more closely with any other observations, but now wish merely to summarize the arguments which, in my opinion, speak against the corpuscular-stream theory of the tails as suggested by Biermann (1953) and advocated by him and his associates at the Max Planck Institute.

It is claimed that the theory accounts as well for the ionization within the heads as for the acceleration of the ions. The ionization is ascribed to a charge-transfer process between the solar protons and the cometary neutral particles. In this connection we need not discuss whether the proton densities are high enough to explain the high ionization rate of the carbon monoxide or carbon dioxide. The real problem is to reconcile the high rate near the nucleus with the low at larger distances, and it is this problem for which the theory can present no answer. I am inclined, as indicated already, to consider this contradiction between the ionization rates as a hint not to connect the observed ionization near the nucleus with the direct influence of an outer force or radiation, but to search for its energy source within the comet. Support is lent this belief if we consider the two other phenomena connected with the appearance of the ions: the formation of the ray structure and the high and regularly decreasing initial velocities. We know nothing about their causes but it seems to me impossible to imagine that the regular development of the tail rays, each ray developing largely independently of the others, is a phenomenon which can be controlled directly by an outer influence.

The theory runs into difficulties also with respect to the repulsive forces, this despite the fact that we need not consider at all the extreme values of 1000 to 10 000 times the solar gravitation which were envisaged by Stumpff to explain the turning of the tail rays. According to Biermann, repulsive forces of the order 100 times the solar gravitation at 1 a.u. from the sun can be explained by the collision theory with proton densities of 10^3 particles per cm^3. But we must remember that this result depends on an assumed density of the cometary particles of the order one to ten. The density in the accelerating stream must be by about three powers of 10 higher than that of the accelerated stream. According to newer estimates the ion density within the tails of brighter comets amounts to 10^2 to 10^3, and we would correspondingly need proton-stream densities of 10^5 and more in order to account for the observ
accelerations. Very probably, solar corpuscle strea
of such densities can, if they exist at all, be only o
localized and sporadic nature. But because of th
distinctly permanent nature it is not possible to conn
the cometary phenomena which I have described w
such occasional streams.

One can also find strong arguments against the hig
density corpuscle theory in a consideration of the exci
tion conditions of the emitting molecules. I will menti
only one argument, connected with the oscillation a
rotation distribution with the C_2 Swan bands. The
molecule cannot get rid of its rotational and oscillatio
energies by way of radiation since it has no permane
dipole movement. Collisions with fast protons shou
of course, increase the internal energies of the molecul
The C_2 molecules at the border of the head have exist
about two days within the atmosphere. There is not t
slightest indication that the molecules near the bord
have gained rotational or oscillational energy compar
with the molecules near the center. If one assumes
effective cross section of 5×10^{-16} cm^2 for the ener
transfer, one estimates that a corpuscle stream with
density above 100 protons per cm^3 cannot exist.

I believe that the arguments mentioned in this pap
together have sufficient weight to show that we mu
give up the collisional theory of cometary tails, a
search for another one.

DISCUSSION

Öpik: Concerning the need for high particle densi
in the corpuscular streams, I think the observations
the spectrum of the zodiacal light by Blackwell sh
that the electron density is certainly less than 100/c
To be sure, if the stream velocity is smaller, the inte
action rises since the cross section is inversely prop
tional to the 4th power of the velocity, but then t
momentum is insufficient. Perhaps a greater difficul
is the motion of the particles in the cometary ta
Repulsive forces of 100 or 1000 times solar were report
first by Bobrovnikoff with Comet Halley. From seve
photographs made in late May and early June 1910,
assumed that every day there were separate elemen
But if all the observations are joined together they sh
a beautiful single trajectory, with average radial
pulsive force of from 60 to 70—quite normal—still t
motion is not that of a central force, the transve
component coming to a full stop. And this is similar
what Dr. Wurm has told us.

Whipple: Is there any well-substantiated eviden
of correlation between tail activity and solar activit
At Liége there have been several papers on this.

Wurm: There have been many papers, but I do n
believe the evidence is good.

——: Are effects of rotation small compared to t
forces you have described?

Wurm: We don't know what the forces actually a otation of the tail rays is certainly not observed.

pik: In the case of Halley's comet the force was tly in the direction of the radius vector.

erzberg: You said that there was an apparent tradiction between the two lifetimes that have been ained? If I understand correctly one is for CO, and other is for CN, C_2 and some others. Is it not con-able that these should be different?

urm: No, I don't think so. Observed also are CH^+ CH neutral.

erzberg: Yes. Do I understand correctly that you ibute the large difference by a factor of 100 to some hanism inside the comet?

urm: There seem to be two mechanisms for ioniza- . The internal one somehow causes the lifetime of ny molecules in the nucleus to be very short, yet this mechanism is not fully efficient and is restricted in space.

Herzberg: Perhaps some kind of shock wave that is produced by the breaking up of the core?

Wurm: This would be difficult since the free path for particles is of the order of the atmosphere.

REFERENCES

Biermann, L. 1953, *Liége Symp. 1953*, 251.
Bobrovnikoff, N. T., 1931, *Lick Obs. Publ.* **17**, Part II.
Miller, F. D. 1957, *Publs. Astron. Soc. Pacific* **69**, 82.
Miller, F. D. and Liller, W. 1956, *Astron. J.* **61**, 10.
Nicolet, M. 1961, *Liége Symp. 1960*, 319.
Stumpff, P. 1959, *Z. Astrophys.* **47**, 225.
Vorontsov-Veliaminov, B. A. 1961, *Soviet Astron.—A. J.* **4**, 674.
Wurm, K. 1947, *Mitt. Hamburger Sternwarte*, Band 8, 57.
——. 1953, *Liége Symp. 1953*, 210.
——. 1961, *ibid. 1960*, 369.
Yoss, K. M. 1953, *ibid. 1953*, 32.

THE ASTRONOMICAL JOURNAL VOLUME 66, NUMBER 8 OCTOBER, 1

Astrometric Observations and Orbits of Comets

Elizabeth Roemer
U. S. Naval Observatory, Flagstaff Station

ANY study of comets begins with observations of position. Crude observations may suffice for finding purposes for spectroscopic or photometric observations of brighter objects. But a large amount of information can be gained, for faint objects as well as for bright ones, by studying the motions, or orbits.

Precise study of the motions of comets has two major aspects: *observation* and *computation*. Observations of position are desired, of considerable *precision*, and extending over as long an interval of *time* as possible. To achieve either of these ends, the application of fairly large instruments is needed. For astrometric purposes comets are not to be regarded as extended objects; the advantage in scale and limiting magnitude of large telescopes is valuable.

OBSERVING PROGRAM AT FLAGSTAFF

At the Flagstaff Station of the U. S. Naval Observatory an effort is made to obtain one pair of plates during each dark of the moon of every comet within reach of the 40-inch Ritchey-Chrétien reflector. Additional observations may be made if they are likely to be useful, as, for example, in the case of newly discovered objects. This program is a modification and expansion of the type of program carried on for some time by H. M. Jeffers of the Lick Observatory, and especially by G. Van Biesbroeck at the Yerkes and McDonald Observatories. Moving objects are recorded regularly to magnitude (pg) 20.5. Since the dividing line between short-period comets and minor planets is by no means clear, certain minor planets are observed whenever the opportunity arises. Some of these minor planets may indeed be old comet nuclei. Included on the program are all the minor planets having a perihelion distance less than 1 a.u. and many of those that have a perihelion distance only slightly greater than 1 a.u., and for which ephemerides are available.

To demonstrate the extent of the program, it may be noted that 19 different comets and nine minor planets were successfully observed during the 12 months ending in June 1961. Eight returning periodic comets were re-observed first at Flagstaff, including four within 16 days in August 1960.

In making the observations, the calculated motion of the object is offset as a general practice, the plate being displaced relative to the crosshairs of the guiding eyepiece. Guiding is done by means of a star located near the edge of the field being photographed. The telescope operates at $f/6.8$, and exposures up to two hours in duration are useful. Appropriate exposure time is expecially important in astrometric investigations. Since estimates of the brightness of comets vary greatly, depending on the instrument and methods by which observations are made, we have found it necessary calculate our own version of predicted magnitudes, pending upon earlier observations of our own, or th of other observers using similar equipment and metho The results of Cunningham (1951, 1952), observ with the Mount Wilson 60-inch and 100-inch telescop 1950 to 1953, have been especially valuable.

Bright comets, as well as faint ones, are observ regularly. Especially in bright objects is there pos bility of a systematic displacement of the center light from the center of gravity. Such a displaceme leads to systematic errors in the orbit, especially the case of such objects as periodic Comet Encke, whi is usually observable, during any specific appariti only before, or only after, perihelion passage. To t best of my knowledge, the U. S. Naval Observator Flagstaff Station, is the only observatory in the world which astrometric observations of comets fainter th mag. 17 are being made regularly at the present tim

MEASUREMENT AND REDUCTION OF PLATES

Since the field of the 40-inch reflector, or of a similar instrument, is fairly small, reference stars a most invariably have to be taken from the *Astrograph Catalogue*. With the epoch of most plates of the Cata logue 40 to 60 years ago, proper motions have had a appreciable effect upon the star positions. The calcul tion of the plate constants of the Catalogue often i volves meridian positions of reference stars from a even earlier epoch, used without application of prop motions. The great improvement in the accuracy positions reduced from the portion of the Paris Zo for which new plate constants have been calculated b Heckmann, Dieckvoss, and Kox (1954) is particular noteworthy. Even with reference stars taken from t *Astrographic Catalogue*, there is an appreciable differen between the magnitudes of the moving objects bei investigated and those of the reference stars. Hen there is likelihood of systematic errors.

Reduction of the measures may be carried out by a of several methods: by dependences, by a modifi plate constant method, or by accurate orientation the plate in measurement and reduction by means an assumed value of the plate scale. The dependen method, with at least six reference stars and a leas squares solution, is used for the reduction of most the results from Flagstaff plates, the computations b ing executed with the IBM 650 of the U. S. Nav Observatory, Washington, D. C. In emergencies, whe results are needed immediately, the plates are generall oriented accurately and the reductions carried out b d at Flagstaff. In our experience these methods pro- better checks in dealing with the *Astrographic* *ilogue.*

CALCULATION OF ORBITS

nly very rarely has every precaution been taken alculation of orbits to ensure that the calculations esent the actual motion of the object to the greatest ible physical accuracy. Very few of the persons ig the computing have had observational experience, cially with large instruments. They are, therefore, always well equipped to evaluate the quality of the ervations on which the computations are based, or to l with the observations in the most effective manner. ely is the attempt made to reduce the observations a consistent catalogue system, even if this can be ie.

n general, a few positions carefully measured on perly exposed plates taken with an instrument of icient focal length and well spaced in time are worth re in practice in defining the orbit than great num- s of positions obtained only when the comet is ght. Computers would often have an easier time, hout loss of precision and sometimes with gain, if an reciable fraction of the total number of observations e simply disregarded. This can be seen in those in- nces in which residuals of individual observations m an improved orbit have been published in detail.

specially for short-period comets, the effort in dictions has generally been to obtain sufficient ac- racy for recovery. The efforts of the volunteer workers the computing section of the British Astronomical sociation have been especially noteworthy and valu- e in making observations possible at repeated returns the numerous members of the short-period Jupiter nily of comets. Necessarily, approximations have n introduced in computing the perturbations, and ne significant perturbations have been neglected, nply to keep the volume of work within bounds. rting orbits have not always been the best available, d almost never the best possible. And, inevitably, stakes in the calculations have occurred from time to ne. Because of misunderstanding, the idea has grown at there are appreciable nongravitational forces opera- ve, and that precise predictions of future positions of mets are impossible.

It should be noted that observations at one apparition not, however, determine the value of the mean mo- n sufficiently well to expect an exact prediction at e next succeeding perihelion passage. Furthermore, e probable error in the mean motion deduced from a st-squares correction to the elements may be largely titious. This fact is well demonstrated by Merton's 927) work on periodic Comet Schaumasse. A least- uares solution by G. Fayet and A. Schaumasse from e observations in 1919 gave a value of the mean daily otion, $n=439''.476\pm0''.7$. By linking the apparitions 1911 and 1919, Merton found the value of the mean motion to be $n=446''.811$. This value of n made the predicted time of perihelion passage in 1927 some *49 days* earlier than the 1919 observations alone indicated. In spite of decidedly unfavorable circumstances the comet was recovered very close to Merton's prediction. Another example is the recovery of Comet Gale by Cunningham in 1938 some $5^h\,23^m$ west of what appeared to be the most likely place predicted on the basis of observations in 1927 (Davidson 1939).

Few orbit methods give a good indication of the real physical determinacy. One notable exception is Cunningham's method, in which a change of the coordinate system yields explicitly the deviation from great circle motion and the length of arc represented by the fundamental observations. A similar insight into the physical accuracy may be obtained by computing variational orbits, on each of which the observations may be represented. This becomes practicable now with the application of large digital computers.

The correction required to bring the predicted time of perihelion passage into accord with observation for periodic comets reobserved in 1960–61 is shown in column 3 of Table I. The total number of observed perihelion passages of each comet appears in column 2. It should be noted that if two perihelion passages have been observed and an effort made to obtain an accurate prediction, the divergence of calculations from observations is very small. The predictions for comets Reinmuth 2, Encke, and Wirtanen are examples.

TABLE I.

Comet	Obs. returns	ΔT (days)	Computer
Reinmuth 2	3	0	E. Rabe
Finlay	7	-1.2	M. P. Candy
Comas Solá	5	(small)	H. Q. Rasmusen, J. M. Vinter Hansen
Harrington	2	-0.6	C. Dinwoodie, B. G. Marsden
Brooks 2	10	(small)	A. D. Dubiago
Encke	46	0	S. G. Makover
Schwassmann-Wachmann 2	6	-0.3	H. Q. Rasmusen
Borrelly	7	$+0.2$	M. G. Sumner, M. P. Candy
Wirtanen	3	0	P. Herget
Forbes	4	$+0.5$	B. G. Marsden
Tempel 2	13	$+0.4$	B. G. Marsden

SECULAR ACCELERATIONS

It is evident from the activity photographed in the head and tail of comets that some nongravitational forces do indeed exist. But the existence of measurable nongravitational accelerations of the center of mass should be regarded as an open question. The amount of any such nongravitational accelerations is vital to theories regarding the structure of comets and their rates of disruption. See, for example, the papers by Whipple (1950), and van Woerkom (1948).

It is a revealing experience to look critically into the published computational work, on the basis of which the existence of nongravitational secular accelerations has been asserted. Divergences from observations are quite small, and the quality of the physical parameters (such as planetary masses) and accuracy of computation that have entered into even the most precise orbits are disappointing in comparison with the size of the residuals.

As an illustrative example, let us take periodic Comet Wolf 1, 1884 III. I choose this object only because the published details of the calculations are quite complete and readily available, and also because I am responsible for all of the accurate positions obtained of this comet at its most recent return in 1958. Kamienski, who has devoted more than 50 years to study of the motion of this object lists (Kamienski 1953, 1959) 72 papers he has published to report his findings. The quality of the computations, carried out by hand methods, is quite remarkable, and this object is nearly unique in that perturbations at the most critical times have been checked by independent calculations by completely different methods. The agreement of these duplicate calculations generally has been quite good, i.e., practically to the limit of the accuracy carried. Nevertheless the small differences that do exist probably are significant in view of the size of the observational residuals, on the basis of which a secular acceleration is deduced. The system of planetary masses used involves differences in the mass of Mercury of some 50%, and of Jupiter of 0.1% from the best modern values. These differences cannot be considered negligible when the attempt is made to represent observations to 1″ accuracy.

The observed motion of P/Wolf 1 may be considered in two parts, separated by a close approach to Jupiter ($\Delta_{\min}=0.12$ a.u.) in 1922. Prior to the close approach the comet moved in an orbit of perihelion distance 1.61 a.u., and afterward in one of perihelion distance 2.45 a.u. Kamienski (1933) found it necessary to introduce an acceleration in the mean motion to represent observations in the smaller orbit:

$$\Delta n=-0''.000\,00042(t-t_0),$$

where $(t-t_0)$ is expressed in days from $t_0=1884$ September 24.0 BMT. The apparitions of the comet in 1925, 1933/34, and 1942 were linked with one set of elements, which, with the inclusion of perturbations due to six planets, represents also observations of the comet in 1950–51 and 1958 with maximum residuals of $-0^{s}.3$. Kamienski suggests that the residuals may be caused partly by uncertainty in the amount of perturbations by Jupiter in the mean anomaly, one part in 8000 being sufficient to reduce the residual to zero, and partly by a continuing secular deceleration. In the larger orbit Kamienski finds (1961) a value for the deceleration term of

$$\Delta n=-0''.000\,00012(t-t_0)$$

(with time counted in the same manner as formerly) the deviation from theory in 1958 is attributed entir to nongravitational forces. This acceleration, one-fou as large as that found in the smaller orbit, is based an observational residual of $(\alpha_0-\alpha_c)\cos\delta=-0$ $=-4''.65$ on June 22, 1958.

As the person responsible for the observations, I not feel that an acceleration deduced from such residu is convincing. Kamienski has implied the same c clusion by suggesting that judgment should be withh until observations can be obtained in 1967. The i portant point to be made here is that gravitatio theory alone, with borderline numerical accuracy computations, and physical constants capable of i provement, is adequate to represent observations o the entire time interval from 1925 to 1958 with residual larger than 4″—a residual quite within t limits of possible observational error. There is, therefo no evidence for appreciable nongravitational forc operating on this comet during this interval.

The observational residuals are somewhat larger f the motion in the smaller orbit, prior to 1922, and t residuals are larger for Comet Encke, which has perihelion distance of 0.3 a.u. But both computatio and observations are more sensitive to effects that le to the appearance of a run of residuals. There is mo likely to be a systematic displacement of the center light from the center of gravity in the brighter, asym metrical image of a comet near the sun. The time inte val of steps in calculating perturbations must l shortened, leading to a rapid increase in the number steps, and hence to an even more rapid buildup roundoff errors in numerical integration. The approx mation of a barycenter is less valid. And the perturb tions by planets whose masses are subject to conside able uncertainty (Jupiter, and, formerly, Mercur and Venus) may be appreciable.

With the emphasis that has been placed recently o comets as probes in studying the interplanetar medium, and the inferences that have been drawn re garding comet models, it may not be out of order t suggest that a great deal of work needs to be done befor much confidence can be placed on conclusions in thes realms. A definitive study of the motion of severa well-observed objects would be extremely useful. Object suspected of a secular acceleration might supply espe cially interesting information. Such a study must star with a rediscussion of original observations, with effort being made to emphasize observations carefully planne and executed with moderate- to large-sized instruments An attempt should be made to reduce positions to consistent catalogue system. Calculations should b carried out to full physical accuracy, and with sufficien guard figures to ensure that such factors as roundof error in long-continued numerical integrations do no destroy significant results. It would be extremely interesting to compute perturbations around a family of variational orbits that do not do an injustice to observa-

s, rather than for the one orbit that gives the best
ematical fit to observations. The differences in
orbits at aphelion, where the perturbations by
ter are largest, may be important. A true estimate
ls to be made of physical uncertainties in predic-
s, to ensure that an adequate search is made. Peri-
comets undoubtedly have been lost in the past
l are being lost at present) because of inadequate
ches. It should be possible to verify results by
putations by different methods, so that mistakes
omputation may be discovered and corrected, as
as to compare the relative merits of different
niques. A great deal of information undoubtedly
be extracted from existing observations with vigor-
and imaginative use of large-scale computing facili-
now available. And in the near future precise orbit
a undoubtedly will be useful in planning the direct
mination of the properties of comets by means of
ce probes.

REFERENCES

ningham, L. E. 1951, *Publs. Astron. Soc. Pacific* **63**, 42, 95,
53, 209.
-. 1952, *ibid.* **64**, 35, 80, 139, 207, 320. See also *Harvard Ann.*
ards, and *I.A.U. Circ.* 1950–53.
idson, M. 1939, *Monthly Notices Roy. Astron. Soc.* **99**, 409.
kmann, O., Dieckvoss, W., and Kox, H. 1954, *Astron. J.* **59**,
43.
nienski, M. 1933, *Acta Astron.* (Ser. a) **3**, 1.
-. 1953, *ibid.* (Ser. c) **5**, 44.
-. 1959, *ibid.* (Ser. a) **9**, 87.
-. 1961, *ibid.* **11**, 33.
ton, G. 1927, *Monthly Notices Roy. Astron. Soc.* **87**, 565.
Woerkom, A. J. J. 1948, *Bull. Astron. Inst. Neth.* **10**, 445.
ipple, F. L. 1950, *Astrophys. J.* **111**, 375.

DISCUSSION

Whipple: This is a very fine work. I should like to
n Miss Roemer in her plea for recalculation of some
bits. Encke's comet especially needs it, for in its early
ys especially the perturbations could not have been
plied very accurately. Cunningham has data, but has
t reduced it as yet. If I had suspected that there may
no secular changes in the period, I don't know whether
would ever have published my icy-conglomerate
odel! (Laughter.)

Eichhorn: If you say the accuracy limit is imposed
the *Astrographic Catalogue* (can't do better than 1″ or 2″), do you attribute this to intrinsic inaccuracy in the positions in the AG, or to proper motions, or to the uncertainty in tying the astrographic measures into a certain fundamental system?

Roemer: It is really a combination of the quality of the reference star positions (primarily observed for the AGK1 and used without proper motions) and the long time interval involved since.

Eichhorn: Are any systematic corrections applied?

Roemer: This is practically impossible to do, and it would probably cause damage. Let the person using the positions apply the corrections he considers desirable. Of course there is the possibility of using field plates, reduced using Yale stars or AGK2 stars, but this more than doubles the work.

——: How large are the typical cometary nuclei that you measure?

Roemer: One practically never observes the nucleus directly. I would give very great weight to the visual observations of van den Bos, Baldet, and V. M. Slipher of the nuclei of comets close to the earth, the indicated size being from $\frac{1}{2}$ to a few km for a typical object.

Herzberg: You mentioned an object with two nuclei. The motion with respect to each other has been measured?

Roemer: I think one can get the velocity of separation, which gives some index of the energy of processes going on in the nuclei. This comet was at such a great distance from the sun that the disruption was not a tidal effect, but something that happened internally in the nucleus.

Herzberg: Would you care to comment on the resemblance between comets and asteroids?

Roemer: The Jupiter family comets cannot be distinguished from asteroids on the basis of orbits alone. When I observed Comet Arend-Rigaux on its last apparition I found that it was completely stellar on all plates. The orbit is similar to that of a minor planet, but the object was designated as a comet because it on occasion showed some diffuseness. When Baade discovered Hidalgo he was undecided whether to call it a minor planet or a comet, but he decided on the former simply because more people were observing minor planets at the time and it would be better taken care of! (Laughter.)

THE ASTRONOMICAL JOURNAL VOLUME 66, NUMBER 8 OCTOBER,

Photoelectric Photometry of Comets

WILLIAM LILLER
Harvard College Observatory

THE recent appearances of several bright comets have resulted, happily, in an increased interest of astronomers with access to photoelectric equipment in comet research. The new observational data have, in turn, provided us with a better understanding of the physical conditions in comets. Most of the observations have been made in broad spectral regions defined, for example, by the standard *UBV* system. A number of astronomers have since acquired narrow-band filters in the event another bright comet puts in an appearance in the near future. The use of interference filters or spectrometers is to be very much preferred over broad-band photometry, of course, because most comets exhibit spectra composed of both molecular emissions and continuous radiation. When using broad-band photometry, one cannot always be sure whether changes in intensity (as a function of time, of plane of polarization, etc.) are to be attributed to the emission bands or to the continuum. There are times, however, when virtually all the radiation is in either the bands or in the continuum. Such a circumstance may occur in a comet tail made of only gas, or of dust, or in the heads of some comets which have a very weak continuum.

Excellent broad-band observations have been made, for instance, by Bappu and Sinvhal (1957), who have used interference filters, by Boiko and Kharitonov (1957), by Hoag (1958), by Johnson (1960), and by Thiessen (1958). Their observations have given us a fairly clear picture of the brightnesses, colors, and the percent polarization of the two bright comets of 1957.

It is particularly interesting to note that Thie found a close correlation between the brightnes Comet 1956 *h* and solar activity, in direct contradic to the results of Beyer (1952), who has been carry out visual observation for many years at the s observatory.

My own work on comets has been almost exclusiv in the field of narrow-band photoelectric photome The instrument used was a photoelectric spectrophot eter (see Liller 1957) located at the focus of a 24-i telescope at the University of Michigan Observato Comets studied so far include 1956 *h* (Arend-Rolan 1957 *d* (Mrkos), Comet Encke, and 1959 *k* (Burnha

The remainder of this paper is divided into th parts: The first contains a summary of the observati of comet head spectra; part II describes briefly cor tail observations; and the last section discusses mo chromatic isophotal contours made of Comet 1959 *k*

I. HEAD SPECTRA

A. Time Variations of 1956 *h*

The discovery of Comet 1956 *h* well in advance perihelion passage made it possible to observe t changes of the spectrum of this comet as it approach the sun, passed perihelion, and then receded from t sun. Figure 1 shows a spectral scan made shortly aft Comet Arend-Roland passed perihelion. As was e pected, the intensities of the emission bands of C_2 a CN relative to the continuum varied, in general, i

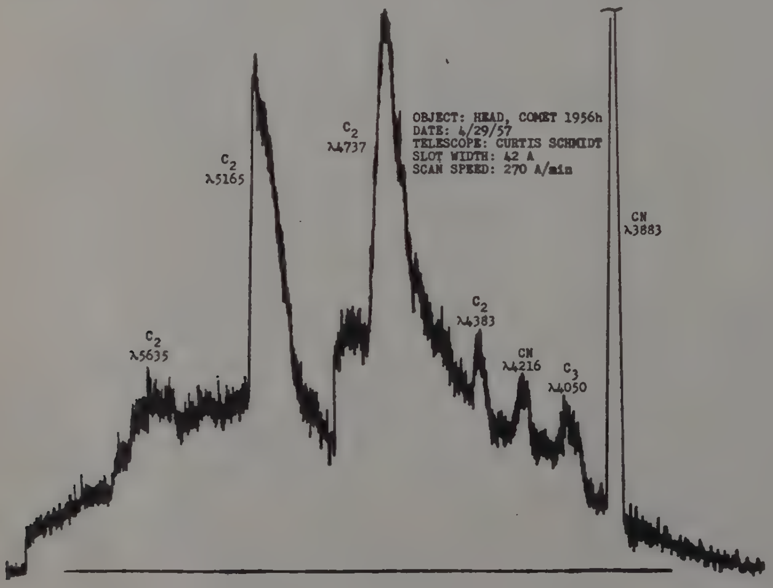

FIG. 1. Photoelectric scan of th spectrum of the head of Comet 1956 (Arend-Roland). A yellow filter w inserted in the light path at wav lengths greater than λ5000 to elimina effects of overlapping orders. Sca made at the focus of the Curti Schmidt telescope, Portage Lak Michigan.

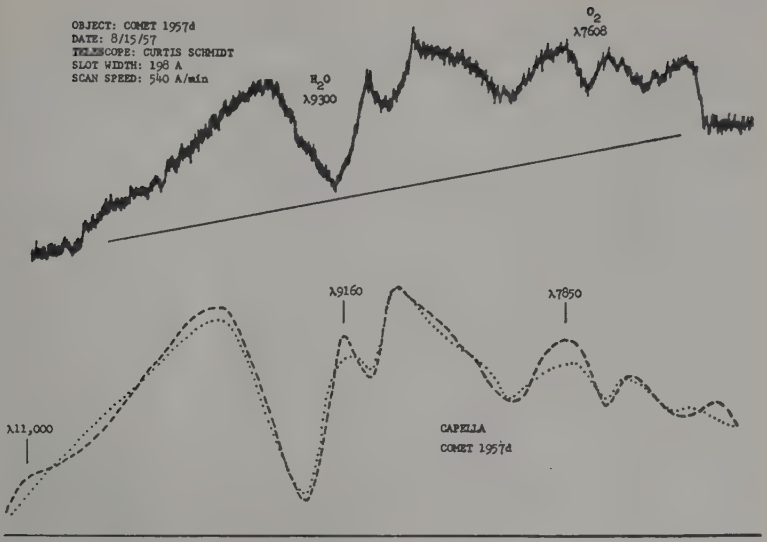

:. 2. Photoelectric scan of the red nfrared spectrum of the head of et 1957 *d* (Mrkos) made at the of the Curtis Schmidt telescope. lla, dotted line; comet, dashed

ely as the heliocentric distance. In units of contin- brightness, the intensity of C_2 (λ5165) increased roximately as the 1.31 power of the heliocentric ance. However, it was particularly interesting to that C_2 did not reach maximum intensity, compared he continuum, until almost exactly one month after helion passage.

B. Variations of Spectra with Comet

'he molecular emission-band spectra of the four ıets which have been observed with the photoelectric ctrophotometer are quite similar. In the photographic on of the spectrum, the bands of C_2, *CN*, and C_3 most conspicuous, and appear with approximately same relative intensities. The sodium D lines were erved in Comets 1956 *h* and 1957 *d* for a brief period ime near perihelion.

'he greatest difference between the head spectra of se comets is the strength of the underlying contin- n. Comets 1956 *h* and 1957 *d* were similar in that y had relatively strong continua. For example, at a iocentric distance of 0.68 a.u., the peak intensity of λ5165 (C_2) band was just twice the intensity of continuum at the same wavelength. For Comet cke this intensity ratio was more than 5 at $r=0.68$; vas over 16 for Comet 1959 *k* at a heliocentric distance).89 a.u. This last value is the only surprising one, ce it has been fairly well established that comets ich have passed close to the sun many times are less ısty" than are very long-period comets. According to segawa (1960), the orbit of Comet 1956 *h* is hyper- ic, while the period of revolution of Comet 1957 *d* is 000 years, according to Schrutka (1961). Presum- y, both of these comets are comparatively "young." the other hand, Comet Encke is an "old" comet with eriod of 3.3 years, and it has probably made over 100 olutions about the sun. The observations of Comet 1959 *k* would, therefore, lead one to believe that it is very "old." It will be very interesting to learn the elements of the orbit of this comet.

C. Spectrum of the Head of Comet 1957 *d* in the Infrared

Shortly after the discovery of Comet 1957 *d*, the writer obtained two scans of the spectrum of this comet out to a wavelength of approximately 10 000 A. A reproduction of one of the original scans and a comparison of it with the spectrum of Capella (Sp. G8III) is shown in Fig. 2. As can be seen, the comet spectrum is primarily of a continuous nature; the greatest difference in brightness between the comet and the solarlike comparison star at approximately 1 μ is possibly due to the (0−0) band of red system of *CN*, according to Swings (1958).

II. TAIL SPECTRA

A more detailed account of the observations of the spectra of the tails of Comets 1956 *h* and 1957 *d* appears elsewhere (Liller 1960). In brief, the results were that the observed energy distributions in the continuous radiations from the tails can be explained by assuming the tails to be made of spherules of iron with diameters of approximately 0.6 μ separated on the average by three or four meters. Reasonable estimates of the volumes of the tails of these comets, the rates of mass loss, and the relative abundance of the other elements leads to total masses for these comets of 10^{18} and 10^{19} g, respectively.

III. ISOPHOTAL CONTOURS OF COMET 1959 *k*

Norman H. Schultz of the University of Michigan Observatory and the writer were able to obtain several monochromatic intensity profiles of Comet 1959 *k* by sweeping the telescope east and west along one declination circle and allowing the comet to move slowly northward or southwards. The isophotal contours show clearly that the images in the light of λ3884 (CN) and λ5165 (C_2) are very nearly equal in size if one considers contours of intensity measured in terms of the intensity of the brightest point of that head isophote. Contours measured in the feeble light of the continuum of this comet showed that this image was from 1.5 to 2 times smaller than the images in the light of the emission bands at a heliocentric distance of approximately 1 a.u.

A single intensity profile of considerable interest was made on April 28, 1960, when Comet 1959 *k* was 1.0 a.u. from the sun and only 0.2 a.u. from the earth. The diameter of the λ5165 (C_2) image appears to have changed by nearly a factor of 2 over a time interval of 70 min. According to Barber (1960), at about the same time the comet was fluctuating by more than a half magnitude in brightness, and on the following night, a very bright aurora was observed in Michigan. Obviously, additional observations of a similar nature are urgently needed to make clear the association between solar activity and comet appearance and brightness.

REFERENCES

Bappu, M. K. V., and Sinvhal, S. D. 1957, *Monthly Notices Roy. Astron. Soc.* **117**, 590.

Barber, D. R. 1960, *Observatory* **80**, 198.

Beyer, M. 1952, *Liège Symp.* **13**, 236.

Boiko, P. N., and Kharitonov, A. V. 1957, *Russian Astron. Circ.* No. 181, 6.

Hasegawa, I. 1958, *I.A.U. Circ.* No. 1619.

Hoag, A. A. 1958, *Publs. Astron. Soc. Pacific* **70**, 203.

Johnson, H. M. 1960, *ibid.* **72**, 10.

Liller, W. 1957, *ibid.* **69**, 511.

——. 1960, *Astrophys. J.* **132**, 867.

Schrutka-Rechtenstamm, G. 1961, *Sky and Telescope* **20**, 329.

Swings, P. 1958, *Trans. I.A.U.* **10**, 240.

Thiessen, G. 1957, *Z. Astrophys.* **43**, 260.

DISCUSSION

ÖPIK: Concerning the interpretation of color polarization, in addition to the two parameters c sidered here (the refractive index and the part radius) there are more parameters such as the distri tion of particle size with radius, which would consid ably change the color, and the composition of particles which need not be pure substances at all. T there are a few dielectric nonabsorbing particles, wh for absorbing particles there are so many different co binations that it may be difficult to unscramble the and tell what particular kind of particles caused One can make a hypothesis for the most probable co position of such dust, but the distribution of the ra must be taken into account as well as the polarizat and color curves.

LILLER: I might add that a frequency distributio the squared shape was taken in the calculations of scatter curves of the individual dielectric and iron p ticles; the variation is by a factor of 2.

DONN: Another parameter perhaps most difficult all to take into account in relation to the interpretat of these curves is the shape of the particles. All one c do theoretically is to consider the cases of spheres spheriods. Actually these kinds of particles are not kind that it is easy to see forming in a comet. One sho know to what extent one can relate the characterist of a randomly oriented group of irregular particles w spherical particles.

HERZBERG: In the slide for Encke's comet the 40 group was practically absent. Is this effect real?

LILLER: This is one band that appears somewh different from one comet to another. In Comet 1959 on one scan it was very strong. But whether this indeed a night-to-night or a photometer variation shou be determined.

E ASTRONOMICAL JOURNAL VOLUME 66, NUMBER 8 OCTOBER, 1961

Problems of the Cometary Nucleus

Fred L. Whipple
Smithsonian Astrophysical Observatory and Harvard College Observatory

INTRODUCTION

OR nearly a century a comet was generally visualized as a "sand bank." Solid particles in a loose gregate of varying sizes were assumed to carry with m a certain amount of gas, to provide the activity the cometary head and tail, under solar activation. nerally the mass was considered to possess gravitanal coherence, that is, to be stable or nearly stable der the influence of solar tidal disruption. Slow, and asionally rapid, disintegrations of comets were exined as arising from solar heating, collisions, or tidesing effects, the loose swarm of particles being conered, in fact, as only in quasi-stable equilibrium for nited periods of time.

Even the requirement of gravitational coherence s more recently abandoned by Lyttleton (1953), who ncluded that "each particle of the comet must deibe a separate, independent orbit around the sun." e sand-bank theory of comets was further strengthed by an ingenious concept due to Levin (1943), o applied the laws of deabsorption of gases to solids cometary nuclei. By the effects of solar heating he counted rather well, quantitatively, for the variation gaseous output and brightness of comets as a function solar distance.

In 1950 the author demonstrated some consequences an icy-conglomerate comet model in which the ucleus of the comet is postulated as a discrete mass of lids which may have been formed from typical interellar material at temperatures of the order of 10–0°K. In the vicinity of the sun, because of solar eating, the materials that sublimate profusely in a acuum at temperatures of the order of 150–500°K rry away from the comet with their vapors the less latile constituents in aggregates variously sized from tremely fine dust to pieces perhaps meters in dimenon. The icy-conglomerate model simulates almost all the observed characteristics of comets. No critical mparison among various comet models has been made, that the icy model is here examined critically. The ajor portion of the present discussion is devoted to the oservational and theoretical evidence relevant to the tual existence of a discrete cometary nucleus, and to s nature.

GAS AND SOLIDS OF A BRIGHT COMET

As Lyttleton has pointed out, direct observation does t *prove* the existence of a discrete cometary nucleus. lso, the orbital calculations made from cometary obserations show that these observations do not always pply exactly to the center of mass of a body moving ecisely under the law of gravitation.

The fact that comets are observed to lose gas and dust to the interplanetary medium is no demonstration that a comet has a discrete nucleus other than a diffuse volume of solid particles with possibly absorbed gases. The hypothesis of a diffuse nucleus, however, sets definite limits on the amount of gas that might be held by solid particles with the observed surface area. Some of the arguments here follow the principles set by Vorontsov-Velyaminov (1946) and lead to similar conclusions.

Wurm (1943) calculated that Halley's comet must have contained some 1.5×10^{32} molecules of C_2 near perihelion with lifetimes of 10^5 sec. For the total passage this adds up to some 2×10^{34} molecules or 4×10^{11} g.

Recent calculations by Wurm for the CO^+ molecule in Comet Arend-Roland, 1956 *h* lead to an estimate of some 8×10^{34} CO^+ molecules in the tail at one time, a mass of 4×10^{12} g. The corresponding values for the tail of Halley's comet would undoubtedly come out larger in view of its greater dimensions. Although we do not know very accurately the lifetime of the CO^+ molecule in space, the material in the tail would surely be replaced at least 10 times during a solar approach, giving the total loss of CO^+ during one passage as a minimum of 10^{36} molecules or 5×10^{13} g.

The apparent surface area of the solid material at the head of Halley's comet at great solar distances had a minimum value of some 10^{13} cm², that is, an apparent radius of 20 km, derived from the assumption of lunar albedo (Wurm 1943; Vorontsov-Velyaminov 1946).

Thus the gaseous layer of C_2 lost by the comet during its perihelion passage would amount to roughly 2×10^{20} mol/cm² of superficial surface area of the solid aggregate. If a monomolecular layer requires some 10^{15} mol/cm² the effective thickness of the absorbed C_2 layer was originally 2×10^5 molecules, or roughly 10^{-2} cm. For the later estimate of CO^+ by Wurm, the corresponding depth of the CO^+ layer comes out 3×10^7 molecules or roughly 1 cm.

There is no reason to believe that the several observed molecules and atoms in the head of a comet are the parent molecules originally present in the comet nor that CO^+ is fundamentally the most abundant molecule. Hence there is every reason to believe that a solid surface layer, centimeters in depth, is a low estimate of the gas loss in one perihelion passage by Halley's or a comparable large comet.

That cometary solids could accumulate 10^{22} or even 10^{20} molecules of gas per square centimeter of surface area during a single revolution about the sun, to maintain quasi-equilibrium in gaseous input and output, is quite unthinkable. If we assume a solar corpuscular radiation of 1000 atoms per cubic centimeter, moving

1000 km/sec and impinging upon Halley's comet continuously at this rate for one revolution, we find 10^{20} atoms/cm^2 rev. Such a rate is inadmissibly high, even at the earth's distance. When we allow for many revolutions (more than 32 for Halley's comet) the observed loss of CO^+ in all is the order of a meter thickness to be applied to the present apparent surface area.

We must conclude that the solids in a bright, new comet must carry a large reservoir of gas, the order of 10^{22} to 10^{23} mol/cm^2 and probably very much more. The corresponding total original gaseous mass of the comet must be at least 10^{17} g, probably a gross underestimate.

Many of the meteoritic solids ejected from comets exist for a considerable period of time in orbits about the sun; probably they are the major constituent of the zodiacal cloud responsible for the zodiacal light and the Fraunhofer corona. The Harvard Meteor Program (Jacchia and Whipple 1960) has shown clearly that visual meteors arise almost solely from comets. Van de Hulst (1947) and Allen (1947) estimate the density of the particulate zodiacal cloud in the neighborhood of the earth at 10^{-23} to 10^{-21} g/cm^3.

The writer (1955) has shown that the zodiacal cloud can be maintained in quasi-equilibrium by the continuous ejection of approximately 1 ton/sec of meteoritic material, if this material is not destroyed until it spirals in close to the sun under the action of the Poynting-Robertson effect. The rate of mass replacement required is independent of the particle dimensions (excepting rather extreme limits), shapes and densities. In fact, however, a major fraction of the mass will be eliminated by other processes, perturbations by the planets, interstellar wind, particle collisions, and sputtering by the solar corpuscular radiation. Thus the actual injection rate necessary to maintain the zodiacal cloud is at least 10^8 g/sec, and possibly as high as 10^9 g/sec, probably from cometary debris.

To date we have no good method of comparing quantitatively the amounts of meteoritic material produced by different comets. Let us assume, fairly reasonably, that the meteoritic material lost by Halley's comet in one perihelion passage is adequate to supply the zodiacal cloud for one year. At a rate of 100 tons/sec, the total mass lost in one perihelion passage would amount to 3×10^{15} g. The "new" Halley's comet, when it made its first perihelion passage, may have contained a mass more than 100 times as great, and possibly today contains 10 times this amount, or the order of 10^{16} to 10^{17} g.

Our knowledge of the masses of meteoroids is still rather uncertain, but for a meteoric body of moderately faint visual magnitude and a velocity of 60 km/sec, such as an Orionid meteor which may arise from Halley's comet, the mass may be the order of 0.01 to 0.4 g. If one meteor of 3.5 mag. is to strike the atmosphere and be visible to a single observer per 10-minute interval, the corresponding space density of meteoritic material will then be in the range 4×10^{-26} to 1.4×10^{-24} g/cm^3 for a one-magnitude range in meteoric size. We do know how to correct from a range of one magnitud find the total space density. Let us adopt a factor about 10 times; the total space density arising from cometary stream will then be some 10^{-25} to 10^{-23} g/c

TABLE I. Mass[a] estimates for a "new" Halley's comet.

Source of estimate	Mass (g)
C_2 in the tail (Wurm)	4×10^{13}
CO^+ in the tail (Wurm)	5×10^{15}
Dust in the zodiacal cloud	10^{16} to 10^{17}
Meteor streams	10^{16} to 10^{18}
Dust in the tail (Liller)	5×10^{16} to 7×10^{17}
Total mass (minimal)	10^{17} to 10^{19}
Radius (density$=1.3$ g/cm^3)	3.1 to 14.6 km

[a] 100 times the mass loss in the recent perihelion passage.

If, as a very rough estimate, the cross section o large stream is 1/5 a.u. in each dimension near earth's orbit, the area is 10^{25} cm^2 and the total volu 10^{41} cm^3.

Thus, for Halley's comet the mass of meteoritic m terial in the stream, if it does indeed produce the Orio and the η Aquarid meteor showers, may be the order 10^{16} to 10^{18} g in total. This mass would then represe a minimum initial mass of the "new" Halley's com Similarly, for Tuttle's comet of 1862, Vorontso Velyaminov calculated a mass of 5×10^{16} g from t Perseids.

Liller (1960) has made a very significant determi tion of the rate at which fine dust is lost by Come Arend-Roland (1956 *h*) and Mrkos (1957 *d*). From t colors, polarizations, brightnesses, and configurati changes of the particulate tails, he deduces, respectivel 5×10^{16} and 7×10^{17} g as the total initial masses fine dust for these comets, in the general "class" Halley's comet. These estimates can be compared wi those based on gases, the zodiacal cloud, and meteor streams, as shown in Table I. The agreement is fair satisfactory, considering the gross uncertainty in th basic data and assumptions. Furthermore, these est mates all concern specifically different cometary mat rial. We conclude that a typical, minimum value f the total mass of a new large comet is the order of 10 g and may easily be 10^{19} g. The corresponding spheric radii, for density 1.3 g/cm^3, are respectively 3.1 an 14.6 km. These values are in good agreement with th present estimate of 15 km for the maximum radius Halley's comet, based on observed magnitude at grea solar distances and on the assumption of a very lo albedo, and with the broad expectations of the ic comet model.

DIFFICULTIES WITH THE "SAND-BANK" COMET MODE

Gas Content

No diffuse sand-bank type or comet model yet pro posed can provide the calculated large ratios of gas t teoritic material. Suppose that the amount of meteor- material is grossly underestimated, or that the eous losses are grossly overestimated. If the meteor- loss in one period from a large comet, such as lley's, is assumed to be the order of a thousand times ater than 10^{16} g/rev the comet's minimum radius n becomes 15 km, comparable to the value from ghtness-albedo determinations at great solar dis- ces. Since the comet must then be effectively a single dy, we have already abandoned the diffuse sand-bank pothesis in making the assumption of such a large ss.

The gas-to-dust ratio in observed large comets ef- tively eliminates the diffuse sand-bank hypothesis the cometary nucleus, unless the gaseous loss has been erestimated by a factor of at least 100. In this case, e hypothesis can be sustained only on the basis that e meteoritic material is highly absorptive of the gases volved, the order of 0.001 to 0.1% of the meteoritic ass.

Meteoritic Masses in Comets

For the minimum dimensions of individual particles the diffuse sand-bank hypothesis, let us take the esent mass of Halley's comet as one-tenth its initial ass, or 10^{17} g, and the density of particles as 3.5 g/cm^3. e then find that the average radius of the particles for comet with an apparent effective area corresponding a 20-km radius sphere, as observed, is 20 m. Such a nclusion as to the size of particles in the sand-bank odel presents no major difficulty, except in the Lyttle- n version, which "is wholly constituted of small dust articles."

Motions in Comets

Plummer (1906) has shown that on the sand-bank odel the secular reduction in period of Encke's comet annot be explained by the Poynting-Robertson effect ecause the relative changes in the elements e and a re not consistent with expectation. Furthermore, cer- ain comets show increases in their periods instead of he shortening observed for Comet Encke, e.g., Comet Volf I, Comet D'Arrest, Comet Pons Winnecke, and ossibly even Halley's comet. No process that solely educes angular momentum, such as the action of a esisting medium or the Poynting-Robertson type ffects can be invoked to explain *both* decreases and in- reases in cometary periods. We can conclude, therefore, that the observed secular changes in the periods of comets have not yet been adequately explained on the sand-bank model. The writer doubts that an explanation can be found.

The existence of negative period changes in comets is also attested by the number of comets and meteor streams with orbits lying entirely within Jupiter's orbit. Perturbations by the planets could not so reduce the aphelion distances for so many objects in the short periods of time available.

The icy model allows for period changes in rotating comets by jet action of the sublimating gas normal to the radius vector. Delays in heat transfer, expected for nucleus surfaces containing meteoritic material, lead to the observed period changes if reasonable physical assumptions and masses are accepted. The required radii of the nuclei are the order of 1 to 10 km, which also allow adequate lifetimes for larger comets.

Hamid and Whipple (1953) have reanalyzed the definitive orbits for 64 long-period comets to derive a weighted mean reduction in effective solar gravity of $\delta k^2/k^2 = -0.53(\pm 0.10 \text{ m.e.}) \times 10^{-5}$. If the effective solar gravity is not to be reduced by a factor of more than -0.53×10^{-5} by solar radiation pressure, the radius of the particles must be of the order of centimeters or greater for densities applying to ordinary stony or metallic particles.

For the sun-grazing comet, 1882 II, the derived value of $\delta k^2/k^2$ is $-0.7(\pm 2.1 \text{ m.e.}) \times 10^{-5}$. If we adopt three times the mean error as an acceptable limit in $\delta k^2/k^2$, the particle dimensions must have been the order of a centimeter or the effect of solar gravity would have been greater than that observed.

We must conclude, therefore, from the motions of comets that (a) the sand-bank hypothesis has not and probably cannot account for the observed secular changes in cometary periods, and (b) that the effective action of solar gravity indicates that the particles in comets probably average at least a centimeter in dimension. The first of these conclusions violates the diffuse sand-bank model. Both conclusions violate the Lyttleton sand bank as he has proposed it.

Sun-Grazing Comets

Russell (1926) has shown that for the great sun-grazing comet, 1882 II, with perihelion passage less than one solar radius of the sun's surface, solar radiation would have vaporized individual particles up to 30 cm in diameter. Lyttleton (1953) admits that such a comet constructed on his model would have vaporized completely. He adopts a temperature of 2000°K which, for a mean molecular weight of 50, leads to a gaseous thermal velocity of about 1 km/sec. He suggests that because this velocity is so small in comparison to the linear velocity of the comet, some 500 km/sec, "any tendency of the gaseous material to expand because of its high temperature would lead only to a small divergence away from the standard orbit, measured by an angle of the order of 2×10^{-3} radian." He then presents calculations by Hoyle to show that recondensation would occur after the solar passage at a linear rate of 10^{-4} cm/hr.

This argument leads to two major difficulties: (a) expansion of the gas along the orbital path, and (b) the effect of light pressure on the small particles while they are in the process of growth. The change in velocity ΔV required to increase the semimajor axis of the comet from the initial value of $a = 83.4$ a.u. to parabolic, if applied along the orbit of the comet is 111 cm/sec. Almost half the material would attain an orbital velocity in the positive sense exceeding the parabolic and all but about 2% remaining would likewise receive an equal velocity change in the negative sense along the orbit, for which the reduced semimajor axis would be less than one-half the original. Thus, on Lyttleton's hypothesis not more than 1 or 2% of the comet could be available for condensation in approximately the original orbit.

If we accept the condensation process assumed by Lyttleton, we see that the particles grew for 50 days with diameters less than 10^{-2} cm. It is quite obvious that these particles would have been moved into hyperbolic orbits while moving under a reduced gravitational attraction caused by light pressure.

There can be no alternative to the argument that the processes suggested by Lyttleton would actually transform his entire sun-grazing comet to the state normally associated with the extended coma and tail of a comet; here the material has been removed completely from the "sphere" of cometary attraction or motion.

The great comet of 1882 II is one of a group of six comets with extremely small perihelion passages and comparable periods, strong evidence that a parent comet survived such a close perihelion passage at least once in the past, and had split up into a number of components that also endured. No "sand-bank" comet could survive such an experience unless the particles composing it were originally at least meters in diameter.

Brightness Variations of Comets

In general the great bursts in brightness are extremely difficult to explain in terms of a "sand-bank" model and appear to require some further, but not necessarily difficult, development of the icy comet model. The regular brightness variations of "old" and "new" appear to contradict expectations for the "sand-bank" model, while other observed properties of the two classes of comets are more or less possible with both models.

The several limitations or difficulties outlined above are definite contradictions to the Lyttleton version of the "sand-bank" model. If one assumes the icy comet model, none of these difficulties appear, except possibly the large cometary bursts in brightness at great solar distances.

The compact "sand-bank" model encounters most of the difficulties of the diffuse model. There is real difficulty in obtaining the required gas-to-dust ratio unless the particles are assumed to be extraordinarily small, or endowed with great gas-containing capacity, or unless we have greatly overestimated the gas-to-dust ratio. Cometary period changes would remain unexplained as would the observed brightness variations generally.

In the author's opinion, following Schatzman's (1953) calculations, a compact "sand-bank" model would eventually become a single structure, the adjacent ticles tending to adhere. Although the structure m never become strong, the nucleus would lose gas tremely slowly after a few solar passages and would, be recognized as a comet. Such nuclei with extren small perihelion distances might act as observed. In case of the asteroid Hidalgo we do observe a truly con ary type of orbit without cometary activity.

Certain characteristics of a cometary nucleus developed below, on the assumption that the nucl is of an icy character with embedded solids of meteor character.

A COMETARY NUCLEUS REQUIRED TO WITHSTAND TIDAL DISRUPTION

What strength of materials in the icy nucleus required to prevent tidal distortion and breakage fo comet such as 1882 II, with an extremely small pe helion distance? Calculations show that the nuclei such comets may possess maximum dimensions of te of kilometers if their internal tensile strength is typi of dirty (H_2O) ice near the freezing point, the order 10^6 to 10^7 dynes/cm^2. Large deviations from spherici could reduce the maximum allowed dimension becau bending forces might be introduced.

ON THE DISAPPEARANCE AND SPLITTING OF COMETS

Mokhnach (1956) has criticized the icy comet mod on the grounds that in disruption a great deal of crus ing of the ices in the nucleus should result in an ou pouring of material and an unobserved enormous burs in luminosity. In the case of a breaking nucleus on must postulate the detailed nature of the breakup before he can draw conclusions as to whether or not a cometary burst should occur. If the nucleus breaks becaus of rapid rotation induced, for example, by the pinwheel-rocket effect, then one should agree with Mokhnach that a large area of new surface should be exposed producing a burst to accompany the splitting of th nucleus.

On the other hand, if one assumes that an irregularly shaped cometary nucleus sublimates away (like an irregular iceberg melting) and splits under a relatively slow rate of rotation, I can see no need for a burst and brightening to accompany the splitting.

In the case of the sun-grazing Comet 1882 II a large quantity of material certainly constituted the luminous "thread" and temporary "beads" after perihelion passage.

COMETARY BURSTS

No adequate theory of cometary bursts has yet been presented. The general concept of collisions between asteroidal-type bodies and cometary nuclei is a rather *ad hoc* type of explanation, and highly improbable. The minimum amount of material required for the Schwassman-Wachmann outbursts is not enormous, the er of 10^4 tons of fine dust. Whitney (1955) has shown t the amount of solar energy that the comet reves between bursts would be quite adequate to duce the effect. He suggests some storing mecham, perhaps a "boiler" type of outburst.

Haser (1955, 1956) has suggested that free radicals h as *OH*, *CN*, etc., imprisoned in crystals such as O, NH_3 and CH_4 or in solid hydrates, might provide e energy for cometary bursts. Donn and Urey (1956) ilarly have suggested that free radicals (originally luded by the writer in the icy comet model) might triggered by corpuscular radiation, by solar far raviolet or by some other form of high-voltage ergy. More recently they have withdrawn this exanation and suggest the possibility that relatively able molecules such as acetylene ($CH{:}CH$) might mbine with other molecules or atoms of the nucleus to ovide considerable explosive energy.

A possible explanation for cometary outbursts may llow from the icy model without the assumption of ee energy in the ices, if the original deposition of atter in the nucleus is taken to be highly irregular.

Also, nonradial forces from sublimating material may sily arise in a cometary nucleus, producing great anges in angular rotation, the "pin-wheel" effect. onfigurations can easily be visualized in which the ntrifugal force established by such a pin-wheel type force could detach a large or small volume by a masve rupture.

Thus it is not clear whether the basic principles of e icy model need the addition of novel hypotheses to ccount for cometary outbursts.

SOME PROPERTIES OF COMETARY MATERIALS

Delsemme and Swings (1952) have made a very mportant contribution to an understanding of the icy omet nucleus by their concept that solid hydrates uch as CH_4+6H_2O may occur in some quantity. The roblem of the enormous differences in vapor pressure etween CH_4 and H_2O is thus resolved in normal comet ctivity. Also, the restriction of an extraordinarily low emperature required in comet formation to solidify CH_4 is relieved.

The general and fundamental problems of the precise hemical and physical structure of an icy comet nucleus re too complex and too little understood for proper reatment at present. In previous papers (1950, 1951, 1955) the author has discussed some physical and chemical aspects of the icy comet model and will not repeat hese discussions and calculations here.

One point is of considerable interest; the photographic meteor studies at Harvard have thrown considerable ight on the nature of cometary solids. McCrosky (1955), for example, finds that many meteoroids are so weak structurally that they crush at a dynamic pressure of 0.02 atm. Also it is clear that photographic meteoroids show an enormous range in character. Jacchia's (1956, 1958) work distinguishes between fragmentation or fragility of meteoroids, on the one hand, and a function of density and luminous efficiency on the other. Each meteor stream, representing an individual comet, shows individual characteristics which differ from stream to stream. Statistically averaged, the characteristics of stream meteors are like those of the sporadic meteors, practically all of cometary origin (Jacchia and Whipple 1960).

The Taurid meteoroids, originating in Encke's comet, are relatively rigid structures, showing practically no fragmentation but possessing average mass-luminosity properties. Also, there are many Taurid fireballs, showing that fairly large structures have survived. Encke's comet must have once been a *very* large comet, for it is known to have contributed huge streams of meteors of which only a few are now observable (Whipple 1940). Hence, we are observing material from the central part of a very "old" comet, in the Oort sense.

The Giacobini-Zinner comet, on the other hand, appears to be small and probably "new." Its meteoroids are featherlike, both extremely fragile and probably of surprisingly low mean density ($\sim$0.01 g/cm^3).

The Geminid meteoroids, of unknown cometary parentage, are of average strength but appear to be extraordinarily dense (or of very high luminous efficiency). Their continued existence with a perihelion distance of only 0.14 a.u. must be related to their high density. Possibly the parent comet was quite large; else how could it have had time to attain such a rare orbit with aphelion distance only 2.6 a.u.? Since large perturbations by the terrestrial planets are unlikely, the aphelion must have been reduced by systematic period shortening, a slow process.

The meteoric data suggest that the centers of "old" comets, in the Oort sense, spew out large and rigid or relatively dense meteoroids, while small comets or the surfaces of "new" comets emit feathery material, weak and of low density. The spectra of comets complement the picture. "Old" comets show primarily the spectra of gases and "new" comets the spectra of scattered sunlight (Oort and Schmidt 1950). Thus the meteoritic material near the centers of "old" comets must generally cohere, so that fine dust is rare, while the unconsolidated dust in small comets and near the surface of "new" comets predominates over the gases in producing light.

The conspicuous occurrence of C_3 molecules in comets with gaseous spectra (Rosen and Swings 1953; Swings, Fehrenbach and Woszczyk 1957) adds an interesting piece to the jigsaw puzzle of cometary nuclei. Can carbon be the first material to condense in a cooling hot cloud of gas, and therefore be more prevalent in centers of the large comets? Or is the carbon in small comets in the form of dust, so that it does not radiate as a molecule? Some important chemical process must be indicated, but what?

An enormous, if not definitive, insight concerning the nucleus and the evolutionary problems of comets could be gained by a space probe made to land on a cometary nucleus. Cores of the nucleus should be stratified like geological sedimentary strata and should give the oldest and least disturbed material record of ancient processes.

The writer wishes especially to thank Karl Wurm and William Liller for their kindness in providing manuscripts of their important articles on comets prior to publication.

REFERENCES

Allen, W. C. 1947, *Monthly Notices Roy. Astron. Soc.* **106**, 137.
Delsemme, A. and Swings, P. 1952, *Ann. d'Astrophys.* **15**, 1–6.
Donn, B. and Urey, H. C. 1956, *Astrophys. J.* **123**, 339.
Hamid, S. E. and Whipple, 1955, *Astron. J.* **58**, 100.
Haser, L. 1955, *Compt. rend.* **241**, 742.
——. 1956, *Bull. acad. sci. Belg.* **42**, 813.
Jacchia, L. 1956, *Astron. J.* **61**, 6; private communication.
——. 1958, *Smithsonian Contrib. Astrophys.* **2**, 181.
Jacchia, L. and Whipple, F. L. 1960, *ibid.* (to be published).
Levin, B. J. 1943, *Russ. Astron. J.* **21**, 48.
——. 1949, *Prirada* No. 10, p. 3.
——. 1957, *Colloq. at Jena.*
Liller, W. 1960, *Astrophys. J.* (to be published).
Lyttleton, R. A. 1953, *Comets and Their Origin* (Cambridge University Press, New York).
McCrosky, R. E. 1955, *Astron. J.* **60**, 170.
Oort, J. H. and Schmidt, M. 1950, *Bull. Astron. Inst. Neth.* **11**, 258.
Rosen, B. and Swings, P. 1953, *Ann. d'Astrophys.* **16**, 82.
Russell, H. N. 1926, *Astronomy* (Ginn and Company, Boston, Massachusetts), Vol. I.
Schatzman, E. 1953, *Physique des Comètes*, Liége Colloque, Louvain, Belgium, p. 313.
Swings, P., Fehrenbach, C., and Woszczyk, A. 1957, *Compt. rend.* **245**, 2152–55.
Van de Hulst, H. C. 1947, *Astrophys. J.* **105**, 471.
Vorontsov-Velyaminov, B. 1946, *ibid.* **104**, 226.
Whipple, F. L. *Proc. Am. Phil. Soc.* **83**, 711.
——. 1950, *Astrophys. J.* **111**, 375, 1952, *ibid.* **113**, 464; 1955, *ibid.* **121**, 750.
Whitney, 1955, *ibid.* **122**, 190.
Wurm, K. 1943, *Mitt. Hamburg Stern. Bergedorf* **15**, 57.

DISCUSSION

——: I am surprised that Whipple has been able to obtain an upper limit to the size of a comet passing close to the sun as a result of perturbations, because this is a case of Roche's limit, which depends on the ratio of the density relative to the size of the body and to the integrated density in a sphere surrounding the perturbing body and passing through the center of the comet. That is, one would expect to derive, not an upper limit to the radius, but an upper or lower limit to the density.

WHIPPLE: The icy-conglomerate idea was partly to give enough internal strength to support the body. If forced to depend on gravity alone this kind of nucleus might not survive. Whether or not the density were below the Roche limit, cracks could cause destruction.

ÖPIK: When comets have grazed the sun, disrup by tidal force is very simply illustrated. Distrib the mass of the sun over a sphere equal to the dista of a comet; this density must be $\frac{1}{2}$ or less than tha the comet nucleus for the nucleus to hold together gravitation. But not a single comet has been obser to hold itself together by gravitation under this con tion, hence to have high density.

DONN: I think Whipple has left out one great vantage of his icy-conglomerate model, in that one make calculations and predictions of what one wo expect to happen and do laboratory work on the str ture of the nucleus. A basic difficulty concerning sand-bank theory is that if small grains once evapor when close to the sun it is questionable whether th could ever recondense, because the density is so l that some of the recombination mechanisms are ve likely not active. It may be interesting to calcula what would happen in the center of a comet like Enck starting off with a density reasonable for an icy n cleus. When you build up to about 10-km radius t internal pressure gets high enough that you sta crushing the low-density snow (in this connection the are estimates on the packing of snow in glacier Beyond 10-km radius the density would increase to value of a few tenths, and then there would be chang due to heating effects also. The preliminary calculatio are reasonable; one can go farther with such calculatio and also carry out experiments. I hope to do this.

——: Is there a perfectly simple mechanism fo changing the periods because the individual plane are in different positions at each perihelion passag so one could see how one could get changes in angula momentum and energy, and perhaps an estimate of ho many would be thrown out of the solar system, an how many would be captured by Jupiter?

WHIPPLE: That, of course, is the basis of thinking b Russell, and Newton also, and Oort takes this int account. But does the period change after one ha taken all the known perturbations into account, a Miss Roemer queried? This needs further investigation

——: Suppose comets originally have gravel-bank structure. Would not the particles in that gravel bank go "through" one another? Would they not eventually kill their kinetic energy and cluster in a compact body with the pieces all touching each other?

WHIPPLE: Schatzmann looked into that in 1953. If the dispersion is too great the time is too long. But it depends on the starting assumptions whether it will happen: I rather think it will.

E ASTRONOMICAL JOURNAL VOLUME 66, NUMBER 8 OCTOBER, 1961

The Survival of Comets and Cometary Material*

ERNST J. ÖPIK†
Department of Physics, University of Maryland

ORMULAS for the probability of collision and orbital change in close encounters with the planets pik 1951) are further developed, auxiliary tables culated, and the theory applied to comets and aster- lal populations.

The probabilities depend on the relative velocity nponents of the particle (comet, asteroid, meteorite) en crossing (not necessarily intersecting) the orbit the planet. Crossing is defined as equality of the liocentric distances. Secular variation of node and rihelion lead repeatedly to intersection. In a Jacobian me rotating with the planet (in circular orbit), the locity components, in units of the planet's orbital locity, are then

$$U_x=\pm[2-A(1-e^2)-A^{-1}]^{\frac{1}{2}} \qquad (1)$$

adial),

$$U_y=+[A(1-e^2)]^{\frac{1}{2}}\cos i-1 \qquad (2)$$

ransversal in plane of planet),

$$U_z=\pm[A(1-e^2)]^{\frac{1}{2}}\sin i \qquad (3)$$

ransversal and normal to the plane),

$$U=\{3-2[A(1-e^2)]^{\frac{1}{2}}\cos i-A^{-1}\}^{\frac{1}{2}} \qquad (4)$$

otal relative velocity vector).

Here A is the semimajor axis of particle, in units of e planet's heliocentric distance, e the eccentricity, d i the average inclination of particle's orbit to that the planet.

The mathematical expectation per orbital revolution the particle, to be called "probability," of an event ith cross section πs^2 is

$$p=s^2U/(\pi|U_x|\sin i), \qquad (5)$$

here s is the target radius.

For physical collisions

$$s=S=R[1+2\mu/(U^2R)]^{\frac{1}{2}}, \qquad (6)$$

here μ is the planet's mass in solar units, and R the lanet's radius.

For 90° average accumulated angular deflection in epeated encounters

$$s=\sigma=\{B\ln[(D^2+B)/(R^2+B)]\}^{\frac{1}{2}}, \qquad (7)$$

here

$$B=16\mu^2/(\pi^2U^4) \qquad (8)$$

nd

$$D=(\tfrac{1}{2}\mu)^{\frac{1}{3}}. \qquad (9)$$

$\pi\sigma^2$ is the cross section for achieving isotropic distribution of the direction of the U vector.

Modifications for an eccentric orbit of the planet are also used.

The angular deflections define the rate of orbital change and elimination by ejection to infinity or to a crossing with a larger planet.

Table I gives some results of the calculations. Objects crossing Jupiter's orbit are chiefly eliminated by orbital change and ejection, and have a relatively short lifetime. Those confined to the region of the terrestrial planets are long-lived, especially those crossing the orbit of Mars alone, and are chiefly eliminated by physical collision. The Mars asteroids have lifetimes greater than the age of the solar system and represent about 50% of their original population. The other groups consist of transient objects, their present number depending upon the balance between elimination and supply from other sources.

As distinct from physical disintegration, the survival time scale of not too small solid remnants of a comet depends solely on the orbital elements and is found to be very much longer than estimated time scales of apparent disintegration. It is suggested that residual nuclei of some dead comets are not dissolved into meteors but survive as asteroids until they are removed by collisions and orbital change.

Comets could not have condensed during the lifetime of the solar system in the region of 50 000–150 000 a.u.; Oort's hypothesis of their origin as asteroids ejected from the inner portions of the solar system can be accepted. The genetic link between the two classes of objects implies that two main ingredients of their material may occur in both, although in different proportions: I, Whipple's icy conglomerate; II, compact meteoritic material. The second is especially capable of survival.

Three contemporary populations of stray bodies are compared and their balance of exchange and decay estimated: (1) group M, the asteroids crossing the orbit of Mars; (2) group A, the Apollo-type asteroids crossing the orbit of the earth and other terrestrial planets; (3) group C, the comets. Group A, of an average lifetime of 10^8 years, cannot have well existed from the beginning and must be currently replenished; cumulative perturbations by Mars on group M, lifetime 6×10^9 years, can supply only a fraction of the loss, the rest being apparently furnished by extinct comet nuclei. A two-stage supply, first through capture by Jupiter, then through perturbations by the terrestrial planets in close encounters, appears to be sufficient to feed into the space inside Jupiter's orbit a number of objects, equal to the number of same size lost by the Apollo group. The main supply comes from comets whose aphelia are close to Jupiter's orbit.

The statistical estimates agree as to the order of mag-

---

* Supported by a grant from the National Aeronautics and Space Administration.

† On leave from Armagh Observatory, Northern Ireland.

TABLE I. Dynamical elimination probabilities and life expectations of crossing objects. J, relative probabilities of eliminati J_c, by collision; J_∞, by ejection; J_J, by deflection to Jupiter crossing; J_E, by deflection to earth crossing.

Object	Comet 1939 IV Väisälä	Comet Giacobini-Zinner (Giacobinids)	Comet 1866 I Tempel (Leonids)	Comet Ha (η Aqua Orionid
Crossings	Jupiter only	Jupiter-earth	earth-Uranus	Venus-Ne
Lifetime, 10^6 yr	0.34	0.50	14.0	38.
J_c	0.026	0.028	0.062	0.061
J_∞	0.974	0.972	0.938	0.939

Object	Comet 1862 III Tuttle (Perseids)	Comet 1942 II Väisälä	Comet Encke (Taurids)	Geminids
Crossings	earth-Neptune	Jupiter-Neptune	Mercury-Mars	Mercury-M
Lifetime, 10^6 yr	162.	37.	265.	245.
J_c	0.057	0.036	0.975	0.98
J_∞	0.943	0.964	...	...
J_J	...	...	0.025	0.01

Object or group	Apollo	Hermes	Icarus	Geographos (1951 RA)	Apollo group average (8 objects)	Mars aste average (34 obje
Crossings	Venus-Mars	Venus-Mars	Mercury-Mars	earth-Mars	Mercury-Mars	Mars only
Lifetime, 10^6 yr	64.	39.	165.	152.	102.	6450.
J_c	0.884	0.926	0.976	0.781	0.871	0.79
J_J	0.116	0.074	0.024	0.219	0.129	...
J_E	...	...	...	...	...	0.20

nitude if asteroid diameters (d, km) are calculated with lunar albedo,

$$\log d = 3.63 + \log r\Delta - 0.2m, \tag{10}$$

where m is the apparent magnitude reduced to full phase, r the heliocentric, and Δ the geocentric distance in a.u., and those of comet nuclei from a formula based on two observed cases,

$$\log d = 2.18 - 0.2m_0, \tag{11}$$

where m_0 is the integrated magnitude reduced to $r=1$, $\Delta=1$ and a 3-inch telescope (Bobrovnikoff-Schmidt reduction). As an independent check, the same formulas yield the correct predicted number of meteor craters in the lunar Mare Imbrium (Öpik 1960).

REFERENCES

Öpik, E. J. 1951. *Proc. Roy. Irish Acad.* **A54**, 165; *Armagh Obs. Contrib.* No. 6.

——. 1960, *Monthly Notices Roy. Astron. Soc.* **120**, 404.

DISCUSSION

WHIPPLE: I have a question for Dr. Öpik about the Apollo group of asteroids. Of those that have been observed, I believe that five out of seven or four out seven are highly selected objects; they're the ones which the motion is such that when they come near earth their angular velocity across the sky is rat small—in meteor terms their elongation is near 90°. is quite possible that the probability of encounter w those asteroids would be higher: In other words, havi this motion the perturbations by the earth will act mo on them than on the others. I wonder whether calcu tions might be carried out for the unknown remaind (at least the two or three others that don't come in this category); perhaps most of the ones not observ are in the second category, and do not have this pro erty. It might be that the probability will fit in bett with the observations on the Mars asteroids.

ÖPIK: Of course. One group needs 39 68 million yea Apollo 64 million years (there are three or four of thes and the others fall nearer Comet Encke with times about 150 to 200 million years. In the probability discovery I allowed for the relative disproportion o the photographic plate, so that the photograph impression is not inversely proportional to the squa but roughly to the first power of the distance from th earth.

ASTRONOMICAL JOURNAL VOLUME 66, NUMBER 8 OCTOBER, 1961

New Investigations on the C_3 Spectrum at 4050 A

B. Rosen
Astrophysical Institute of the University of Liége and National Research Council, Ottawa, Canada

URING the last few years, the team at the Astrophysical Institute of the University of Liége succeeded in obtaining a number of high-dispersion tra of some relatively bright comets, which show articular the structure of the *CH*, *NH*, *CN*, and ands with considerably more detail than on pre- sly reported spectrograms. Owing to the weakness he underlying continuum, the spectrum of the comet nham (1959 *k*) was particularly appropriate for a ise determination of the position of as many as 55 ssion features in the 4050 cometary system of C_3. wever, even the new high-dispersion spectra are not icient to attempt a classification of the 4050 group, in a forthcoming paper giving details of their ob- vations, Swings, Fehrenbach, Dossin, and Haser 61) stress the need of new laboratory investigations cerning the C_3 bands.

t is well known that the cometary bands of C_3 are ily excited in different kinds of laboratory sources that the main 4050 A band, which undoubtedly ongs to the (0,0) transition, has been studied under h resolution and analyzed by Douglas (Douglas 1; Clusius and Douglas 1954) at Ottawa. The rota- nal analysis combined with isotopic substitution has ealed that the C_3 molecule is linear in both states some molecular constants have been obtained. But rotational analysis of the whole system is far from ng complete and all attempts to achieve a vibrational alysis have been so far completely unsuccessful; in t, in the whole region between 3800–4200 A, con- ning in laboratory emission spectra many thousands lines, regular rotational structure can be observed only in the (0,0) band itself and even the position of other band heads have been differently reported by various authors and do not always coincide with reported cometary features.

A few years ago, G. Herzberg observed that the strongest cometary band at 4050 A appeared in absorption after flash photolysis of diazomethane. The best conditions for the development of this absorption have been quite recently carefully studied by Herzberg and Shoosmith, and excellent spectrograms with very high dispersion (about 0.3 A/mm) were obtained a few weeks ago. All the cometary features are clearly recognizable in the absorption spectrum and the intensity distribution is very similar in both kinds of spectra. Regular rotational structure is seen not only in the main band but also in several other bands; the analysis is now under way. The complete vibrational and rotational analysis of the whole system will take a long time. In fact, there are definite indications of complications due to vibronic interaction and to Fermi resonance. The only (preliminary) result obtained up to now concerns the ν_1' frequency, which can be evaluated to about 890 cm^{-1}. But we hope that the available laboratory spectra will be adequate for a complete analysis and might give, together with new high-dispersion cometary spectra, a useful contribution to cometary physics.

REFERENCES

Clusius, K. and Douglas, A. E. 1954, *Can. J. Phys.* **32,** 319.
Douglas, A. E. 1951, *Astrophys. J.* **114**, 466.
Swings, P., Fehrenbach, Ch., Dossin, F., and Haser, L. 1961, *Ann. d'Astrophys.* (to be published).

THE ASTRONOMICAL JOURNAL VOLUME 66, NUMBER 8 OCTOBER, 19

The Distribution of Stars in the Sculptor Dwarf Galaxy

PAUL W. HODGE*
Mount Wilson and Palomar Observatories, Carnegie Institution of Washington, and California Institute of Technology

(Received July 5, 1961)

Star counts on six Schmidt plates, covering the Sculptor dwarf galaxy and the surrounding area, provide information on the distribution of the brightest stars in the system. Equidensity contours drawn from the counts are smooth ellipses with ellipticity 0.35. Density profiles along the major axis do not agree with Hubble's or de Vaucouleurs' interpolation formulas for luminosity profiles of giant ellipticals. The size of the Sculptor system as observed agrees well with the computed tidally limited size caused by the attraction of our Galaxy on its outer stars.

I. INTRODUCTION

THE distribution of luminosity across giant elliptical galaxies has been given a great deal of attention (most recently by Mrs. Liller 1960). Similarly the distribution of light and stars in globular clusters is being studied in detail (King, in preparation). The present paper is one of a series which examines the distribution of luminosity with radius for objects intermediate in their characteristics between the giant ellipticals and the globular clusters, namely, the dwarf elliptical galaxies.

The first paper (Hodge 1961) examined the structure of the Fornax dwarf galaxy by means of star counts, the surface brightness of the object being far too low for the standard photoelectric or photographic methods of measurement. The present paper gives the results of study of a similarly faint and extended object, the Sculptor dwarf elliptical.

Since Shapley's discovery of the Sculptor dwarf (Shapley 1938, 1939), relatively little has been published about its characteristics. Baade and Hubble (1939) used the 100-inch telescope to confirm Shapley's conclusion that the Sculptor system resembled an enlarged globular cluster by their discovery of RR Lyrae variables in it. Later Thackeray (1950) obtained an important and extensive series of plates from which he was able to determine periods and light curve characteristics for a number of the variables.

In his announcement of the discovery of the Sculptor system, Shapley (1938) tabulated the results of star counts on the discovery plate. The writer has extended Shapley's studies by means of star counts on six new plates. These have provided fairly complete data on the stellar distribution, which may now be compared with those for other dwarf ellipticals and for giant galaxies.

II. OBSERVATIONAL MATERIAL

The six plates used for the present study were obtained with the ADH Baker-Schmidt telescope at the Boyden Observatory, South Africa. The Schmidt correcting plate was diaphragmed to 24 inches to avoid vignetting. Three of the plates were exposed on 103a emulsion behind a GG-11 filter and three on 103a emulsion behind a GG-13 filter; the color system equivalent to V and B of the UBV system.

The exposures represent a range in magnitude lim exact magnitudes are not available, but it can be es mated that the deepest plate, ADH 5059, reach approximately $B=19.1$. This estimate is based on t fact that at the limit of the plate lie several of t variables identified by Baade and Hubble (1939); th estimate of the mean magnitudes of these objects maximum is 19.12 (pg).

A 2.5-mm grid was used for counting all stars in area of 2.2 square degrees, centered on the Sculpt system. The grid was oriented NS and EW, ve nearly parallel with the axes of the object (s below). Each plate was counted at one sitting so th uniformity would be maintained. The plates we counted to the limiting magnitude and each w counted once. From experience with similar star coun made on the Fornax dwarf elliptical, it was decid that the reproducibility of counts on a particular pla is greater than from plate to plate, so that it is bett to count many plates each once than one plate man times.

In the richest portion of the galaxy the star densi on the deepest plate, ADH 5059, reaches a maximu value of eight stars per square minute of arc. The imag diameter on this plate is less than 0.05 mm=0.06 thus the probability of a star being obscured by anoth on this plate is very small, of the order of 0.02. We ca conclude that saturation of images, as found on one the plates used for the Fornax galaxy (Hodge 196 does not occur in the present material.

TABLE I. Observational data.

Plate No.	Color	Exposure (minutes)	Stars counted Total	Stars counted Members of Sculptor	Foregroun (stars per □′)
5109	V	10	2281	254	0.28
5088	V	20	2878	565	0.31
5111	V	30	2737	509	0.31
5058	B	60	3350	882	0.34
5061	B	60	3676	1104	0.35
5059	B	60	4630	1529	0.42

---

* National Science Foundation Postdoctoral Fellow, 1960–61. Present address: Berkley Astronomical Department, University of California.

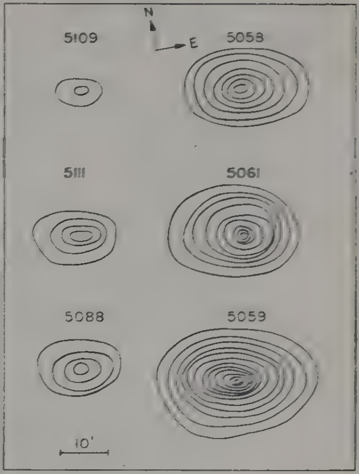

Fig. 1. Equidensity contours drawn from the star counts. The outer contour line represents a projected density of 1.5 stars per square minute of arc. The contour interval is 0.6 star.

Table I lists the plates used and the total numbers stars counted on each. The number given there for total number of the member stars of Sculptor was tained by subtracting the expected numbers of back- ound stars, as determined from surrounding more tant areas, from the number counted within the area the galaxy itself. As pointed out below, the Sculptor stem has a definite limiting radius where the star nsity reaches zero; for this reason the number of inted members for each plate could be obtained ambiguously.

DISTRIBUTION OF STARS

Lines of Equidensity

Contour diagrams illustrating the counts for each ate in the form of equidensity lines are given in Fig. 1. ch was constructed directly from the recorded counts enveloping within a particular curve the squares with particular count, in steps of five stars per counting uare. The contours plotted in Fig. 1 include the reground stars in their counts. The outer equidensity e is in each case that for 12 stars per counting square .5 stars per square minute of arc), and the contour terval is five stars per counting square (0.6 stars per uare minute of arc).

The diagrams in Fig. 1 were used to determine the neral properties of the shape of the system: orient- tion, ellipticity, and symmetry. The actual profiles of ellar density and subsequent analysis are based rectly on the counts.

Isophotes

It would be of considerable interest to have an sophotal diagram of the Sculptor system so as to be le to compare its properties with those of galaxies r which luminosity density is directly observable. It possible to artificially construct such a diagram if the sumption is made that the luminosity function of the ulptor system is similar to that of M3. We know from apley's (1938) work that this is probably true, at ast for the top 1.5 mag. (pg). Similarly, Baade and Miss wope (1961) find that the top of the luminosity func- on of the Draco dwarf system also resembles that of 3. The fact that Baum (1959) finds that dwarf ellip- cals (unlike giants) have integrated colors similar to ose of globular clusters is further evidence that the art of the luminosity function responsible for most of e light is probably similar to the normal globular uster luminosity function.

To convert star densities into isophotes, it is necessary know what fraction of the total luminosity of the stem is contributed by the unresolved stars in the stem. For this purpose, we can use Sandage's (1954) mputation of the fractional light for stars at M_{pv} and righter in M3. The depth of the counts in Sculptor on late ADH 5088, the deepest visual plate, is approximately 1.6 mag., as judged from photoelectric sequences on similarly exposed ADH plates. Thus the counts reach $M_{\mathrm{pv}}\approx -1.4$, and the counted stars account for 0.28 of the total light of the system, if our assumptions are correct.

Figure 2 shows the artificially constructed isophotal map of the Sculptor system, based on the star counts on plate ADH 5088 (smoothed) and Sandage's luminosity function. The map indicates that in visual light the luminosity density at the center of the system reaches 23.9 mag. per square second, while at a distance of 30′ from the center along the major axis this value has dropped to 27.7 mag. per square second.

Ellipticity

The ellipticity of the Sculptor system, defined by

$$\epsilon = 1 - b/a, \tag{1}$$

has been derived by measuring it for all curves in the raw isodensity diagrams. The mean value for all 39

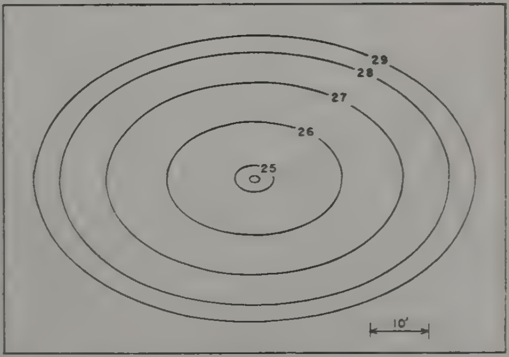

Fig. 2. Artificially constructed isophotal map of Sculptor, based on assumptions of a globular-cluster-like luminosity function, invariant across the galaxy. Contours are labeled in units of magnitudes per square second.

TABLE II. Profiles along the major axis.[a]

	5111		5109		5088		5061		5059		5058
r	*E*	*W*	*E*	*W*	*E*	*W*	*E*	*W*	*E*	*W*	*E*
0	25.0	25.0	10.8	10.8	22.2	22.2	40.2	40.2	64.0	64.0	36.0
3	16.0	21.0	10.6	7.3	20.0	20.5	36.0	37.7	54.0	45.5	33.2
6	8.5	18.2	10.0	7.0	19.8	16.5	33.1	27.9	40.2	38.3	24.7
9	7.2	15.2	9.3	5.7	8.0	11.8	18.0	25.0	26.5	32.5	11.7
12	5.5	12.3	4.3	5.0	5.8	10.5	11.3	18.1	23.5	21.7	9.0
15	4.8	9.2	7.3	2.8	8.5	4.0	8.0	13.3	18.0	17.0	11.0
18	3.0	3.5	5.0	3.5	6.5	4.0	6.7	8.0	9.8	12.0	7.6
21	2.8	4.0	3.5	2.7	3.8	3.8	3.5	5.2	6.3	7.5	5.0
24	3.8	1.2	3.5	3.3	3.0	3.0	3.8	6.0	4.7	5.0	4.2
27	4.2	3.3	3.8		4.5	5.0	5.7	4.1	7.0	4.2	3.3
30	4.0		3.5		3.3		4.7	3.3	4.7	4.0	5.0
33	3.5		2.2		2.8		3.5	3.7	5.5	4.2	4.2
36	2.2		2.0		2.8		4.0	3.3	3.7	4.0	2.5
39	2.8		1.8		3.5		2.3	3.0	4.3	3.8	2.7
42	2.5		1.5		4.2		3.5		3.7		2.3
45	2.5		3.2		4.6		3.0		3.2		1.5
48	3.6		3.5		1.2		4.3				
51			3.0		3.3						
54			1.2		2.0						
57			1.8		2.0						
60			2.5								

[a] Average number of stars per counting square (8 □′).

curves is 0.35±0.05. A plot of ϵ against r shows that there is no detectable variation of ellipticity with distance from the center, as had been found for the Fornax dwarf (Hodge 1961) and for giant ellipticals (Liller 1960).

Orientation

From measures of the orientation of all the curves in the isodensity diagrams, the orientation of the Sculptor dwarf is found to be 98° from the north, measured eastwards. This value has a probable error of about 2°.

Symmetry

Unlike the Fornax dwarf system, the Sculptor galaxy seems to be perfectly symmetrical. Neither from the isodensity diagrams nor from the detailed profiles is there any suggestion that the object is not a perfectl symmetrical ellipsoid.

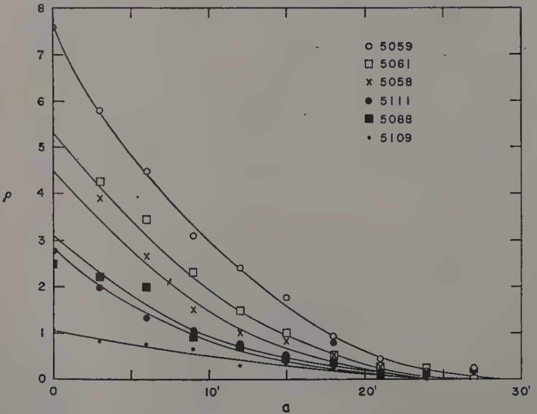

FIG. 3. Major axis profiles for the six counted plates. The projected density is in units of stars per square minute of arc.

Density Profiles

Table II lists the star densities, determined for di ferent distances along the major axes of the system for each of the six plates. The values given in Table II are averages of the number of stars per counting square for the two or three squares intersected by the major axis and/or a line 3′ long perpendicular to the axis and centered on it at at distance r from the center of the object. The values in Table II include foreground stars.

The east and west halves of the major axis are averaged together in Table III, which gives profiles in terms of stars per square minute of arc, with the foreground stars (Table I) subtracted out. Figure 3 shows a plot of these points, with smooth curves drawn through them by eye.

The six curves can be combined to give a mean curve only if the luminosity function and the color-

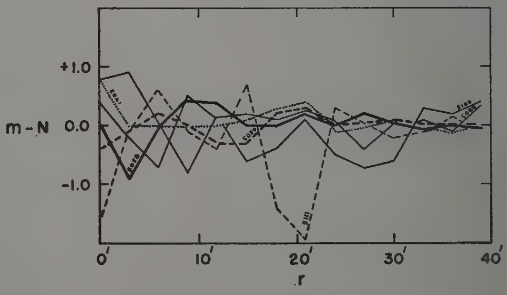

FIG. 4. The difference between the normalized density for each plate and the mean density at that point.

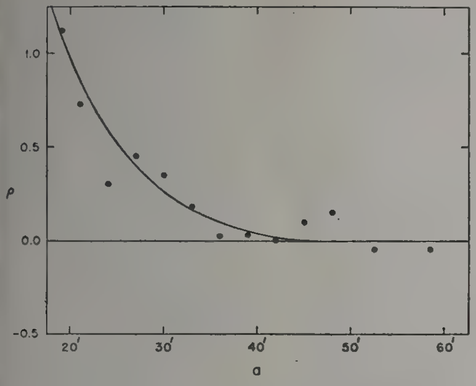

FIG. 5. The outer mean contour points, showing the adopted curve drawn through them.

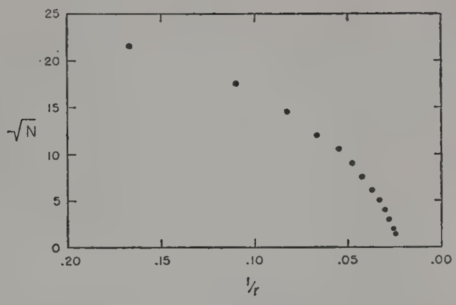

FIG. 6. The mean density distribution plotted in units for the radius determination.

agnitude diagram are invariant with distance from e center of the system. To test this, the profiles given Table III have each been multiplied by the approiate factor to bring the smoothed curves in Fig. 3 gether at $r=6'$. The mean of these normalized profiles is been taken, giving the three deepest plates double eight. Finally, the normalized points N for each plate ive been subtracted at each given distance r from the ean profile M. The difference $M-N$ is plotted in Fig. as a function of r. The figure shows that there is no ppreciable slope for the lines of any of the plates. Thus e conclude that the tops of the luminosity function id color-magnitude diagram are sufficiently invariant ith distance that we may have confidence in a mean ajor axis profile derived from all six plates.

A mean profile, computed as described above, is iven in the last column of Table III. The tabulated alues are the computed ones out to a distance of $=15'$, beyond which they are smoothed values read om a curve drawn through the computed points (Fig.). This profile, derived from all six counts, is considered ie most representative of the galaxy, and is therefore sed in all of the following analysis.

Radius

In the case of the Fornax system, it was found that ie galaxy had an actual radius, determined by the fact iat the stellar density reached a definite zero value. 'his radius was read from a curve showing the density lotted against the reciprocal of the radius, as done for ie globular cluster M15 by King (1961). Such a plot f the outer parts of the Sculptor galaxy is shown in 'ig. 6. The radius of the system derived from this plot $r=46'\pm3'$ for the major axis. This means that if the istance modulus is $m-M=19.6$ (Baade and Hubble 939), then the linear radius of the Sculptor dwarf long the major axis is $r=1.1$ kpc.

Shapley's Star Counts

In his initial paper on the Sculptor system, Shapley 1938) gave a table of counts made on the discovery plate, A18005, for an area of 4° centered on the galaxy. The plate used was of very unusually high sensitivity so that the limiting magnitude of the counts was approximately 19.5 pg. In order to compare Shapley's data with that of the present work, a major-axis profile was computed from his counts (Table IV). First the background count was established by averaging the counts from 70 squares in the four corners of his grid, where the squares were all at a distance appreciably greater than the radius derived above (46′ for the major axis and 30′ for the minor). The background was found to be 0.58 stars per square minute of arc. Table IV gives the star density along the *E–W* axis, which is very nearly the major axis, obtained by averaging the two sides and subtracting the background. The table indicates that either foreground fluctuations or counting irregularities happen to depress the foreground count along the major axis in the very outer two steps of the grid, so as to make the major axis look larger than the value obtained when a reliable foreground count is used to determine the zero point. This would explain Shap-

TABLE III. Major-axis profiles and mean profile.

a	5109	5088	5111	5058	5061	5059	Mean Profile
	Stars per square minute						
0′	1.06	2.47	2.80	4.12	4.67	7.58	7.22
3	0.83	2.23	1.98	3.91	4.25	5.80	5.94
6	0.78	1.97	1.34	2.69	3.46	4.49	4.70
9	0.65	0.94	1.07	1.53	2.33	3.14	3.12
12	0.30	0.72	0.78	1.02	1.48	2.41	2.09
15	0.35	0.48	0.55	0.84	0.98	1.77	1.47
18	0.25	0.35	0.79	0.58	0.56	0.94	1.13
21	0.10	0.17	0.98	0.29	0.19	0.44	0.83
24	0.14	0.07	−0.01	0.16	0.26	0.19	0.58
27	0.19	0.29	0.14	0.12	0.26	0.28	0.38
30	0.15	0.11	0.17	0.21	0.15	0.13	0.26
33	−0.01	0.05	0.11	0.16	0.10	0.19	0.16
36	−0.03	0.05	−0.05	0.02	0.10	0.06	0.09
39	−0.06	0.14	0.02	0.05	−0.02	0.09	0.04
42	−0.10	0.22	−0.01	−0.05	0.08	0.04	0.02
45	0.11	0.27	−0.01	−0.15	0.02	−0.02	
48	0.15	−0.15	0.12		0.18		
51	0.09	0.11					
54	−0.14	−0.05					
57	−0.06	−0.05					
60	0.03						

ley's statement that the diameter of the Sculptor system might be as large as 2°.

Figure 7 shows the outer portion of the curve derived

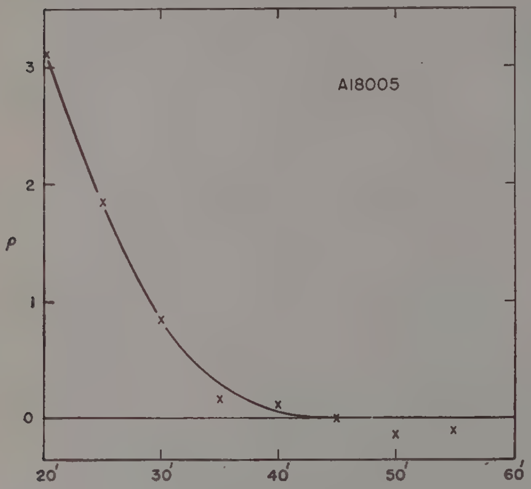

Fig. 7. The outer density distribution from Shapley's counts. The background was established from larger areas at greater distances than shown here.

from Shapley's counts. The curve drawn smoothly through these points has been used to find the radius of the galaxy to compare it with that derived above from the present work. Figure 8 shows the curve used, which gives a value for the radius (measured 8° *from* the major axis) of $r=40'$. This value is very reasonable when compared with 46' obtained above for the major axis, indicating satisfactory agreement between the two independent studies.

Table IV. Major-axis profile after Shapley.

r Minutes of arc	p Stars per □'
0'	12.70
5	9.76
10	6.28
15	4.38
20	3.12
25	1.84
30	0.84
35	0.16
40	0.12
45	0.00
50	−0.16
55	−0.16

Transparency

The images of galaxies lying in the direction of the Sculptor system have been counted on two plates. The projected density of these objects is tabulated as a function of distance from the center of the Sculptor galaxy in Table V. The data show no apprec diminishing of the background galaxy count be the Sculptor system, especially when it is taken account that a distinct cluster of galaxies lies dire south of the system at a distance of about 50'.

Table V. Galaxies behind the sculptor system.

Outer radius of ring (minutes of arc)	No. galaxies per 1000 □'
10	44
20	41
30	42
40	50
50	55
60	50
70	49

IV. DISCUSSION

In general shape, the major-axis profile of the Sculp system is very similar to that of the Fornax syst (Hodge 1961), with the exception that the densi gradient of the outer portions of Sculptor is somewh steeper. Figure 9 compares the observed density di tribution with the formula

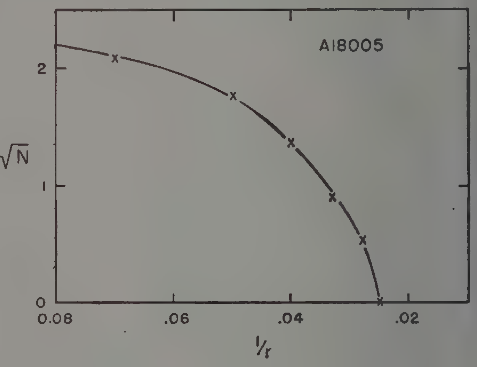

Fig. 8. The curve used to determine the radius from Shapley's counts.

$$N=N_0/(r/a+1)^2, \qquad ($$

where N is the projected density, N_0 is the centr density, r is the distance along the major axis, and is a scale parameter, equal to r at $N=\frac{1}{4}N_0$. This formul is Hubble's luminosity law for giant ellipticals, writte in terms of star density on the assumption that th luminosity function is constant throughout the galax The observed curve does not fit the computed one, an adjusting the values of a or N_0 does not improve the fi As in the case of Fornax, the curve fits the predictio moderately well out to a distance of $1a$ (13'), after whic it falls off much more steeply than the prediction.

Similarly the Sculptor dwarf does not conform t

Vaucouleurs' law (de Vaucouleurs 1948). For his ula a galaxy's luminosity distribution forms a ight line when plotted in the units of Fig. 10. The ve there cannot be considered a straight line.

Gravitationally Limited Radius

he similarity of the Sculptor with the Fornax system gests that its radius, too, may be determined by the vitational attraction on its outer stars by the axy. The expression for the gravitational limited ius is (approximately)

$$r=R_g(M/2M_g)^{\frac{1}{3}} \tag{3}$$

n Hoerner 1957, Burbidge and Sandage 1958), where the tidal radius, R_g is the distance to the Galaxy, is the mass of Sculptor, and M_g is the mass of the axy.

t is necessary, before computing the gravitationally ited radius, to have an estimate of the mass of the tem. In the case of Sculptor the mass cannot be asured directly. Instead we are left with two possible ans of obtaining a rough guess at its mass.

irst, we may compare its luminosity function with t of a globular cluster of known mass. Such a comparison assumes equality of the luminosity functions the two kinds of systems. Shapley's luminosity ction (1938) indicates that Sculptor is 15.2 times as h as the globular M3, if we compare the two in the erval between the brightest stars and 0.5 mag. low the horizontal branch. This is necessarily uncern because of the lack of knowledge of the similarity dissimilarity of the two systems. However, the comrison can give an estimate of the mass of Sculptor, ing Sandage's mass for M3 (1954). The result is $=2\times 10^6\, M_\odot$.

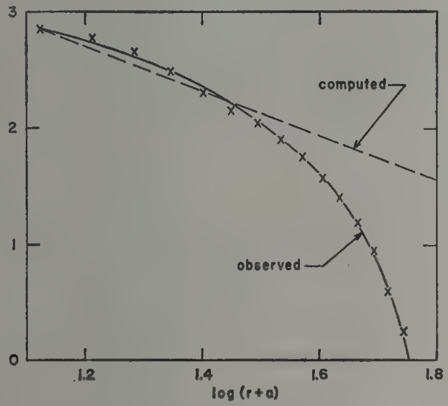

. 9. The density distribution plotted in units in which Hubble's law (dashed lines) gives a straight line.

Another estimate can be made from Sculptor's solute magnitude, assuming a mass-to-light ratio for the system. Shapley (1939) gives its apparent magnitude as approximately 9.0, photographic. If its mass-to-light ratio is the same as for globular clusters, of the order of 2 (Sandage 1954), then the mass of the Sculptor dwarf is $M=4\times 10^6\, M_\odot$. A larger mass-to-light ratio leads to a proportionally larger estimate of the mass, but enlarges the estimated limiting radius only by the cube root of this increase. Using Brandt's (1960) value for the mass of the Galaxy, Baade and Hubble's (1939) value for the distance of Sculptor, and $3\times 10^6\, M_\odot$ as the mass of Sculptor, the computed tidal limit is $r=1.7$ kpc. This is slightly larger than the observed radius of 1.1 kpc, and is comparable to it considering the uncertainties involved in the mass estimates and considering the fact that the tidal radius applies to the situation of nearest approach of the system to our Galaxy. Uncertainties in the distance are large, but not very important in this connection, as they tend to cancel each other out in the comparison of the two radii.

V. SUMMARY

The Sculptor dwarf galaxy is very similar in nearly every respect to the previously studied dwarf in Fornax. Its stars are smoothly distributed in a symmetrical elliptical configuration of ellipticity 0.35. The distribution of star density with radius does not agree in shape with that of giant elliptical galaxies. The radius of the Sculptor dwarf is 46′, approximately 1.1 kpc; this agrees well, within the uncertainties, with the computed tidal radius imposed on the system by the mass of the Galaxy.

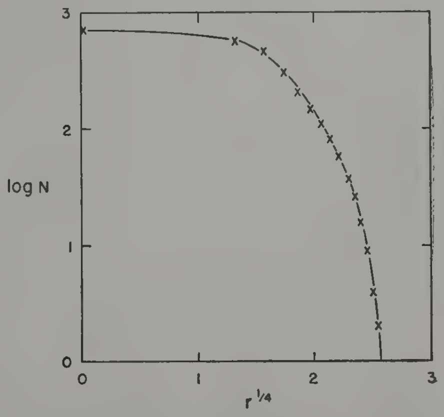

FIG. 10. The density distribution plotted in units in which de Vaucouleurs' law gives a straight line.

ACKNOWLEDGMENTS

I am indebted to Professor H. Haffner and Professor D. H. Menzel who made it possible for me to obtain the plates of Sculptor at the Boyden Observatory. It is also a pleasure to thank Dr. Ira Bowen and the Mt. Wilson and Palomar Observatories for their hospitality during the period in which this paper was written.

REFERENCES

Baade, W. and Hubble, E. P. 1939, *Publs. Astron. Soc. Pacific* **51**, 40.
Baade, W. and Swope, H. S. 1961, *Astron. J.* **66**, 300.
Baum, W. A. 1959, *Publs. Astron. Soc. Pacific* **71**, 106.
Brandt, J. C. 1960, *Astrophys. J.* **131**, 553.
Burbidge, E. M. and Sandage, A. R. 1958, *ibid.* **127**, 527.
Hodge, P. W. 1961, *Astron. J.* **66**, 249.
von Hoerner, S. 1957, *Astrophys. J.* **125**, 451.
Hubble, E. P. 1930, *ibid.* **71**, 131.
King, I. 1961, *Astron. J.* **66**, 47.
Sandage, A. R. 1954, *ibid.* **59**, 162.
Shapley, H. 1938, *Harvard Bull.* **908**, 1.
——. 1939, *Proc. Natl. Acad. Sci. U. S.* **25**, 565.
Thackeray, A. D. 1950, *Observatory* **70**, 144.
de Vaucouleurs, G. 1948, *Ann. d'Astrophys.* **11**, 247.

THE ASTRONOMICAL JOURNAL VOLUME 66, NUMBER 8 OCTOBER, 1

Multicolor Photoelectric Photometry of Bright Galaxies.* I

William Grant Tifft†
Mount Wilson and Palomar Observatories, Carnegie Instituion of Washington, and California Institute of Technology

(Received May 22, 1961)

Photoelectric observations are presented for 57 galaxies and 52 stars as obtained with a blue-sensitive photocell. The response bands have effective reciprocal wavelengths of 2.66, 2.39, 2.07, and 1.68 (micron units). In addition, 8 galaxies and 19 stars have been observed in the red and infrared. The effective reciprocal wavelengths for the red response bands are 1.55, 1.26, 1.14, and 1.00. From one to five aperture sizes have been used in the photometry of each galaxy, with an average of three per galaxy. All the observations have been reduced to an absolute energy color system by means of direct comparisons between the response of the photocell and filter combinations and the response of a thermocouple. A subsequent paper will contain the bulk of the discussion of the data.

INTRODUCTION

NUMEROUS investigations involving extragalactic photometry have been carried out; among the most extensive investigations are those of Stebbins and Whitford (1952), Pettit (1954), Holmberg (1958), and de Vaucouleurs (1961). Some six-color observations were obtained by Stebbins and Whitford (1948); however, most of the available photometry on extragalactic systems has been limited to two colors and, in the case of photoelectric work, to only one or at best relatively few aperture sizes for each galaxy. This present paper extends photoelectric observations, similar to the Stebbins and Whitford six-color data, to a larger sample of galaxies with up to five aperture sizes used in the measurement on each system. Some measurements have been made in eight colors using two photocells; however, the vast majority of the observations were taken in four colors using a blue-sensitive photocell. The results of the work are presented in two papers; this paper includes the observations and describes the photometric system and procedure, while a later paper will contain a discussion of the observations.

INSTRUMENTATION AND TECHNIQUES

Photoelectric Equipment

The blue sensitive photometer employed utilized an unrefrigerated type 6094 EMI photocell. The 11-stage end-on EMI photocell was normally operated with total applied voltage of 1300 v, and the output f through a dc amplifier and recorded on a Bro recorder. Red and infrared observations were obtain with a type 16 PM-1 Farnsworth photomultiplier tu The 16-stage end-on photocell was operated und dry-ice refrigeration with a total applied voltage 2200 v from an electronic power supply. The first o servations were obtained with the Farnsworth photoc in conjunction with a chopper stabilized amplifi Later observations were taken with an electromet tube amplifier. As with the EMI photocell the amplifi output was recorded on a Brown recorder.

The sensitivity curves of the EMI and Farnswor phototubes were determined as a function of waveleng for use in absolute energy calibration of the co system. The calibration was carried out by compari the response of the phototubes with that of a therm couple. The source of illumination was a tungsten lam viewed through a Hilger-Muller double-pass quar monochromator. Both the thermocouple and photoce entrance windows were placed in the same position, close as possible to the exit slit of the monochromato Because of the great sensitivity of the photocel compared to the thermocouple, it was necessary introduce light attenuation, in the form of diaphragm in the light beam before it entered the monochromat when the photocells were used. The thermocoup output was read with a sensitive galvanometer, an the photocell output was fed through an amplifier an recorded on either a Brown or Varian recorder.

The calibration was carried out in three sessions

---

* Thesis submitted in partial fulfillment of the requirements for the Ph.D. degree at the California Institute of Technology, 1958.

† Presently at A. J. Dyer Observatory, Vanderbilt University.

Farnsworth photocell under dry-ice refrigeration ween λ5500 and λ16 000, the EMI photocell between 500 and λ8000, and the EMI photocell between 500 and λ4900. The photocells were operated at 500 v ken from an electronic supply. Throughout the cali- ation the entrance and exit slits of the monochromator re set equal and the center slit at about twice the dth of the other two. For the Farnsworth and longer ivelength EMI calibration the exit slitwidth corre- onded to 240 A in the emergent spectrum at λ5850. or the ultraviolet EMI calibration the exit slitwidth rresponded to 260 A in the emergent spectrum at λ4045. ne measuring procedure consisted of scanning the tire range of interest with the thermocouple, then peating the scan with the photocell, and then repeat- g the thermocouple scan as a check. The two thermo- uple scans agreed satisfactorily in all cases. The avelength scale of the monochromator was calibrated visual observations and photoelectric scanning. ssible errors in the wavelength calibration range om 5 A at λ4500 to as much as 50 A at λ10 000.

In view of the technique employed, the only impor- nt differences in the light seen by the thermocouple d photocell arise from the light attenuation dia- hragming, and slight differences in the viewing at the it slit, particularly the viewing of light scattered from e jaws of the exit slit. Both of these effects are prob- bly small. Visual inspection of the emergent light ggests that a small amount of light is scattered into e beam from adjacent spectral regions, probably by attering at the jaws of the central slit. The effect ppears to be small and in any case the wavelength ifference of the light from the main bundle is small. hotoelectric scanning in the ultraviolet beyond the hototube cutoff and in the far infrared gives zero esponse, implying that scattering over large wavelength ifferences is virtually zero. Table I gives the measured hototube response relative to the thermocouple as a unction of reciprocal wavelength. The values are normalized to read 1.000 at maximum sensitivity. The values are not corrected for the effect of finite slitwidth.

TABLE I. Normalized response of photocells.

1/λ	*P*	1/λ	*P*	1/λ	*P*	1/λ	*P*
			EMI Photocell				
.90	.626	2.45	1.000	2.00	.707	1.55	.00790
.85	.699	2.40	.999	1.95	.632	1.50	.00234
.80	.763	2.35	.994	1.90	.550	1.45	.00059
.75	.821	2.30	.980	1.85	.447	1.40	.000157
.70	.869	2.25	.962	1.80	.328	1.35	.000033
.65	.910	2.20	.933	1.75	.222	1.30	.0000068
.60	.946	2.15	.895	1.70	.144	1.25	.0000012
.55	.974	2.10	.839	1.65	.0673		
.50	.993	2.05	.776	1.60	.0224		
			Farnsworth Photocell				
1.70	.297	1.40	.587	1.10	1.000	0.80	.00275
1.65	.323	1.35	.675	1.05	.953	0.75	.00013
1.60	.356	1.30	.761	1.00	.767	0.70	.000015
1.55	.397	1.25	.840	0.95	.468		
1.50	.448	1.20	.909	0.90	.159		
1.45	.512	1.15	.966	0.85	.026		

TABLE II. Filter system.

Band	Filters
1	Corning 9863+approximately Corning 7380
2	Schott BG-12+Schott GG-13
3	Corning 5030 (1.6 mm)+Corning 3387
4	Corning 3480
5	Federal Engineering special interference filter
6	Federal Engineering special interference filter+Corning 2434
7	Federal Engineering special interference filter+Schott RG-10
8	Heimann No. 205

Filter System

Corning and Schott glass filters or filter combinations were used to define four response bands in conjunction with the EMI photocell. Special interference filters made by Federal Engineering (Madison, Wisconsin) were used for three of the four red and infrared pass bands. For the far infrared a Heimann filter was used. Clear glass was cemented to three of the four glass filters, and the far-infrared filter, to bring them all to the thickness of the thickest glass filter. In the case of the ultraviolet filter the added glass cuts out light below λ3400 normally transmitted by the filter. The interference filters were not adjusted in thickness but are nearly the same as the others. Table II lists the filter components and thickness when different from stock values. The filters and response bands they define are designated by serial numbers in order of wavelength. This numeral notation is used throughout the paper.

Filter transmissions were determined as a function of wavelength with a Hilger-Muller double-pass quartz monochromator by viewing the emergent beam alternately through a filter and directly. The measured filter transmission F, combined with the photocell response P from Table I, and the reflectivity of aluminum M, according to Allen (1953), define the response function G. Using the reciprocal wavelength units,

$$G(x)=P(x)F(x)M^2(x),\quad x=1/\lambda. \tag{1}$$

The response functions include two aluminum reflections, since all observations were made at the Newtonian focus of the Mount Wilson reflectors. Table III gives the eight $G(x)$ functions; Fig. 1 illustrates the response functions.

Observing Program and Technique

All observations were made at the Newtonian focus of the 60-inch and 100-inch telescopes at Mount Wilson during 1957 and early 1958. All red observations were made with the 100-inch telescope, while the EMI photocell was used at both reflectors. Five circular diaphragms were used in the program, from 0.8 to 7.0

Table III. $G(x)$ functions.

$1/\lambda$	G_1	$1/\lambda$	G_2	$1/\lambda$	G_3	$1/\lambda$	G_4
2.90	.007	2.75	.009	2.30	.007	1.80	.002
2.85	.058	2.70	.056	2.25	.200	1.75	.041
2.80	.166	2.65	.139	2.20	.356	1.70	.082
2.75	.292	2.60	.240	2.15	.415	1.65	.043
2.70	.370	2.55	.338	2.10	.418	1.60	.014
2.65	.388	2.50	.392	2.05	.384	1.55	.005
2.60	.346	2.45	.419	2.00	.325	1.50	.001
2.55	.220	2.40	.428	1.95	.253		
2.50	.093	2.35	.418	1.90	.174		
2.45	.025	2.30	.384	1.85	.102		
2.40	.006	2.25	.336	1.80	.047		
2.35	.002	2.20	.271	1.75	.017		
		2.15	.181	1.70	.005		
		2.10	.083				
		2.05	.019				
		2.00	.003				

$1/\lambda$	G_5	$1/\lambda$	G_6	$1/\lambda$	G_7	$1/\lambda$	G_8
1.700	.007	1.450	.004	1.350	.001	1.150	.004
1.675	.064	1.425	.028	1.325	.003	1.125	.027
1.650	.145	1.400	.093	1.300	.010	1.100	.103
1.625	.181	1.375	.198	1.275	.029	1.075	.238
1.600	.189	1.350	.307	1.250	.080	1.050	.369
1.575	.172	1.325	.360	1.225	.184	1.025	.446
1.550	.149	1.300	.371	1.200	.312	1.000	.441
1.525	.148	1.275	.404	1.175	.407	0.975	.384
1.500	.199	1.250	.455	1.150	.383	0.950	.298
1.475	.208	1.225	.486	1.125	.318	0.925	.198
1.450	.087	1.200	.453	1.100	.250	0.900	.107
1.425	.024	1.175	.312	1.075	.242	0.875	.052
1.400	.009	1.150	.156	1.050	.274	0.850	.018
1.375	.004	1.125	.055	1.025	.170	0.825	.008
1.350	.002	1.100	.018	1.000	.043	0.800	.002
1.325	.002	1.075	.007	0.975	.010		
1.300	.001	1.050	.003	0.950	.002		
1.275	.001	1.025	.002				
1.250	.001	1.000	.001				
1.200	.001	0.975	.001				
1.150	.002						
1.100	.006						
1.050	.007						
1.000	.004						
0.950	.002						
0.900	.001						

mm in diameter in steps of about three in area. The diameters, measured in a measuring engine, are given in Table IV along with their actual angular size in the focal planes of the 60-inch and 100-inch telescopes.

Galaxies were selected for observation according to the following restrictions: (1) With the exception of M31, M32, M33, and NGC 205, all galaxies lie between +30° and +90° galactic latitude. This restriction was put on the selection to reduce effects of galactic absorption. Proper calibration of the galactic absorption effect would have required observations of a much larger sample of galaxies. (2) The majority of the galaxies observed are bright noncluster field galaxies with small redshifts. A few representative galaxies from the Virgo and Coma clusters were also included. (3) All the Hubble extragalactic types are represented, including examples over the full range of inclination from edge-on to face-on. (4) Whenever possible, galaxies were taken from the list of systems for which Morgan and Mayall (1957) have given spectral types. To complete representation of structural types, additional galaxies we selected from the Humason, Mayall, and Sanda (1956) redshift catalogue. (5) With one accidental e ception, all galaxies are free from interference by brig field stars.

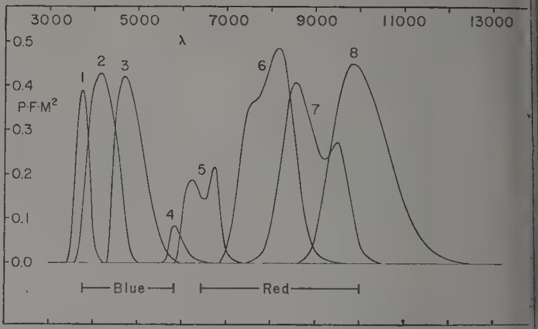

Fig. 1. Response functions for the photometric system.

In addition to the galaxies, a selection of stars w observed to determine stellar colors on the photometr system. The majority of the stars observed range fro spectral type F to M and include representatives of th main sequence, normal and high-velocity giants, an subdwarfs. A few blue stars were measured.

Stellar settings and settings on galaxies with wel defined nuclei were done visually. In a few cases speci regions of galaxies were measured by offsetting from th nucleus or a nearby reference star. Nearly all galax measurements were made directly above sky by of setting the photometer between the galaxy and preselected clear sky region. A typical observing ru on each galaxy with each diaphragm size employe consisted of five deflections, one in each of the fou colors in order of increasing wavelength followed by repetition of the first color as a check. For faint galaxie multiple deflections were taken to increase accuracy Throughout each measurement run an offset guide sta was used to keep the object centered while bein measured and to permit recentering after offset to sky

Two stars were used as primary reference and ex tinction stars when using the EMI photocell; thes were the very blue star Feige 95 (Feige 1958) and nearby reddish star. Eight other stars were used a secondary standards. One star was used for a standar in the red work. Extinction measurements generall were taken at the beginning and end of each night an

Table IV. Measuring diaphragms.

	Diameter in minutes of ar	
Diameter in mm	60-inch	100-inch
0.809	0.365	0.216
1.328	0.600	0.354
2.264	1.023	0.604
4.032	1.822	1.075
7.028	3.177	1.874

ntervals of one to three hours throughout the night. ntifications, magnitudes, colors, and observational bable errors for the reference stars are given in ble VIII.

bservations were reduced to outside the atmosphere fairly standard techniques. For both the four blue- and four red-cell colors, reduction was carried out terms of one magnitude and three-color indices. Ex- ction coefficients were allowed to vary from night night, and all the available observations were con- ered together to derive the best set of extinction coef- ents. A careful investigation of the dependence of inction on color showed significant effects only for color index 2–3 and the magnitude 3.

Calibration of the Color System

Once atmospheric extinction has been removed from otoelectric measurements, instrumental magnitudes n be represented by

$$m = -2.5\log\int E(x)G(x)dx + \text{const.} \qquad (2)$$

is the absolute energy curve of the object observed, d G has been defined in Eq. (1). If we expand $E(x)$ Eq. (2) in a Taylor series about an arbitrary x_0, we n reduce the result to the form

$$= -2.5\log\Big\{E(x_0)\int G(x)dx + \frac{dE}{dx}\Big|_{x_0}\Big[\int xG(x)dx - x_0\int G(x)dx\Big] + \frac{1}{2}\frac{d^2E}{dx^2}\Big|_{x_0}\int (x-x_0)^2G(x)dx + \dots\Big\} + C. \qquad (3)$$

ow define the set of moments γ:

$$\gamma_1 = x_0; \quad \gamma_1\int G(x)dx = \int xG(x)dx, \qquad (4)$$

$${}_N\int G(x)dx = \int (x-x_0)^N G(x)dx, \quad N=2,3,4,\dots. \qquad (5)$$

nserting the moments in Eq. (3) the first derivative erm vanishes, so we have

$$= -2.5\log\Big\{E(\gamma_1) + \frac{1}{2}\frac{d^2E}{dx^2}\Big|_{\gamma_1}\gamma_2 + \dots\Big\} - 2.5\log\int G(x)dx + C. \qquad (6)$$

o the extent that terms in γ_2 and higher derivatives may be neglected we have

$$m = -2.5\log E(\gamma_1) - 2.5\log\int G(x)dx + C. \qquad (7)$$

Thus, given the integrals of the G functions, we can determine the shape of the energy curve. It is of course obvious that observations with response functions G cannot show detail in the energy distribution over intervals of x significantly less than the bandwidth of the G functions. As the monochromatic energy distribution E is smoothed over larger and larger intervals Δx, until Δx approaches the bandwidth of the G functions, values of $E(\gamma_1)$ computed from Eq. (7) will be better and better approximations to the energies read from the smoothed energy distribution at the γ_1 points. This is the case since smoothing the energy distribution reduces the terms neglected in Eq. (7). Except possibly in the ultraviolet and violet, most observed energy distributions smoothed over Δx intervals comparable to the G function bandwidths have fairly small second and higher derivatives. Thus, relative energies, computed from Eq. (7), generally give a good determination of the shape of the true smoothed energy distribution. Errors in the determination of the G functions generally set the limit of accuracy attainable. Further discussion of the validity of the effective wavelength approximation is given later in this section.

Transposing Eq. (7) and writing

$$m_E = -2.5\log E(\gamma_1), \quad \Delta = 2.5\log\int G(x)dx, \qquad (8)$$

we have

$$m_E = m_{\text{obs}} + \Delta + C. \qquad (9)$$

If we now define

$$H(a,b) = \Delta(a) - \Delta(b), \qquad (10)$$

then color indices may be placed on an absolute energy basis by taking

$$C_E(a,b) = C_{\text{obs}}(a,b) + H(a,b). \qquad (11)$$

Values of Δ, H, γ_1, and γ_2 for the photometric system are given in Table V. The absolute values of Δ in Table V have no particular significance since no attempt was made to determine C in Eq. (9). The Δ values do show, however, the relative "constant energy" areas

TABLE V. Calibration constants of the photometric system.

Band	Δ	γ_1	γ_2	Color	H
1	2.683	2.664	0.006	1–3	−0.343
2	3.371	2.392	0.023	2–3	0.345
3	3.026	2.068	0.016		
4	0.141	1.682	0.009	3–4	2.885
				3–6	4.830
5	1.696	1.554	0.005	5–6	−0.922
6	2.618	1.262	0.005		
7	2.280	1.136	0.003	6–7	0.338
8	2.270	1.001	0.002	6–8	0.348

Table VI. Computed and observed colors for the sun and 10 Lacertae.

Color	$B(T)$	10 Lac Obs.	Δ	Sun Comp.	Sun Obs. G2	Δ	$\bar{\Delta}$
1–3	−0.255	−0.254	−0.001	1.154	1.148	0.006	0.00
2–3	−0.156	−0.156	0.000	0.506	0.492	0.014	0.01
3–4	−0.261	−0.203	−0.058	0.302	0.387	−0.085	−0.07
3–6	−[illegible]	...	...	0.41	0.41	0.00	0.00
5–6	−0.318	−0.314	−0.004	0.021	0.038	−0.017	−0.01
6–7	−0.174	−0.233	0.059	−0.027	−0.082	0.055	0.06
6–8	−0.388	−0.589	0.201	−0.013	−0.204	0.191	0.20

Δ = Computed minus observed

of the bands within the systems for each photocell. Since the constant C is different for the EMI and Farnsworth photocells, Eq. (10) does not apply for the determination of $H(3,6)$ in Table V. $H(3,6)$ was found by using the Minnaert (1953) solar energy curve to calculate the 3–6 color index expected for the sun according to the general color-index equation

$$(A-B)=-2.5\log\left[\int E(x)G_A(x)dx\Big/\int G_A(x)dx\right]+2.5\log\left[\int E(x)G_B(x)dx\Big/\int G_B(x)dx\right]. \tag{12}$$

Comparing the calculated solar color with the observed instrumental 3–6 color index of a G2V star, interpolated from the available observations, yielded the value of H given in Table V.

In Table III it will be noted that the response function for band 5 shows a secondary maximum to the infrared side of the primary maximum. Corrections to remove the effect of the secondary maximum have been applied to all the 5–6 colors. This has been done by calculating the correction for various energy distributions and expressing the correction as a function of the observed 5–7 color index. The correction was related to 5–7 since the secondary maximum in response band 5 corresponds closest to band 7. The corrections in no cases exceeded 0.12 mag. and are probably quite well determined. In calculating the data for band 5 in Table V the response function was cut off at $x=1.225$, the correction having accounted for the remainder of the function.

After application of the special corrections to the 5–6 color indices, all color index measurements on the natural instrumental system were reduced to an absolute energy system by use of Eq. (11) and Table V. It is in this form that all color indices are given in Table VIII to XII. Band 3 instrumental magnitudes have been reduced to approximate visual magnitudes by addition of a constant determined by comparing stellar instrumental band 3 magnitudes with published visual photoelectric magnitudes. Because of the limited number and type of stellar observations obtained, no attempt has been made to relate the magnitudes or colors more closely to any conventional system. De Vaucouleurs (1961) using the observations contai in this paper, as originally tabulated in thesis form, discussed linear relationships of the color system to t Johnson-Morgan U, B, V system. In using such re tionships, however, one should bear in mind that wh systems differ widely in response functions transf mations are generally nonlinear, especially in the short wavelength regions. Furthermore, the transformatio will differ according to the type of object considere so transformations based upon stars will not necessar apply strictly to galaxies. If it is desired to transf the observations in this paper to any other syster while retaining the maximum precision, it is recor mended that direct integrations be performed over t desired response bands. Equation (12) can be used f this purpose with G_A and G_B referring to the desire system and $E(x)$ taken from a smooth plot of each i dividual object, or group of very similar objects, take from the data in this paper.

As a final item relating to the color system calibratio we consider deviations of the calibration from a tru absolute energy system. Two energy distributio available for comparison with the observations ar those of the sun and a blackbody approximation to 1 Lacertae. Using the $G(x)$ functions absolute energ color indices were computed, for the Minnaert (1953 solar energy distribution and a 20 000° blackbody according to Eq. (12). Table VI shows the compariso between computed and observed color indices. Th color indices of 10 Lacertae are direct observations whil the color indices compared with the solar values ar interpolated among available observations to represent a G2V star.

The agreement of the residuals from 10 Lacertae and the sun, according to Table VI, is quite good. Relatively small calibration errors are indicated for all color indices except 6–8, with only 3–4, 6–7, and 6–8 showing significant residuals. Since 10 Lacertae has no observed 3–6, and the solar color index has been matched to calibrate 3–6 initially, this material gives no check on the calibration of 3–6.

Additional comparisons of the color system with outside information are afforded by comparison with absolute energy calibrated flux scans according to Code (1958 personal communication). Magnitudes were read off the scans at the effective $1/\lambda$ points, and colors

TABLE VII. Comparison of observed colors with colors from Code scans.

Color	10 Lac (O9V) Code	Obs.	55 Cyg (B3Ia) Code	Obs.	55 Cas (B[illegible]) Code	Obs.
1–3	−0.24	−0.25	−0.39	−0.41	−0.55	−0.51
2–3	−0.14	−0.16	−0.32	−0.22	−0.22	[illegible]
3–4	−0.31	−0.29	−0.29	−0.53	−0.22	−0.27
3–6	−0.77					
5–6	−0.30	−0.32				
6–7	−0.13	−0.23				
6–8	−0.25	−0.59				

Color	σ Boo (F2V) Code	Obs.	31 Com (G0III) Code	Obs.	β Com (G0V) Code	Obs.
1–3	−0.78	−0.73	−1.19	−1.1[illegible]	−1.00	−1.06
2–3	−0.25	−0.28	−0.50	−0.54	−0.42	−0.45
3–4	−0.18	−0.23	−0.40	−0.44	−0.34	−0.56
3–6	−0.22	−0.01	−0.56	−0.45	−0.46	−0.55
5–6	−0.02	−0.05	−0.11	−0.05	−0.07	−0.02
6–7	−0.00	−0.11	−0.05	−0.06	−0.08	−0.09
6–8	−0.00	−0.30	−0.14	−0.16	−0.08	−0.19

Color	a Code	b Obs.	c Obs.	Σ Code-Obs	p.e.	Σ (Table VI)
1–3	−0.91	−0.89		−0.08	0.01	−0.10
2–3	−0.25	−0.35		−0.02	0.01	−0.0[illegible]
3–4	−0.20	−0.28		−0.05	0.01	−0.0[illegible]
3–6	−0.25		−0.15	−0.14	0.02	
5–6	−0.02		−0.02	−0.05	0.01	−0.04
6–7	−0.02		−0.10	−0.07	0.02	−0.06
6–8	−0.03		−0.25	−0.30	0.01	−0.2[illegible]

π³ Ori (F6V).
110 Her (F6V).
θ Boo (F7V).

rmulated. Table VII gives comparisons between colors erived from the flux scans and direct observations of te same or comparable objects. The mean residuals re in good general agreement with those in Table VI. lthough some small systematic differences appear to e present. It should be noted that these residuals have een computed for comparison only and have not been pplied to the observations.

In making comparisons with Code's observations in he violet and ultraviolet, it was necessary to smooth over appreciable energy fluctuations shown by the relatively high resolution of the spectral scans. In order to investigate how closely the mean magnitudes integrated over the response bands resembled the mean level of the radiation in the immediate vicinity of the λ_0 points for bands 1, 2, and 3, direct integrations were performed over bands 1, 2, and 3 for some representative objects. The derived mean magnitudes were then compared with the locally smoothed magnitudes at the λ_0 points directly from the spectral scans. The

TABLE VIII. Reference and extinction stars.

Star		p.e.		p.e.		p.e.		p.e.	N
	1–3		2–3		3–4		3		
−40°129	0.967	0.0021	0.400	0.0019	0.354	0.0019	9.867	0.0029	7
Anon 1	0.867	0.002	0.306	0.001	0.285	0.012	11.282	0.126	2
Anon 2	0.889	0.0082	0.402	0.0016	0.324	0.0057	12.498	0.0019	13
eige 32	−0.226	0.0020	−0.165	0.0025	−0.260	0.0061	12.394	0.0018	13
eige 95	−0.236	0.0014	−0.169	0.0010	−0.250	0.0036	12.895	0.0009	71
Anon 3	1.844	0.0019	0.792	0.0013	0.619	0.0015	11.785	0.0009	69
Boo	2.674	0.0056	1.106	0.0020	0.554	0.0026	3.891	0.0082	5
Anon 4	2.975	0.019	1.251	0.005	0.977	0.005	14.644	0.005	2
Anon 5	0.827	0.0049	0.538	0.0052	0.255	0.0038	11.144	0.0036	4
110 Her	0.893	0.0022	0.354	0.0014	0.280	0.0012	4.170	0.0019	5
	5–6		6–7		6–8		3–6		
HD 81192	0.190	0.001	−0.002	0.001	−0.067	0.004	0.92	…	20

Anon 1: 8.6 N, 5.1 W of NGC 3031 (M81) nucleus
Anon 2: 2.3 S, 0.3 W of Feige 32
Anon 3: 6.0 N, 0.1 E of Feige 95
Anon 4: 1.2 N, 9.3 W of NGC 6239 nucleus
Anon 5: 7.9 N, 6.6 W of NGC 6239 nucleus, probably BD+43°2653

TABLE IX. Stellar colors determined with the blue photocell.

Star[a]	Spectrum	1–3	2–3	3–4	3
μ Cas	G5Vp	1.16	0.56	0.45	5.18
53 Cas	B8Ib	0.51	0.20	0.27	5.48
HD 81192	G7III+hv	1.69	0.77	0.62	6.66
θ UMa	F6III	0.91	0.36	0.30	3.13
π Leo	M2III	3.26	1.35	1.24	5.12
ζ Leo	F0III	0.88	0.25	0.18	3.35
+51°1696	G0sd	0.86	0.43	0.40	9.87
HD 103095	G8sd	1.26	0.59	0.50	6.52
HD 108910	K3+III hv	2.93	1.21	0.98	7.23
31 Com	G0III	1.19	0.54	0.44	4.99
β Com	G0V	1.06	0.45	0.36	4.29
HD 122563	G0III	1.34	0.64	0.64	6.40
HD 124752[b]	K0V	1.63	0.71	0.56	8.61
α Boo	K2IIIp	2.42	1.05	0.82	0.25
θ Boo	F7V	0.94	0.40	0.31	4.02
ρ Boo	K3III	2.67	1.11	0.85	3.89
σ Boo	F2V	0.73	0.28	0.23	4.35
HD 128902	K2III hv	2.96	1.25	1.01	6.15
+26°2606	F4sd	0.64	0.30	0.31	9.68
HD 134063	G5III+hv	1.65	0.78	0.60	7.95
HD 134439	K0sd	1.26	0.60	0.52	9.13
5 Ser A	F8III–IV hv	1.03	0.44	0.32	5.00
HD 140283	F5sd	0.69	0.32	0.33	7.21
λ Ser	G0V	1.05	0.43	0.46	4.50
δ Oph	M1III	3.27	1.33	1.08	3.20
γ Her	A9III	0.89	0.25	0.13	3.60
η Dra[b]	G8III	1.74	0.75	0.58	2.90
HD 148349	M2+III: hv	3.42	1.43	1.25	5.69
η Her	G4III	1.70	0.75	0.57	3.63
48 Her	K1II–III hv	2.38	1.04	0.81	6.84
γ Dra	K5III	3.20	1.31	1.03	2.68
HD 168322	G8III hv	1.82	0.79	0.63	6.29
110 Her	F6V	0.89	0.35	0.28	4.17
κ Cyg	K0III	1.87	0.79	0.60	3.98
σ Dra	K0V	1.64	0.67	0.50	4.78
16 Cyg A	G2.5V	1.22	0.52	0.40	6.00
16 Cyg B	G4V	1.24	0.54	0.42	6.26
HD 186776	M3III hv	3.09	1.28	1.04	6.81
55 Cyg	B3Ia	0.41	0.22	0.30	4.78
HD 199191	G8III hv	1.74	0.78	0.61	7.31
61 Cyg A	K5V	2.30	0.96	0.87	5.49
61 Cyg B	K7V	2.48	1.04	1.03	6.44
HD 201891	F9sd	0.81	0.36	0.33	7.35
10 Lac	O9V	−0.25	−0.16	−0.20	4.59

[a] θ UMa, HD 103095, 31 Com, HD 124752, BD+26°2606, HD 134063 and HD 134439 were measured twice. HD 128902 and 10 Lac were measured three times. ρ Boo and 110 Her were measured five times. All other stars were measured only once.

[b] Measures include light of a faint companion.

agreement was found to be excellent in bands 1 and 3, while in band 2 the integrated magnitude was a few hundredths of a magnitude brighter than the smoothed scan predicted. For the Minnaert (1953) solar energy curve, comparison of integrated mean magnitudes in all response bands with magnitudes read directly at the γ_1 points showed excellent agreement for band 1 and all the red and infrared points. The integrated magnitudes for bands 2, 3, and 4 fell slightly below local fluctuations in the solar energy distribution. However, the smooth curve drawn through all the integrated magnitudes at the γ_1 points averages out local fluctuations very w The general conclusion would seem to be that the col and magnitudes given in this paper are quite rep sentative of the actual energies, locally smoothed, the γ_1 points. It also seems probable that the co system, including the mean corrections in Table V does not deviate very appreciably from an absolu energy system.

OBSERVATIONS

Stellar Observations

Table VIII gives colors, band 3 magnitudes, probab errors of the colors and magnitudes, and the number observations on each object, for all stars used for refe ence and extinction. Stars are listed in order of rig ascension. Stars without common designations are inc cated by "anon" and are identified in notes followi the table.

Table IX contains colors and band 3 magnitudes f all the stars observed with the EMI photocell excep the fainter stars in Table VIII. Spectral and luminosit classes are given for all the stars. The notation "hv after the spectral class indicated that the star was take from the list of high-velocity stars given by Keenan an Keller (1953). These stars tend to show population I characteristics. HD 122563, although not listed b Keenan and Keller, is an extreme example, color metrically, of this class. Giants not marked "hv" o "p" are more or less normal population I objects. Tabl X gives the colors and spectral classes for all star observed in the red. Both Tables IX and X are in orde of right ascension.

TABLE X. Stellar colors determined with the red photocell.

Star[a]	Spectrum	3–6	5–6	6–7	6–8
HD 81192	G7III+hv	0.92	0.24	−0.00	−0.07
π Leo	M2III	2.17	0.87	0.13	0.2
ζ Leo	F0III	0.05	−0.08	−0.12	−0.3
HD 103095	G8sd	0.63	0.18	−0.03	−0.13
HD 108910	K3+III hv	1.67	0.48	0.07	0.06
31 Com	G0III	0.45	0.05	−0.06	−0.16
β Com	G0V	0.35	0.02	−0.09	−0.19
HD 122563	G0III	0.97	0.24	0.00	−0.03
θ Boo	F7V	0.15	−0.02	−0.10	−0.25
ρ Boo	K3III	1.23	0.28	0.02	0.04
σ Boo	F2V	−0.01	−0.05	−0.11	−0.30
HD 128902	K2III hv	1.54	0.46	0.08	0.15
+26°2606	F4sd	0.15	−0.00	−0.07	−0.21
HD 134063	G5III+hv	0.77	0.20	−0.01	−0.04
HD 134439	K0sd	0.62	0.13	−0.05	−0.08
λ Ser	G0V	0.55	0.01	−0.10	−0.26
δ Oph	M1III	2.05	0.71	0.09	0.18
γ Her	A9III	−0.13	−0.12	−0.14	−0.32
10 Lac	O9V	···	−0.31	−0.23	−0.59

[a] HD 81192 was measured 20 times and served as standard reference star for the group. β Com was measured twice and ζ Leo, HD 108910, 31 Com, and σ Boo were measured twice in 6–7 and 6–8. All other values are single determinations.

TABLE XI. Extragalactic colors determined with the blue photocell.

Object	Type	Field	1–3	2–3	3–4	3	Remarks
NGC 205	Ep	1.02	1.14	.50	.54	11.34	
		0.36	1.07	.46	.40	13.04	
NGC 221	Ep	1.02	1.61	.74	.66	9.28	M32
		0.36	1.61	.74	.69	10.12	
NGC 224	Sb	3.18	1.80	.80	.73	6.60	M31
		1.82	1.83	.83	.70	7.31	
		1.02	1.85	.83	.73	8.20	
		0.60	1.84	.83	.73	9.10	
		0.36	1.87	.85	.74	9.93	
NGC 598	Sc	1.02	0.70	.35	.45	11.52	M33, a
NGC 2903	Sc	3.18	1.09	.52	.54	9.65	
		1.82	1.11	.51	.57	10.30	
		1.02	1.06	.51	.60	10.99	
		0.60	1.01	.48	.56	11.60	
		0.36	0.88	.42	.55	12.16	
Haro 22	:	0.60	0.55	.37	.10	14.84	
NGC 3031	Sb	1.02	1.76	.81	.74	9.49	M81
		0.36	1.87	.85	.77	10.62	
NGC 3115	E7	1.82	1.69	.81	.64	9.80	
		1.02	1.68	.82	.66	10.14	
		0.36	1.79	.84	.67	10.95	
NGC 3351	SBb	3.18	1.27	.60	.63	10.33	M95, Leo group
		1.82	1.33	.66	.66	10.86	
		1.02	1.30	.66	.64	11.34	
		0.60	1.15	.61	.62	11.77	
NGC 3368	Sa	3.18	1.44	.68	.66	9.88	M96, Leo group
		1.82	1.50	.72	.68	10.25	
		1.02	1.59	.76	.69	10.77	
		0.60	1.64	.78	.73	11.34	
NGC 3510	SBc	0.60	0.68	.34	.25	14.04	Haro 26
		0.35	0.67	.33	.36	14.65	
		0.60	0.57	.33	.12:	14.94	8″.0 *W*, 32″.0 *N*
NGC 3810	Sc	3.18	0.87	.42	.49	10.86	Leo group
		1.02	0.98	.48	.53	11.80	
		0.36	1.22	.59	.64	13.18	
NGC 3998	S0	1.82	1.65	.80	.65	10.98	UMa cloud
		1.02	1.67	.80	.66	11.26	
		0.60	1.69	.80	.68	11.58	
		0.36	1.73	.84	.67	11.90	
NGC 4216	Sb	1.02	1.78	.82	.74	11.26	Virgo cluster
		0.36	1.92	.88	.80	12.06	
		1.82	1.34	.60	.59	12.62	54″.2 *E*, 136″ *N*
NGC 4245	SBa	1.87	1.47:	.73:	...	11.76:	
		1.08	1.55	.72	.65	12.11	
		0.60	1.55	.74	.66	11.57	
		0.22	1.49	.71	.68	13.53	
NGC 4274	Sa	3.18	1.56	.75	.71	10.85	
		1.02	1.64	.77	.73	11.72	
NGC 4278	E1	3.18	1.62	.78	.64	10.61	
		1.82	1.60	.76	.64	10.81	
		1.02	1.61	.78	.66	11.11	
		0.60	1.67	.81	.65	11.45	
NGC 4283	E0	1.02	1.70	.80	.62	12.53	
NGC 4374	S0	1.82	1.72	.81	.69	10.20	13″.6 *S*, b
		0.60	1.76	.83	.71	11.01	Centered

TABLE XI (*continued*)

Object	Type	Field	1–3	2–3	3–4	3	Remarks
NGC 4406	E4	1′.82	1.68	.77	.64	10.30	M86, Vir cl.
		0.60	1.74	.79	.66	11.30	
NGC 4449	I	1.82	0.51	.24	.23	10.28	c
		0.36	0.46	.20	.23	12.33	d
Anon	E0	0.60	1.57	.84	.78	13.58	e
NGC 4486	E0	3.18	1.68	.78	.69	9.62	M87, Vir cl.
		1.82	1.71	.81	.68	9.97	
		1.02	1.72	.82	.68	10.45	
		0.60	1.69	.80	.71	11.02	
		0.36	1.71	.82	.72	11.66	
NGC 4501	Sc	3.18	1.37	.64	.65	10.09	M88 Vir cl.
		1.82	1.44	.69	.69	10.58	
		1.02	1.59	.75	.74	11.25	
		0.60	1.73	.81	.78	11.93	
		0.36	1.82	.84	.79	12.51	
NGC 4548	SBb	3.18	1.39	.68	.71	10.74	Virgo cluster
		1.82	1.51	.69	.61	11.23	
		1.02	1.61	.77	.73	11.80	
		0.36	1.67	.77	.70	12.89	
NGC 4565	Sb	1.02	1.73	.83	.77	11.38	
		0.36	1.95	.92	.88	12.78	
		0.60	1.39	.67	.66	14.31	69″.2 *W*, 82″.7 *N*
		1.02	1.09	.54	.58	13.82	174″ *W*, 193″ *N*
NGC 4579	Sb	3.18	1.44	.69	.62	10.10	Virgo cluster
		1.82	1.48	.70	.58	10.55	
		1.02	1.58	.75	.68	11.04	
		0.60	1.60	.78	.68	11.51	
		0.36	1.61	.79	.71	11.97	
NGC 4627	:	0.60	1.05	.45	.42	14.08	f
NGC 4631	Sc	1.02	1.03	.46	.54	12.52	Offset, g
		1.02	0.47	.25	.36	12.24	Offset, g
		1.02	0.74	.38	.41	11.97	Offset, g
NGC 4643	SB0	1.87	1.65	.76	.69	11.04	
		0.60	1.72	.81	.68	11.68	
		0.22	1.74	.83	.70	12.72	
NGC 4698	Sa	3.18	1.54	.70	.66	10.90	Virgo cluster
		1.82	1.56	.74	.66	11.20	
		1.02	1.64	.78	.62	11.60	
		0.60	1.64	.76	.66	12.04	
		0.36	1.64	.76	.71	12.51	
NGC 4699	Sb	3.18	1.41	.67	.66	9.88	
		1.82	1.48	.72	.64	10.19	
		1.02	1.55	.75	.66	10.38	
		0.60	1.60	.76	.66	10.78	
		0.36	1.65	.76	.67	11.24	
NGC 4713	Sc	1.82	0.60	.30	.34	11.86	
		1.02	0.62	.31	.32	12.38	
NGC 4762	Sa	0.60	1.61	.75	.58	11.82	Virgo cluster
		1.02	1.37	.63	.66	14.16	65″.1 *E*, 108″ *N*
NGC 4865	E6	0.60	1.64	.84	.64	14.05	Coma cluster
		0.22	1.64	.77	.68	14.53	
NGC 4874	S0	1.08	1.70	.84	.68	13.00	Coma cluster
		0.60	1.69	.85	.68	13.49	
		0.35	1.75	.89	.69	13.98	
NGC 4881	E1	0.60	1.53	.86	.60	14.17	Coma cluster
		0.22	1.73	.86	.65	14.84	

TABLE XI (*continued*)

Object	Type	Field	1–3	2–3	3–4	3	Remarks
NGC 4889	E4	0′.60	1.76	.89	.66	12.94	Coma cluster
		0.22	1.81	.90	.68	13.90	
NGC 4907	SBb	1.08	1.43	.70	.64	13.80	Coma cluster?
		0.60	1.45	.72	.61	14.16	
		0.35	1.65	.79	.71	14.77	
		0.22	1.71	.85	.69	15.25	
IC 4051	E1	1.08	1.68	.84	.63	13.84	Coma cluster
		0.35	1.70	.83	.70	14.48	
NGC 4911	Sb	0.60	1.24	.58	.60	13.72	Coma cluster?
		0.22	1.51	.80	.75	15.04	
NGC 4921	Sa	1.87	1.48	.70	.62	12.86	Coma cluster?
		1.08	1.57	.78	.67	13.42	
		0.60	1.64	.82	.68	14.03	
		0.35	1.70	.84	.69	14.49	
NGC 5005	Sb	1.82	1.41	.68	.62	10.44	
NGC 5055	Sb	1.02	1.21	.58	.56	12.17	54″.2 *N*, M63
		1.02	1.14	.57	.62	12.69	54″.2 *S*
NGC 5194	Sc	1.82	1.09	.52	.56	10.10	M51
		1.02	1.13	.55	.57	10.61	
		0.60	1.26	.58	.62	11.18	
		0.36	1.36	.62	.61	11.85	
		1.02	0.99	.46	.52	12.11	46″.1 *E*, 57″.0 *S*
NGC 5195	Ep	1.02	1.69	.80	.80	11.11	M51 companion
NGC 5248	Sc	3.18	1.02	.47	.56	10.62	
		1.82	1.09	.52	.56	11.08	
		1.02	1.14	.57	.60	11.72	
		0.60	1.14	.55	.64	12.28	
		0.60	0.84	.37	.46	13.99	57″.0 *E*, 48″.8 *S*
NGC 5363	I	1.02	1.73	.83	.66	11.10	h
NGC 5457	Sc	1.82	1.14	.54	.52	10.90	8″.1 *W*, M101
		0.60	1.17	.57	.56	12.51	Centered
NGC 5560	(SBc)	1.02	1.14	.56	.61	13.10	
NGC 5566	SBa	1.82	1.56	.74	.64	11.22	
		0.60	1.66	.80	.67	11.90	
		0.36	1.70	.79	.71	12.22	
NGC 5576	E4	1.02	1.56	.76	.63	11.60	
NGC 5633	Sb	1.02	0.94	.43	.50	12.67	
		0.36	1.05	.53	.51	13.62	
NGC 5850	SBb	1.08	1.69	.81	.66	12.42	
		0.35	1.75	.82	.71	13.32	
NGC 5907	Sb	0.60	1.60	.76	.73	12.91	
		1.02	1.37	.67	.57	12.83	19″.0 *E*, 51″.5 *S*
		1.02	1.16	.54	.56	13.29	46″.1 *E*, 111″ *S*
		1.02	0.86	.38	.47	13.76	84″.1 *E*, 198″ *S*
NGC 6239	(Sc)	1.82	0.71	.36	.31	12.52	
		1.02	0.72	.39	.32	12.76	
		0.36	0.64	.39	.35	13.90	
NGC 6503	Sc	1.82	1.06	.51	.56	10.86	
		0.60	1.23	.59	.62	12.27	

---

[a] Centered on brightest patch, slightly *SE* of photographic center.

[b] M84, Virgo cluster.

[c] Centered on the over-all structure.

[d] Centered on stellarlike nucleus slightly *E* of the general center of the galaxy.

[e] Virgo cluster dwarf elliptical galaxy, 7′ *N*, 4′.4 *W* of NGC 4486.

[f] Small galaxy just *N* of NGC 4631. This galaxy resembles an elliptical galaxy except that it has no significant nucleus.

[g] Since this galaxy shows no distinct nucleus, offsets have been made from a star near the edge of the galaxy and directly *N* of the center. Taken in e order listed in the table the offsets are 54″.2 *E*; 103″ *W*, 48″.8 *S*; 78″.6 *E*, 27″.1 *S*. Although no real nucleus is seen, the measure 54″ *E* of the offset ar may include light from the outer part of a central bulge. Both other regions measured include bright visual patches, probably *H*II regions.

[h] A fairly bright star near the nucleus is included in the measures.

Table XII. Extragalactic colors determined with the red photocell.

Object	Type	Field	5–6	6–7	6–8	3–6	6	Remarks
NGC 224	Sb	1.′08	.53	.09	.21	1.36	6.76	M31
		0.60	.54	.11	.24	1.34	7.75	
		0.35	.54	.12	.25	1.32	8.67	
NGC 2903	Sc	1.08	.36	.10	.19	0.98	9.95	
		0.60	.38	.11	.19	0.99	10.61	
		0.35	.39	.09	.21	1.00	11.20	
NGC 3115	E7	1.08	.40	.10	.20	1.31	8.79	
		0.60	.40	.08	.20	···	9.12	
		0.35	.42	.08	.19	1.51	9.46	
NGC 3351	SBb	1.08	.40	.08	.17	1.13	10.17	M95, Leo group
		0.60	.41	.10	.15	1.18	10.59	
		0.35	.35	.07	.18	···	11.07	
NGC 3810	Sc	1.08	.27	.03	.13	0.89	10.84	Leo group
		0.60	.25	.08	.23	···	11.43	
		0.35	.37	.10	.12	1.14	12.09	
NGC 4486	E0	1.08	.40	.10	.19	1.12	9.28	M87, Vir cl.
		0.60	.40	.10	.22	1.13	9.89	
		0.35	.38	.11	.20	1.10	10.60	
NGC 4631	Sc	1.08	.23	.16	.30:	0.80:	11.12	a
NGC 5248	Sc	1.08	.35	.10	.20	1.01	10.66	
		0.60	.33	.09	.17	1.10	11.17	
		0.35	.32	.11	.20	···	11.70	

[a] 78″.7 *E*, 27″.2 *S* from reference star. See Table XI.

Extragalactic Observations

Table XI gives the color indices and band 3 magnitudes for all galaxies observed with the EMI photocell. The NGC number or other identification is given for each system along with the Hubble structural type taken from the Humason, Mayall, and Sandage (1956) redshift catalogue, wherever possible. One type, given in parentheses, was determined by the author. The galaxy Haro 22 was taken from a list of blue galaxies given by Haro (1956). The aperture employed for each measurement is given in minutes of arc, and unless otherwise indicated the diaphragm was centered on the nucleus. The last column of Table XI contains remarks, including references to notes following the table.

Table XII contains all extragalactic observations obtained in the red. The material is arranged as in Table XI with the addition of the color index 3–6 which ties together the blue and red observations. In order to formulate 3–6 it was necessary to interpolate among band 3 magnitudes to derive the value of 3 corresponding to the field size used to measure 6. This problem arose because of the different scales of the 60-inch and 100-inch telescopes, and the fact that all galaxies measured in the red at the 100-inch had been measured in the blue at the 60-inch. However, for the diaphragms employed in measurement, a given field size at the 60-inch telescope corresponds closely to the field size of the next larger diaphragm at the 100-inch telescope. Thus the interpolation corrections were small and it is unlikely that serious errors are present in 3–6 due to the interpolation. Stellar colors in Table X are of course independent of diaphragm size.

Observational Errors

Observational errors may be divided into two categories, internal random errors of measurement on each individual galaxy or star, and tie-in systematic errors between different galaxies or galaxies and stars or between different nights. Some information is available for estimating the random errors of measurement on individual galaxies by comparing the first and last measurement made with each diaphragm size. The first and last measures were almost always taken with the ultraviolet filter when using the EMI photocell; thus at least two determinations of 1–3 are available for each diaphragm size on nearly every galaxy. An investigation of the 1–3 residuals about the final mean value shows, as expected, a very good correlation with the band 3 magnitude, due allowance being made for the different light-gathering powers of the 60-inch and 100-inch telescopes. Brighter than 3=12.5 at the 60-inch or 13.7 at the 100-inch, 1–3 measurement errors are consistently less than 0.02 mag. Extra deflections were taken for the faintest systems, so it is doubtful if random errors as great as 0.05 mag. exist in 1–3 at any magnitude. 3–4 random errors should be about the same as in 1–3 since deflections in 1 and 4 were quite similar in most cases. Because of the increased sensitivity of bands 2 and 3, random errors in 2–3 probably do not exceed 0.02 or

3 mag. at any magnitude. Relatively little informa-
n is available for estimating errors in the red obser-
tions; however, what repeat observations are avail-
le rarely show deviations of individual measures from
e mean larger than 0.02 mag. for any of the red
otocell color indices.

Tie-in systematic errors between galaxies and stars
d between different nights are much more difficult to
termine than random errors. Except for a few cases
the red, no repeat measurements were made on
laxies using the same field diaphragm. Reference stars
re referred to frequently but provide no check on
sidual errors after reduction since the standards
ovided the basis for extinction determinations. For
e or six galaxies some observations using different
aphragm sizes were obtained on different nights. On
e basis of these observations, assuming smooth color
adients with radius, night-to-night systematic errors
rely exceed 0.03 to 0.04 mag. in all colors. It is
ubtful if any exceed 0.1 mag.

Systematic errors for magnitudes in band 3 or band
are larger than systematic errors in the color indices.
his is the case primarily because magnitude extinc-
on is much more variable than color extinction and
arder to determine accurately. Differential magnitudes
etween various diaphragm sizes are probably as reli-
ble as the colors, but the actual values of individual
agnitudes are definitely less accurate. In view of the
wer accuracy of magnitude determinations, the color
dex 3–6 relating the measures with the two photocells
s the least reliable color. Correlations of 3–6 with
ther colors imply that few if any discrepancies as
arge as 0.1 are present in the 3–6 colors.

Two factors preclude any precise comparison with
ost other extragalactic observations. The uncertainties
f color system transformations has already been men-
ioned and will enter into any comparison of dissimilar
ystems. A second consideration arises from aperture
ffects. Since color varies with radius in most types of
alaxies, and different observers have used widely
aried apertures, a direct comparison between observers
s difficult. Errors arising from the above sources are
ore or less comparable with normal photoelectric
recision. De Vaucouleurs (1961) has shown that the
tellar observations contained in this paper are quite
onsistent with standard U, B, V data. Furthermore,
here are no obvious inconsistencies in the extragalactic
bservations in comparison with de Vaucouleurs. A
ore detailed comparison would not seem to be war-
anted at this time.

DISCUSSION

Comparison of Stellar and Extragalactic Color Indices

As an introduction to the analysis of the extragalactic
olors given in this paper we consider first a comparison
etween stellar and extragalactic color indices. Variations of color index with such parameters as radius, inclination, velocity, and galactic latitude are neglected here and are considered in detail in the second paper in this series. Figures 2 through 6 present five color-color diagrams of the stellar and extragalactic observations. In the first three figures, 1–3 is plotted as ordinate against the progressively longer wavelength color indices 2–3, 3–4, and 3–6. In the last two figures 5–6 is used as ordinate with 6–7 or 6–8 as abscissa. In each figure stellar observations are shown to the left. Lines have been drawn to represent particular types of stars, viz., main-sequence stars, normal giants, high-velocity giants, and subdwarfs, whenever separation into groups is suggested. The red observations are insufficient to make significant distinctions. The lines representing the different types of stars are repeated in the right portion of each figure, where the extragalactic observations are shown. Different symbols have been used for the various basic extragalactic structural types.

Table XIII. Comparison of high- and low-velocity star color indices.

Color	G8III hv	G8III	G8sd	K2.5+III hv	K3III
1–3	1.78	1.74	1.26	2.94	2.67
2–3	0.78	0.75	0.59	1.23	1.11
3–4	0.62	0.58	0.50	1.00	0.85
3–6				1.60	1.23
5–6				0.47	0.28
6–7				0.08	0.02
6–8				0.10	0.04

G8III hv mean of HD 168322 and HD 199191
G8III Eta Draconis
G8sd HD 103095
K2.5+III hv mean of HD 108910 and HD 128902
K3III Rho Bootis

In Figs. 2 and 3 in particular, the separation of stars into distinct groups is quite clear. Particularly interesting is the separation of the high-velocity giants from the normal giants in the same manner as the subdwarfs deviate from the main sequence. The high-velocity-giant point deviating most extremely in Figs. 3 and 4 is HD 122563, which shows extreme population II spectral characteristics. Another comparison between the high-velocity giants and the normal giants is shown in Table XIII, where color indicates at equal spectral type are compared. The Table XIII examples, as well as others that may be taken from the stellar color index measurements, indicate that the high-velocity giants are consistently redder than the normal giants at the same spectral type. If equality of spectral type is to mean equality in effective temperature, then similarity of the far-red energy distributions, where line absorption has little effect on the energy distributions, should correspond to equal spectral class. Metal-poor stars, such as are generally considered to occur among the high-velocity stars, should show, if anything, less line blanketing than the low-velocity stars, and hence if they deviate at all in color index from low-velocity stars they should show bluer color indices at short

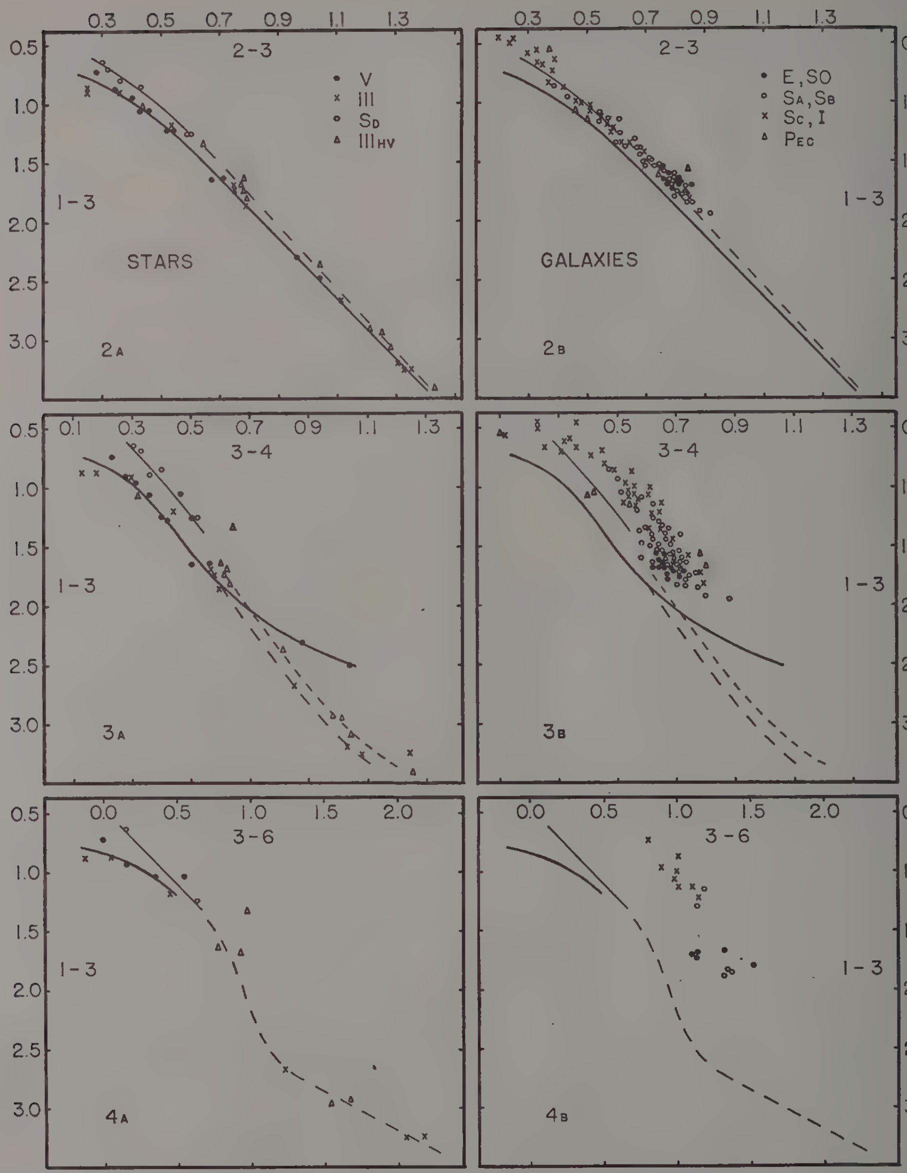

Figs. 2–4. Color-color relationships for stars (left) and galaxies (right). The lines are discussed in the text. Coma cluster galaxies are not plotted, and in the most crowded portions of the figures some points have been omitted for clarity. The most extreme red points are nuclei of spirals seen edgewise, hence heavily reddened.

wavelengths. This effect is well known in the subdwarfs, and since the same apparently holds true for the high-velocity giants it would appear that the high-velocity giants have been classified too early in spectral type.

In each of the color-color relationships the extragalactic colors are seen to lie in a fairly distinct sequence displaced from, but nearly parallel to, the stellar pattern. The displacement is readily explained as a natural consequence of the composite nature of the galaxies. Consider, for example, that a certain type of galaxy has an energy distribution resembling a G4III star over the spectral region from band 1 to band 3; i.e., 1–3 for the galaxy is equal to 1–3 for a G4III star. Now as we examine the galaxy's energy distribution further to the red, energy contributions from stars of later and later spectral types become increasingly important. Thus the galaxy will yield a color index 3–4, which resembles a star of spectral type later than G4III, say K1III. Passing still further to the red, we would find that 3–6 for the galaxy resembles 3–6 of a

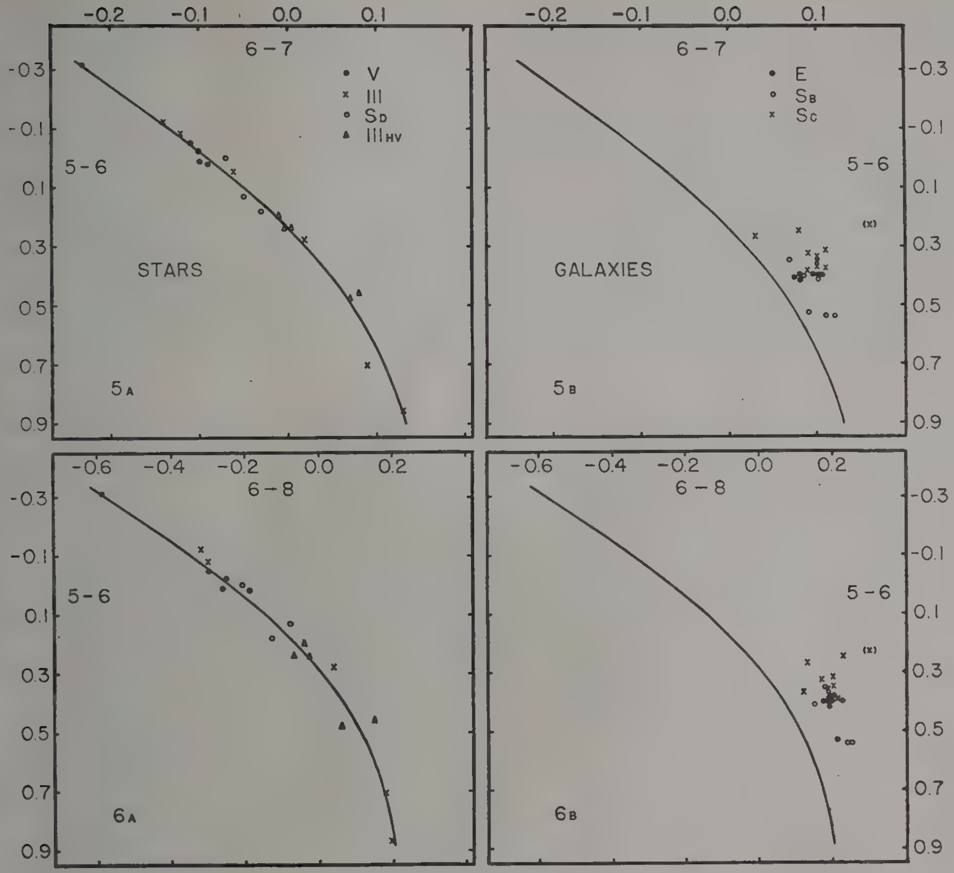

FIGS. 5–6. Color-color relationships for stars (left) and galaxies (right) in the infrared.

3III star. Thus when we plot one color index against nother for the galaxy, the longer wavelength color ndex is found to be too red to correspond to a star hich matches the galaxy in the shorter wavelength olor index. This is just what is observed and illustrated n Figs. 2 through 6. Note that as progressively longer olor base lines are employed the difference in the pectral type of the stars matching the two color ndices increases, hence the deviation of the galaxy olors from the colors of any one type of star grows.

The reddest color one would expect to observe in a alaxy, neglecting reddening by interstellar or interalactic matter, should be representative of the latest pectral type giants. Figure 6 shows that the 6–8 olors begin to resemble M-giant star colors, clearly ndicating the considerable importance of M giants, or ven cooler stars, as contributors to the integrated mergent energy from extragalactic systems. For the luest galaxies it is interesting to compare the measurenents, particularly in Fig. 3, with the blue galaxy neasurements of Hiltner and Iriarte (1958). These alaxies appear to form the blue end of the extragalactic sequence, and presumably represent galaxies containing a large number of young blue stars, but still enough late-type stars to produce the composite effect. There is no indication that the Hiltner and Iriarte observations do not fit smoothly on the sequence indicated by the data in this paper. Further consideration of the synthesis of extragalactic colors is given in the second paper of this series.

In addition to demonstrating the composite structure of galaxies, Figs. 2 through 6 show the well-known effect that structural type is correlated with color. The Sc and SBc spirals are clearly bluer than the Sa or Sb systems, and the elliptical galaxies form a fairly homogeneous group among the redder systems.

ACKNOWLEDGMENTS

The author wishes to express his appreciation to the California Institute of Technology and the Mount Wilson and Palomar Observatories for having made facilities available for this work. Acknowledgment is also due to the National Science Foundation for fellow-

ship support preceding and during the time this work was carried out.

REFERENCES

Allen, C. W. 1953, *Astrophysical Quantities* (Athlone Press, London).
Feige, J. 1958, *Astrophys. J.* **128**, 267.
Haro, G. 1956, *Bol. Obs. Tonantz. y Tacub.* No. 14, 8.
Hiltner, W. A. and Iriarte, B. 1958, *Astrophys. J.* **128**, 443.
Holmberg, E. 1958, *Medd. Lunds Astron. Obs.* Ser. II, No. 136.
Humason, M. L., Mayall, N. U., and Sandage, A. R. 195 *Astron. J.* **61**, 97.
Keenan, P. C. and Keller, G. 1953, *Astrophys. J.* **117**, 241.
Minnaert, M. 1958, *The Sun*, edited by G. P. Kuiper (Universi of Chicago Press, Chicago), Chap. 3.
Morgan, W. W. and Mayall, N. U. 1957, *Publs. Astron. So Pacific* **69**, 291.
Pettit, E. 1954, *Astrophys. J.* **120**, 413.
Stebbins, J. and Whitford, A. E. 1948, *ibid.* **108**, 413.
——. 1952, *ibid.* **115**, 284.
de Vaucouleurs, G. 1961, *Astrophys. J. Suppl.* No. 48, **5**, 233.

IE ASTRONOMICAL JOURNAL VOLUME 66, NUMBER 8 OCTOBER, 1961

Determination of Differential Limb Darkening of Eclipsing Binaries from Multicolor Photometric Observations. I

K. Serkowski
*Lowell Observatory, Flagstaff, Arizona**

(Received July 15, 1961)

The linear equations are presented which describe the observed color indices of an eclipsing binary during the eclipse as functions of the difference of limb darkening coefficients, difference of intrinsic colors, and corrections to the rectification constants. The ratio of radii of the components of the eclipsing binary, the ratio of their luminosities in one color, and the coefficients of limb darkening in this color are the only elements of the system upon which the coefficients of these equations depend. A least-squares solution of the equations describing the color indices of YZ Cassiopeiae observed by Kron gives for the star eclipsed in primary minimum a difference of limb darkening coefficients $u^{4500}-u^{6700}=0.35\pm0.02$ (m.e.) which is about twice as large as the value 0.16 ± 0.08 resulting from independent solutions in each color.

I. INTRODUCTION

THE problem of determining the elements of an eclipsing binary from two-color photometric ob-ervations can be, in general, reduced to a least-squares olution of the system of equations with corrections to e elements on one side and the observed brightnesses r their differences on the other side. Part of the equa-ons describes the changing brightness in one color nly. The remaining equations can be written in one of wo forms; they may contain either the brightnesses in nother color or the color indices.

The second form of these equations seems better ecause the color index is as a rule measured more ccurately than the brightness. This is especially true r the differential photometers containing several ultiplier tubes which are becoming more and more ommon. The color indices measured by such photom-ters are to a large extent free of the disturbing influence f atmospheric scintillation.

The equations describing the color indices are almost ndependent of equations describing the brightnesses n one color. Each of these systems of equations contains separate set of unknowns: In each of these systems the erm containing the corrections to unknowns deter-nined by the other system are negligibly small. Hence ach group of equations can be solved separately.

The most interesting quantity obtained by solution f equations describing the color indices of an eclipsing inary during the eclipse is the difference of limb arkening coefficients in two colors. This difference can e determined with much higher accuracy than can ach of the coefficients separately; the reason is that in he equations describing the brightnesses of eclipsing inary in one color the coefficients of the correction to he radius of eclipsed star are almost exactly propor-ional to those of the correction to the coefficient of limb arkening (cf. Irwin 1947). Hence the accuracy of a imultaneous determination of limb darkening and adius of eclipsed star is very low.

Methods of determining the differential limb darkening from two-color photometric observations have been proposed by Irwin (1947), by Kopal (1946), and by Russell and Merrill (1952). However, these methods do not pretend to be of high accuracy and do not permit us to estimate the error of the result. In an attempt at a somewhat more accurate approach we are considering in this paper all the first-order effects upon which the color index of eclipsing binary may depend during the eclipse.

II. CHANGES IN COLOR CAUSED BY DIFFERENCES IN INTRINSIC COLORS AND IN LIMB DARKENING

A. Fractional Loss of Light

The surface brightness J of a given point on the surface of spherical star is with fairly high accuracy given by the equation (Kopal 1949)

$$J(\gamma)=J(0)(1-u-v+u\cos\gamma+v\cos^2\gamma), \qquad (1)$$

where γ is the angle between the direction to observer and the normal to the surface of a star at a given point while u and v are the limb darkening coefficients fulfilling the inequality $0\leqslant v\ll u<1$.

The fractional loss of light f of the eclipsed star is defined as the ratio of integrals:

$$f=\left[\int_s J(\gamma)\cos\gamma d\sigma\right]\left[\int_S J(\gamma)\cos\gamma d\sigma\right]^{-1}, \qquad (2)$$

where s is the area of the eclipsed part of the stellar surface, S is the total area of that hemisphere of the eclipsed star which is directed towards us, and $d\sigma$ is the surface element. Evaluating the integrals in (2) we find (cf. Kopal 1949)

$$f=\frac{6}{6-2u-3v}\left[(1-u-v)f^U+\tfrac{2}{3}uf^D+\tfrac{1}{2}vf^Q\right]; \qquad (3)$$

here f^U is the value which f assumes for $u=v=0$, f^D that assumed for $u=1$ and $v=0$, and f^Q the value assumed for $u=0$ and $v=1$. These values are proportional to the associated alpha functions α_i^0 tabulated by Kopal (1947):

$$f^U=\alpha_0^0;\quad f^D=\tfrac{3}{2}\alpha_1^0;\quad f^Q=2\alpha_2^0. \qquad (4)$$

---

* Present address: Warsaw University Observatory, Warsaw, oland.

We shall denote by δ the apparent distance of the projected centers of the two component stars and by r_a, r_b, the radii of these stars; throughout this paper the subscript a will always refer to the smaller star and b to the larger star. We denote further, in accordance with usual notations,

$$k=r_a/r_b, \tag{5}$$

$$p=(\delta-r_b)/r_a, \tag{6}$$

and we define the normalized fractional loss of light $\alpha(k,p)$ by the equation

$$\alpha(k,p)=f(k,p)/f(k,-1). \tag{7}$$

We shall now consider two cases: occultation (the eclipse of the smaller star) and transit (the eclipse of the larger star).

Occultation. In this case we have $f_a(k,-1)=1$ and hence $\alpha_a(k,p)=f_a(k,p)$. Introducing the modified limb darkening coefficients

$$x_a=\frac{4u_a}{6-2u_a-3v_a}, \quad y_a=\frac{3v_a}{6-2u_a-3v_a}, \tag{8}$$

and making use of (3) we write the normalized fractional loss of light for the occultation in the form

$$\alpha_a=\alpha^U+(\alpha_a{}^D-\alpha^U)x_a+(\alpha_a{}^Q-\alpha^U)y_a, \tag{9}$$

where α^U, α^D, and α^Q are defined by formula (7), in which f is replaced by f^U, f^D, or f^Q, respectively. Writing (9) for two wavelengths λ_1 and λ_2 and subtracting we find

$$\alpha_a{}^{\lambda_1}-\alpha_a{}^{\lambda_2}=(\alpha_a{}^D-\alpha^U)(x_a{}^{\lambda_1}-x_a{}^{\lambda_2}) +(\alpha_a{}^Q-\alpha^U)(y_a{}^{\lambda_1}-y_a{}^{\lambda_2}). \tag{10}$$

Transit. Equation (3) gives for this case

$$f_b{}^U(k,-1)=k^2, \tag{11}$$

$$f_b{}^D(k,-1)=\tfrac{3}{2}k^2\Phi(k), \tag{12}$$

$$f_b{}^Q(k,-1)=(4-3k)k^3, \tag{13}$$

where the function $\Phi(k)$ is tabulated by Tsesevich (1940, Table 5). Introducing modified limb darkening coefficients

$$x_b=\frac{u_b\Phi(k)}{1-u_b-v_b+u_b\Phi(k)+\frac{1}{2}(4-3k)kv_b}, \tag{14}$$

$$y_b=\frac{\frac{1}{2}(4-3k)kv_b}{1-u_b-v_b+u_b\Phi(k)+\frac{1}{2}(4-3k)kv_b}, \tag{15}$$

we have, by (3), (7), and (11)–(13),

$$\alpha_b=\alpha^U+(\alpha_b{}^D-\alpha^U)x_b+(\alpha_b{}^Q-\alpha^U)y_b, \tag{16}$$

and finally, by subtracting Eqs. (16) written for wavelengths λ_1 and λ_2, we have

$$\alpha_b{}^{\lambda_1}-\alpha_b{}^{\lambda_2}=(\alpha_b{}^D-\alpha^U)(x_b{}^{\lambda_1}-x_b{}^{\lambda_2}) +(\alpha_b{}^Q-\alpha^U)(y_b{}^{\lambda_1}-y_b{}^{\lambda_2}). \qquad \text{(1}$$

B. Relation between $\alpha^{\lambda_1}-\alpha^{\lambda_2}$ and Color Index of t Eclipsing Binary

Denoting by l the rectified fractional light of th eclipsing system expressed in terms of the combine luminosities of its constituent stars and by L_a, L_b, th fractional luminosities of the smaller and the larg component, we have for an occultation the fractiona loss of light

$$f_a=(1-l)/L_a, \qquad \text{(18}$$

and for a transit

$$f_b=(1-l)/L_b. \qquad \text{(19}$$

We denote further by p_0, α_0, and λ the values of p, α and l for internal tangency in the case of total or annula eclipses (in this case $p_0=-1$ and $\alpha_0=1$) and for th deepest eclipse in the case of partial eclipses. Takin now the ratio of the fractional loss of light for a give p to that for p_0 we get for an arbitrary type of eclips the normalized fractional loss of light

$$\alpha=[(1-l)/(1-\lambda)]\alpha_0, \qquad \text{(20}$$

and hence

$$\alpha^{\lambda_1}-\alpha^{\lambda_2}=\frac{\alpha_0{}^{\lambda_1}}{1-\lambda^{\lambda_1}}(1-l^{\lambda_1})-\frac{\alpha_0{}^{\lambda_2}}{1-\lambda^{\lambda_2}}(1-l^{\lambda_2}). \qquad \text{(21}$$

Equation (21), after adding and subtracting the ter $\alpha_0{}^{\lambda_1}l^{\lambda_2}(1-\lambda^{\lambda_1})$, is

$$\alpha^{\lambda_1}-\alpha^{\lambda_2}=\frac{\alpha_0{}^{\lambda_1}}{1-\lambda^{\lambda_1}}(l^{\lambda_2}-l^{\lambda_1})+\left(\frac{\alpha_0{}^{\lambda_1}}{1-\lambda^{\lambda_1}}-\frac{\alpha_0{}^{\lambda_2}}{1-\lambda^{\lambda_2}}\right) \times(1-l^{\lambda_2}). \qquad \text{(22}$$

We shall consider the two types of eclipses separately

Occultation. Since $\alpha_a=f_a$, we have, by (18) and (20)

$$\alpha_{0a}/(1-\lambda_a)=1/L_a, \qquad \text{(23}$$

where α_{0a} is the value of α_0 for occultation. Let u introduce the parameter Z_0 depending only upon th difference in intrinsic colors of stars constituting th eclipsing binary system and defined by the equation

$$Z_0=1-\frac{L_b{}^{\lambda_2}/L_b{}^{\lambda_1}}{L_a{}^{\lambda_2}/L_a{}^{\lambda_1}}. \qquad \text{(24}$$

If the color indices C of the constituent stars are define by the equation

$$C=-2.5\log(L^{\lambda_2}/L^{\lambda_1}), \qquad \text{(25}$$

their difference is related to Z_0 by the equation

$$C_a-C_b=2.5\log(1-Z_0). \qquad \text{(26}$$

Iultiplying (22) by $L_a^{\lambda_1}$ we have, by (23)–(24),

$$^{\lambda_2}-l^{\lambda_1}=(\alpha_a^{\lambda_1}-\alpha_a^{\lambda_2})L_a^{\lambda_1}-(1-l^{\lambda_2})(1-L_a^{\lambda_1})Z_0. \quad (27)$$

ilarly, multiplying (10) by $L_a^{\lambda_1}$, we get, by using), the expression for the difference in light of an psing binary in two wavelengths

$$-l^{\lambda_1}=(\alpha_a^D-\alpha^U)(x_a^{\lambda_1}-x_a^{\lambda_2})L_a^{\lambda_1} +(\alpha_a^Q-\alpha^U)(y_a^{\lambda_1}-y_a^{\lambda_2})L_a^{\lambda_1} -(1-l^{\lambda_2})(1-L_a^{\lambda_1})Z_0. \quad (28)$$

e system of equations (28) written for different ises of the eclipse can be used for determining the intities $x_a^{\lambda_1}-x_a^{\lambda_2}$, $y_a^{\lambda_1}-y_a^{\lambda_2}$, and Z_0 by the method least squares.

Transit. Introducing the function $Y(k, -1)$ defined the equation

$$k, -1)=f_b(k, -1)/k^2 = \left\{1+\left[\frac{1}{\frac{3}{2}\Phi(k)}-1\right]x_b+\left[\frac{1}{(4-3k)k}-1\right]y_b\right\}^{-1}, \quad (29)$$

have, by (19)–(20),

$$\alpha_{0b}/(1-\lambda_b)=[k^2Y(k, -1)L_b]^{-1}, \quad (30)$$

l hence, by (22),

$$-l^{\lambda_1}=k^2Y^{\lambda_1}(k, -1)(\alpha_b^{\lambda_1}-\alpha_b^{\lambda_2})L_b^{\lambda_1} -\{1-[Y^{\lambda_1}(k, -1)L_b^{\lambda_1}]/ [Y^{\lambda_2}(k, -1)L_b^{\lambda_2}]\}(1-l^{\lambda_2}). \quad (31)$$

ce $y_b \ll 1$, and since $|[1/\frac{3}{2}\Phi(k)]-1|<0.17$ for 0.21, the following approximate expression is valid en k is not small:

$$\frac{(k, -1)}{(k, -1)}\approx 1-\left[\frac{1}{\frac{3}{2}\Phi(k)}-1\right](x_b^{\lambda_1}-x_b^{\lambda_2}) -\left[\frac{1}{(4-3k)k}-1\right](y_b^{\lambda_1}-y_b^{\lambda_2}). \quad (32)$$

Defining the parameter Z_t depending on the differ- e in intrinsic colors,

$$Z_t=1-\frac{L_a^{\lambda_2}/L_a^{\lambda_1}}{L_b^{\lambda_2}/L_b^{\lambda_1}}=\frac{Z_0}{Z_0-1}, \quad (33)$$

l multiplying (17) by $k^2Y^{\lambda_1}(k, -1)(1-L_a^{\lambda_1})$ we have, (31)–(32),

$$-l^{\lambda_1}=a_1(x_b^{\lambda_1}-x_b^{\lambda_2})+a_2(y_b^{\lambda_1}-y_b^{\lambda_2}) -(1-l^{\lambda_2})L_a^{\lambda_1}Z_t, \quad (34)$$

ere the coefficients are

$$=k^2Y^{\lambda_1}(k, -1)(1-L_a^{\lambda_1})(\alpha_b^D-\alpha^U) +(1-L_a^{\lambda_1}Z_t)[1-1/\tfrac{3}{2}\Phi(k)](1-l^{\lambda_2}), \quad (35)$$

$$=k^2Y^{\lambda_1}[(k, -1)(1-L_a^{\lambda_1})(\alpha_b^Q-\alpha^U) +(1-L_a^{\lambda_1}Z_t)[1-1/(4-3k)k](1-l^{\lambda_2}). \quad (36)$$

The approximation is fairly good for k not smaller than 0.20. The terms containing Z_t in (35)–(36) are in most cases negligibly small and successive approximations are not necessary for determining Z_t.

Simultaneous solution of Eqs. (28) and (34), i.e., a simultaneous solution for both primary and secondary eclipses, is possible when Z_0 and Z_t are replaced by one unknown, which can always be done if only we know the approximate value of, say, Z_0. Denoting this approximate value of Z_0 by $\bar{Z}_0$ and denoting

$$\bar{Z}_t=\bar{Z}_0/(\bar{Z}_0-1),$$

the expansion of Z_t in the Taylor series with only the first two terms retained is

$$Z_t\approx\bar{Z}_t-[(Z_0-\bar{Z}_0)/(\bar{Z}_0-1)^2]. \quad (37)$$

After substituting (37) into (34) we transfer the constant term $(1-l^{\lambda_2})L_a^{\lambda_1}\bar{Z}_t$ to the left side of (37). Similarly we substitute $Z_0=\bar{Z}_0+(Z_0-\bar{Z}_0)$ into (28) and transfer the constant term $(1-l^{\lambda_2})(1-L_a^{\lambda_1})\bar{Z}_0$ to the left side of this equation. The unknown $Z_0-\bar{Z}_0$ is now determined by the simultaneous solution of Eqs. (28) and (34). If $(1-\lambda_b^{\lambda_2})L_a^{\lambda_1}>(1-\lambda_a^{\lambda_2})(1-L_a^{\lambda_1})$, it is better to express Z_0 in terms of Z_t and not the reverse; the difference between the two procedures, however, is very small if the approximate value $\bar{Z}_0$ is sufficiently close to the true value.

The simultaneous solution of Eqs. (28) and (34) for primary and secondary eclipses can be made not only in the case of a circular orbit but also in the case of elliptical orbit of small eccentricity. The geometrical elements p_0, r_a, r_b, and i (inclination of the orbit) obtained in the case of an elliptical orbit from each eclipse separately on the assumption of a circular orbit are somewhat different, but the ratio k is the same for both solutions. And k is the only geometrical element upon which Eqs. (28) and (34) depend.

C. Computation of $\alpha^D-\alpha^U$ and $\alpha^Q-\alpha^U$

To make a solution of Eqs. (28) and (34) we must know the elements k and L_a from a solution based on the observations in one color, say λ_1. We must also assume (or determine from the observations in one color) the coefficients of limb darkening $u_a^{\lambda_1}$, $u_b^{\lambda_1}$, $v_a^{\lambda_1}$, and $v_b^{\lambda_1}$ in this color. Knowing these elements we compute for every normal point of the light curve the normalized fractional losses of light for wavelength λ_1, using for partial phases of the occultation the equation

$$\alpha_a^{\lambda_1}=(1-l^{\lambda_1})/L_a^{\lambda_1}; \quad (38)$$

for totality we have $\alpha_a^{\lambda_1}=1$ and for transit

$$\alpha_b^{\lambda_1}=(1-l^{\lambda_1})/k^2Y^{\lambda_1}(k, -1)(1-L_a^{\lambda_1}). \quad (39)$$

The values $\alpha_a^{\lambda_1}$ and $\alpha_b^{\lambda_1}$ found from (38) and (39) are entered into Tsesevich's (1940) table of the function $p(k,\alpha)$ for the assumed value of u^{λ_1}. The values p, TABLE I. $(\alpha^D-\alpha^U)k^2\times10^4$. Transit.

$p \backslash k$	1.00	0.95	0.90	0.85	0.80	0.75	0.70	0.65	0.60	0.55	0.50	0.45	0.40	0.35	0.30	0.25
1.00	0	0	0	0	0	0	0	0	0	0	0	0	0	0	0	0
0.95	− 34	− 32	− 30	− 28	− 25	− 23	− 20	− 18	− 16	− 13	− 11	− 9	− 8	− 6	− 4	− 3
0.90	− 81	− 78	− 74	− 69	− 63	− 57	− 51	− 46	− 40	− 34	− 29	− 24	− 20	− 15	− 12	− 8
0.85	−129	−126	−121	−113	−105	− 96	− 86	− 77	− 68	− 58	− 50	− 41	− 34	− 26	− 20	− 14
0.80	−172	−173	−167	−158	−147	−135	−122	−109	− 96	− 84	− 71	− 60	− 48	− 38	− 29	− 21
0.75	−208	−215	−211	−201	−189	−174	−159	−142	−126	−109	− 93	− 78	− 64	− 50	− 38	− 27
0.70	−237	−251	−250	−242	−228	−212	−194	−175	−155	−135	−116	− 97	− 79	− 62	− 47	− 34
0.65	−258	−282	−285	−279	−265	−248	−228	−206	−183	−160	−137	−115	− 94	− 74	− 56	− 40
0.60	−271	−307	−316	−312	−299	−281	−259	−235	−211	−184	−158	−133	−109	− 86	− 65	− 47
0.55	−275	−325	−341	−341	−330	−312	−289	−263	−236	−207	−178	−150	−123	− 97	− 74	− 53
0.50	−271	−336	−361	−366	−357	−340	−316	−289	−260	−229	−197	−166	−136	−108	− 82	− 59
0.45	−260	−342	−376	−386	−381	−364	−341	−313	−282	−249	−215	−182	−149	−118	− 90	− 65
0.40	−240	−341	−386	−402	−401	−386	−364	−335	−302	−268	−232	−196	−161	−128	− 98	− 70
0.35	−213	−334	−391	−415	−417	−405	−383	−354	−321	−285	−247	−209	−172	−137	−104	− 75
0.30	−179	−322	−391	−423	−430	−421	−400	−372	−338	−300	−261	−221	−182	−145	−111	− 80
0.25	−139	−304	−387	−427	−439	−433	−414	−386	−352	−314	−273	−232	−192	−153	−116	− 84
0.20	− 93	−282	−378	−427	−446	−443	−426	−399	−365	−326	−284	−242	−200	−159	−122	− 88
0.15	− 43	−255	−366	−424	−448	−450	−435	−409	−375	−336	−294	−250	−207	−165	−126	− 91
0.10	+ 12	−225	−350	−418	−448	−454	−442	−417	−384	−344	−302	−257	−213	−170	−130	− 94
0.05	+ 70	+191	−331	−408	−445	−455	−446	−423	−390	−351	−308	−263	−218	−174	−133	− 96
0.00	+131	−155	−309	−396	−440	−454	−448	−426	−395	−356	−313	−268	−222	−178	−136	− 98
−0.05	+194	−116	−285	−381	−432	−451	−447	−428	−397	−359	−316	−270	−225	−180	−138	− 99
−0.10	+258	− 76	−259	−365	−422	−445	−444	−427	−398	−360	−318	−272	−226	−181	−139	−100
−0.15	+322	− 35	−231	−346	−409	−437	−439	−424	−396	−360	−318	−272	−226	−182	−139	−100
−0.20	+385	+ 6	−203	−326	−395	−427	−432	−419	−393	−357	−316	−271	−226	−181	−138	−100
−0.25	+446	+ 46	−174	−305	−380	−415	−424	−412	−387	−353	−312	−269	−224	−179	−137	− 99
−0.30	+504	+ 86	−146	−284	−363	−402	−413	−403	−380	−347	−307	−264	−220	−177	−135	− 98
−0.35	+558	+123	−117	−262	−345	−387	−400	−393	−371	−339	−301	−259	−216	−173	−132	− 96
−0.40	+606	+157	− 91	−240	−326	−370	−386	−380	−360	−329	−292	−252	−210	−168	−129	− 93
−0.45	+648	+187	− 66	−218	−307	−353	−370	−365	−346	−318	−282	−243	−202	−162	−124	− 90
−0.50	+680	+212	− 44	−197	−287	−334	−352	−349	−331	−304	−270	−233	−194	−156	−119	− 86
−0.55	+704	+231	− 24	−177	−267	−314	−333	−330	−314	−288	−256	−221	−184	−147	−113	− 81
−0.60	+715	+244	− 9	−159	−247	−293	−311	−310	−295	−271	−240	−207	−172	−138	−106	− 76
−0.65	+712	+248	+ 2	−143	−227	−271	−288	−287	−273	−251	−222	−191	−159	−127	− 97	− 70
−0.70	+694	+242	+ 8	−128	−206	−248	−263	−262	−249	−228	−202	−174	−144	−115	− 88	− 63
−0.75	+657	+227	+ 9	−115	−186	−222	−236	−234	−222	−203	−179	−154	−128	−102	− 78	− 56
−0.80	+597	+199	+ 4	−104	−164	−194	−205	−203	−191	−174	−153	−131	−109	− 86	− 66	− 47
−0.85	+511	+158	− 5	− 93	−141	−163	−170	−166	−156	−141	−124	−106	− 87	− 69	− 53	− 38
−0.90	+393	+102	− 19	− 80	−112	−126	−128	−124	−115	−104	− 91	− 77	− 63	− 50	− 38	− 27
−0.95	+232	+ 37	− 28	− 58	− 72	− 77	− 76	− 72	− 66	− 59	− 51	− 43	− 35	− 28	− 21	− 15
−1.00	0	0	0	0	0	0	0	0	0	0	0	0	0	0	0	0
q																
0.10	0	+ 11	+ 28	+ 46	+ 63	+ 78	+ 92	+103	+112	+118	+121	+121	+118	+112	+103	+ 92
0.20	0	21	52	84	115	144	168	189	204	214	219	218	212	201	184	161
0.30	0	29	72	117	160	200	233	261	281	295	301	299	290	273	248	217
0.40	0	36	89	145	198	244	288	321	346	362	368	365	353	332	301	262
0.50	0	42	104	168	230	285	333	371	399	417	424	420	405	380	344	298
0.60	0	46	115	187	255	316	369	411	442	461	468	463	446	417	377	327
0.70	0	50	124	201	274	340	396	441	474	494	502	496	478	446	403	348
0.80	0	52	130	211	288	357	416	463	497	518	526	519	500	467	421	363
0.90	0	54	134	217	296	368	428	476	511	532	540	533	513	478	431	372
1.00	0	+ 54	+135	+219	+299	+371	+432	+480	+516	+537	+545	+538	+517	+482	+435	+375

found for every normal point from these tables, are entered into the tables of $\alpha^D-\alpha^U$ and $\alpha^Q-\alpha^U$, which should be tabulated as functions of k and p. The tables of $\alpha^D-\alpha^U$ can be easily obtained by taking the differences of functions $\alpha^D(k,p)$ and $\alpha^U(k,p)$ tabulated by Tsesevich (1939, Table III and 1940, Table D). The function $\alpha^D-\alpha^U$ is tabulated for occultation by Irwin (1947, Table 4) and for transit in Table I of the present paper (multiplied by k^2). Values of $\alpha^D-\alpha^U$ for $k=0.96$, 0.97, 0.98, and 0.99 can be obtained from the tables of α^U published for these arguments by Merrill (1950) and tables of α^D which can be obtained from the Princeton University Observatory on request.

For annular phases of a transit eclipse, $(\alpha^D-\alpha^U)k^2$ is tabulated in Table I as a function of arguments k and q. The values of q can be found from the table of $q(k,X)$ given by Tsesevich (1940, Tables XVI and XVIa), where X is computed from the equation

$$X=(\alpha_b{}^{\lambda_1}-1)/A^x(k); \qquad (40$$

the values $A^x(k)$ are also tabulated by Tsesevich (1940 Tables XVIII–XXI), who denotes by x our u. Th values $\alpha^D-\alpha^U$ for annular phases can be found als directly from the formula

$$\alpha_b{}^D-\alpha^U=[A(k)/A^x(k)](\alpha_b-1), \qquad (41$$

where $A(k)$ is tabulated by Tsesevich (1940, Tabl XVII).

The terms $\alpha^Q-\alpha^U$ are not yet tabulated. They ca be simply expressed in terms of the "boundary inte grals" $I_{1,0}{}^0$ and $I_{-1,2}{}^0$ tabulated by Kopal (1947). Fo occultation we have

$$\alpha_a{}^Q-\alpha^U=\frac{kp+1}{k^4}[I_{-1,2}{}^0-2(kp+1)I_{1,0}{}^0], \qquad (42$$

where the boundary integrals are taken from p tables for the argument α defined by the formula

$$\cos\alpha=\tfrac{1}{2}(k^2p^2+2kp-k^2+2)/(kp+1). \qquad (43)$$

For the partial phases of transit eclipse we have

$$\alpha_b{}^Q-\alpha^U=\frac{(k^{-1}+p)k}{4-3k}\left[I_{-1,2}{}^0-2\left(\frac{1}{k}+p\right)I_{1,0}{}^0\right] -\left[1-\frac{1}{(4-3k)k}\right]\alpha^U, \qquad (44)$$

where the boundary integrals are taken from p tables for α defined by

$$\cos\alpha=\tfrac{1}{2}(kp^2+k+2p)/(kp+1). \qquad (45)$$

Finally, for annular phases of transit eclipse we have

$$\alpha_b{}^Q-\alpha^U=\frac{(q-1)(k-1)}{4-3k}\left[I_{-1,2}{}^0-(q-1)\left(1-\frac{1}{k}\right)\right] +\frac{1}{(4-3k)k}-1, \qquad (46)$$

where the boundary integral is taken from a tables for α defined by

$$\cos\alpha=\{(1-k^{-1})q^2+4[(1+\tfrac{1}{2}k^{-1})q-1]\}/ \{(1-k^{-1})q^2-4[(1-\tfrac{1}{2}k^{-1})q-1]\}. \qquad (47)$$

III. INFLUENCE OF THE ERRORS OF RECTIFICATION

A. Analysis of the Observations outside the Eclipses

The harmonic analysis of the observations outside of eclipse is done by solving by the method of least squares the two independent systems of linear equations:

$$l_0{}^{\lambda_1}-1=A^{\lambda_1}-B^{\lambda_1}\cos\theta+C^{\lambda_1}\sin^2\theta, \qquad (48)$$

$$l_0{}^{\lambda_2}-l_0{}^{\lambda_1}=(A^{\lambda_2}-A^{\lambda_1})-(B^{\lambda_2}-B^{\lambda_1})\cos\theta +(C^{\lambda_2}-C^{\lambda_1})\sin^2\theta, \qquad (49)$$

where θ is the phase counted from primary minimum and l_0 is nonrectified fractional light of the eclipsing binary expressed in terms of the mean of lights at phases $\theta=90°$ and 270° taken as unity.

The rectified fractional lights l^{λ_1} and the differences $l^{\lambda_2}-l^{\lambda_1}$, which have to be entered into Eqs. (28) and (34) are computed, following Kopal (1959), from the equations

$$l^{\lambda_1}=l_0{}^{\lambda_1}(1-A^{\lambda_1}-C^{\lambda_1}\sin^2\theta)+B^{\lambda_1}\cos\theta +(1-l_0{}^{\lambda_1})(\alpha^{\lambda_1}-b^{\lambda_1}\cos\theta-\gamma^{\lambda_1}\cos^2\theta), \qquad (50)$$

$$\begin{aligned} l^{\lambda_2}-l^{\lambda_1}= {}&(l_0{}^{\lambda_2}-l_0{}^{\lambda_1})[(1-A^{\lambda_1}-\alpha^{\lambda_1}+\gamma^{\lambda_1}) \\ &+b^{\lambda_1}\cos\theta-(C^{\lambda_1}+\gamma^{\lambda_1})\sin^2\theta] \\ &-l_0{}^{\lambda_2}[(A^{\lambda_2}-A^{\lambda_1})+(C^{\lambda_2}-C^{\lambda_1})\sin^2\theta] \\ &+(B^{\lambda_2}-B^{\lambda_1})\cos\theta+(1-l_0{}^{\lambda_2}) \\ &\times[(\alpha^{\lambda_2}-\alpha^{\lambda_1}+\gamma^{\lambda_2}-\gamma^{\lambda_1})-(b^{\lambda_2}-b^{\lambda_1})\cos\theta \\ &+(\gamma^{\lambda_2}-\gamma^{\lambda_1})\sin^2\theta], \qquad (51) \end{aligned}$$

where the constants A, B, C, and their differences are the values obtained from the least-squares solution of Eqs. (48)–(49), while the coefficients α, b, and γ cannot be determined from the observations and must be estimated theoretically; the methods of such estimations are described by Kopal (1959). In general, $|\alpha|+|b|+|\gamma|\ll|A|+|B|+|C|$.

B. Correction of the Errors of Rectification

Among the terms in Eq. (51) the terms $l_0{}^{\lambda_2}(A^{\lambda_2}-A^{\lambda_1})$ and $(B^{\lambda_2}-B^{\lambda_1})\cos\theta$ can have absolute values much larger than any of the other terms except the first because the coefficients $l_0{}^{\lambda_2}$ and $\cos\theta$ can be near unity during the eclipse; the other terms in (51) contain factors such as $\sin^2\theta$ or $l_0{}^{\lambda_2}-l_0{}^{\lambda_1}$, which are in most cases much smaller than unity during the eclipse. Since $A^{\lambda_2}-A^{\lambda_1}$ and $B^{\lambda_2}-B^{\lambda_1}$ obtained from the solution of Eqs. (49) are not exact values we shall denote the true values of these coefficients by $A^{\lambda_2}-A^{\lambda_1}+\delta_A$ and $B^{\lambda_2}-B^{\lambda_1}+\delta_B$. The inexact value $l^{\lambda_2}-l^{\lambda_1}$ obtained from (51) should be replaced in (28) and (34) by the true value $l^{\lambda_2}-l^{\lambda_1}-l_0{}^{\lambda_2}\delta_A+\delta_B\cos\theta$. The corrections δ_A and δ_B should be treated as additional unknowns in these equations which now take the final form

Occultation:

$$\begin{aligned} &l^{\lambda_2}-l^{\lambda_1}+(1-l^{\lambda_2})(1-L_a{}^{\lambda_1})\bar{Z}_0 \\ &=(\alpha_a{}^D-\alpha^U)L_a{}^{\lambda_1}(x_a{}^{\lambda_1}-x_a{}^{\lambda_2}) \\ &\quad+(\alpha_a{}^Q-\alpha^U)L_a{}^{\lambda_1}(y_a{}^{\lambda_1}-y_a{}^{\lambda_2})-(1-l^{\lambda_2}) \\ &\quad\times(1-L_a{}^{\lambda_1})(Z_0-\bar{Z}_0)+l_0{}^{\lambda_2}\delta_A-\delta_B\cos\theta; \qquad (52) \end{aligned}$$

Transit:

$$\begin{aligned} &l^{\lambda_2}-l^{\lambda_1}+(1-l^{\lambda_2})L_a{}^{\lambda_1}\bar{\bar{Z}}_t \\ &=a_1(x_b{}^{\lambda_1}-x_b{}^{\lambda_2})+a_2(y_b{}^{\lambda_1}-y_b{}^{\lambda_2}) \\ &\quad+[(1-l^{\lambda_2})L_a{}^{\lambda_1}/(\bar{\bar{Z}}_0-1)^2](Z_0-\bar{\bar{Z}}_0) \\ &\quad+l_0{}^{\lambda_2}\delta_A-\delta_B\cos\theta. \qquad (53) \end{aligned}$$

In most cases the quadratic terms $y^{\lambda_1}-y^{\lambda_2}$ can be neglected and Eqs. (52)–(53) can be solved by the method of least squares for the five unknowns: $x_a{}^{\lambda_1}-x_a{}^{\lambda_2}$, $x_b{}^{\lambda_1}-x_b{}^{\lambda_2}$, $Z_0-\bar{Z}_0$, δ_A, and δ_B.

It should be emphasized that the purpose of introducing the additional unknowns δ_A and δ_B is not so much to increase the accuracy of determining the differential limb darkening as to increase the reliability of the mean errors obtained from the least-squares solution. The mean errors obtained by neglecting these two unknowns would be systematically in error.

It should be noted that the term

$$(1-l_0{}^{\lambda_2})(\alpha^{\lambda_2}-\alpha^{\lambda_1}+\gamma^{\lambda_2}-\gamma^{\lambda_1})$$

in (51) is varying proportionally to the terms containing Z_0 in Eqs. (52)–(53). This means that the error of the term $\alpha^{\lambda_2}-\alpha^{\lambda_1}+\gamma^{\lambda_2}-\gamma^{\lambda_1}$ contributes to the error of Z_0 and does not affect the other unknowns.

If the solution is not made simultaneously for both eclipses, the unknown δ_B should not be determined. Considering only one eclipse, we have

$$\delta_B\cos\theta\approx(1-l^{\lambda_2})\,\mathrm{sgn}(\cos\theta)\delta_B+l^{\lambda_2}\,\mathrm{sgn}(\cos\theta)\delta_B,\tag{54}$$

where $\mathrm{sgn}(\cos\theta)$ equals $+1$ for primary eclipse and -1 for secondary. The two terms on the right side of (54) are varying proportionally to the terms in (52)–(53) containing Z_0 and δ_A, respectively, which means that δ_B does not need to be determined separately. Making a solution of Eqs. (52) without determining δ_B we obtain, instead of Z_0 and δ_A, the quantities $Z_0+[\mathrm{sgn}(\cos\theta)\times(\delta_B+\delta_b)-\delta_{\alpha+\gamma}]/(1-L_a^{\lambda_1})$ and $\delta_A-\mathrm{sgn}(\cos\theta)\delta_B$, where δ_b and $\delta_{\alpha+\gamma}$ are corrections to the terms $b^{\lambda_2}-b^{\lambda_1}$ and $\alpha^{\lambda_2}-\alpha^{\lambda_1}+\gamma^{\lambda_2}-\gamma^{\lambda_1}$, respectively.

The contributions to $l^{\lambda_2}-l^{\lambda_1}$ resulting from the effects of spherical harmonic distortion of order higher than the second (cf. Kopal 1959) consist of terms varying proportionally to $\cos\theta$, those varying proportionally to $l_0^{\lambda_2}$, and terms independent of phase. The terms of the two first types contribute to δ_A and δ_B, respectively. The terms independent of phase are eliminated together with δ_B only in the case when the solution is not made simultaneously for both eclipses. These terms are in most cases negligibly small.

The rectification eliminates only the part of the photometric terms resulting from the aspherical shape of stars. The remaining terms which can not be eliminated are called perturbations within minima. An estimate of the influence of these terms (as given by Kopal 1959) on $l^{\lambda_2}-l^{\lambda_1}$ was made for moderately distorted stars for which $r_a+r_b=0.50$. It was found that for such stars the errors of $l^{\lambda_2}-l^{\lambda_1}$ due to perturbations within minima should not exceed 0.003. This means they are negligible for the present accuracy of photometric observations. The methods described in this paper should not, however, be applied to eclipsing binaries for which r_a+r_b exceeds, say, 0.55. This maximum value should be diminished if the difference in intrinsic colors of stars constituting a binary is very large since in this case the influence of perturbations becomes also larger.

C. Weights of Observational Equations and Additional Equations Describing the Observations outside of Eclipses

Let us suppose that, as is usually the case, the differences $l^{\lambda_2}-l^{\lambda_1}$ must be expressed in stellar magnitudes to make their mean errors independent of the brightness of the eclipsing binary. If the considered normal point is formed of n observations of unit weight, the equation (52) or (53) corresponding to this normal point must be multiplied by $n^{\frac{1}{2}}/(l^{\lambda_1}+l^{\lambda_2})$. The equations multiplied by such factors will have equal weight. Let the color index, expressed in magnitudes and corresponding to an observation of unit weight made during the eclipse, be characterized by the mean error ϵ. It can be shown that the mean error of the left side of Eq. (52) or (53) multiplied by the afore-mentioned weighting facto equals $(\ln 10)\epsilon/5$ or 0.4605ϵ. The mean error of this lef side is usually an order of magnitude larger than th product of an unknown on the right side and the mear error of its coefficient. The errors of these coefficient result from the uncertainty in determining α^{λ} fron observed brightness by means of Eq. (38) or (39) If only the amplitude of light variations is much large than the amplitude of color variations, the errors of th coefficients of the unknowns in Eqs. (52)–(53) hav negligible influence on the results of solution. Thi condition is essential for validity of the method presented in this paper.

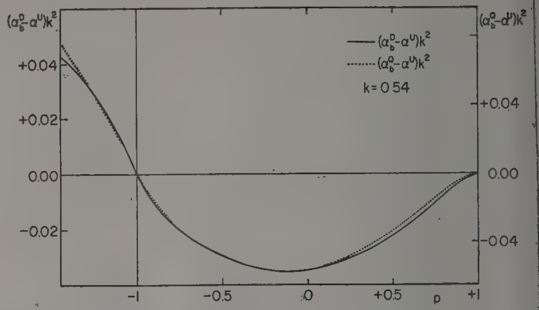

FIG. 1. Coefficients $(\alpha^D-\alpha^U)k^2$ and $(\alpha^Q-\alpha^U)k^2$ for primary eclips of YZ Cassiopeiae (transit).

In order that the unknowns δ_A and δ_B may be reliabl determined, Eqs. (52)–(53), following the procedur first introduced by Piotrowski (1948), must be supplemented by two additional equations containing information about the accuracy with which $A^{\lambda_2}-A^{\lambda_1}$ an $B^{\lambda_2}-B^{\lambda_1}$ are determined from the harmonic analysis o the observations outside of eclipse. These will be equations of the form $\delta_A=0$ and $\delta_B=0$ multiplied by such factors that the weight of these equations is the same as that of all the other equations of the form of (52)–(53 multiplied by the weighting factors. Let the mean error of $A^{\lambda_2}-A^{\lambda_1}$ and $B^{\lambda_2}-B^{\lambda_1}$ as obtained from the least squares solution of Eqs. (49) be $\epsilon_{\Delta A}$ and $\epsilon_{\Delta B}$, respectively. Now the two additional equations are

$$0.4605(\epsilon/\epsilon_{\Delta A})\delta_A=0, \qquad (55$$

$$0.4605(\epsilon/\epsilon_{\Delta B})\delta_B=0; \qquad (56$$

we can easily see that if the mean errors of δ_A and δ in Eqs. (55)–(56) are $\epsilon_{\Delta A}$ and $\epsilon_{\Delta B}$, the error of the lef side of each of these equations equals 0.4605ϵ.

IV. EXAMPLE. DIFFERENTIAL LIMB DARKENING OF YZ CASSIOPEIAE

The eclipsing binary YZ Cassiopeiae was selected a an example because the coefficients of limb darkenin have been determined for this system with an accurac much greater than for any other eclipsing binary. Th binary was observed by Kron (1939, 1942) in blue an

TABLE II. Results for YZ Cassiopeiae.

	Assumed				Obtained				
Solution	k	u_b^{4500}	u_a^{4500}	L_a^{4500}	$x_b^{4500}-x_b^{6700}$	$u_b^{4500}-u_b^{6700}$	$x_a^{4500}-x_a^{6700}$ $=u_a^{4500}-u_a^{6700}$	Z_0	$B^{4500}-B^{6700}$
I	0.540	0.49	0.45	0.063	0.330 ±.013	0.368 ±.014	−0.05 ±.27	0.438 ±.012	+0.004 ±.001
II	0.532	0.60			0.325 ±.011	0.342 ±.012	−0.09 ±.24	0.435 ±.010	+0.004 ±.001
Kron (Kopal, Shapley)	0.542 ±.012	0.49 ±.06	0.45 ±.16	0.063 ±.002		0.16 ±.08	−0.03 ±.24	0.439	+0.003

red colors (effective wavelengths 4500 and 6700 A) and independent solutions were made by this author for the observations in each color. The geometrical elements obtained from these solutions are slightly different. According to Kopal and Shapley (1956) the quadratic terms in the law of limb darkening (our coefficients v) must be taken into account if the observations in both colors have to be explained by the same set of geometrical elements.

This opinion is not supported by the present analysis, which shows that the observations in both colors can be well explained by a single set of geometrical elements without introducing the quadratic terms in the law of limb darkening. The coefficients $\alpha^Q-\alpha^U$ of the unknown $y^{\lambda_1}-y^{\lambda_2}$ in (10) and (17) are, in the case of YZ Cassiopeiae, almost exactly proportional to the coefficients $\alpha^D-\alpha^U$ of the unknown $x^{\lambda_1}-x^{\lambda_2}$. This is shown on Figs. 1 and 2, where both these coefficients are plotted as a function of p.

The proportionality of the coefficients of $y^{\lambda_1}-y^{\lambda_2}$ to those of $x^{\lambda_1}-x^{\lambda_2}$ excludes the possibility of independent determination of these two unknowns. For that reason the solution of Eqs. (52)–(53) for Kron's observations of YZ Cassiopeiae was made on the assumption that $v^{\lambda_1}=v^{\lambda_2}=0$. For estimating the influence of the assumed values of k and of the blue coefficient of limb darkening on the final results two least-squares solutions were made, each for a different set of initial elements. The first set of assumed values of k, L_a^{4500}, and u^{4500} is almost identical with values given for YZ Cassiopeiae in the catalogue by Kopal and Shapley (1956) and with values obtained from the blue observations by Kron (1942). The other set is based on the value of the radius of the smaller star obtained by Kron from the observations in the red light only. This second set of elements does not represent the blue observations as well as the first set; the mean O–C is about 30% larger.

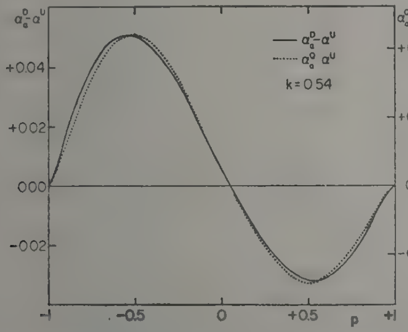

FIG. 2. Coefficients $\alpha^D-\alpha^U$ and $\alpha^Q-\alpha^U$ for secondary eclipse of YZ Cassiopeiae (occultation).

The results of both solutions are given with their mean errors in Table II. We can see that a rather large change of the initially assumed elements has very little influence on the values of $x^{4500}-x^{6700}$ and Z_0 obtained from the solution. The difference $u^{4500}-u^{6700}$ is somewhat more strongly affected because it depends explicitly on the assumed value of u^{4500}. The theoretical changes of color computed from the results of both solutions are compared in Fig. 3 with values of $l^{6700}-l^{4500}$ resulting from Kron's observations. The curves computed from both solutions almost coincide. This means that the mean errors given in the upper part of Table II should be increased only slightly to take into account the uncertainty of the assumed values of k, u^{4500}, and L_a^{4500}.

The most probable value of the difference of limb darkening coefficients for star eclipsed in primary minimum

$$u^{4500}-u^{6700}=0.35\pm0.02 \text{ (m.e.)} \tag{57}$$

is about two times larger than the value resulting from

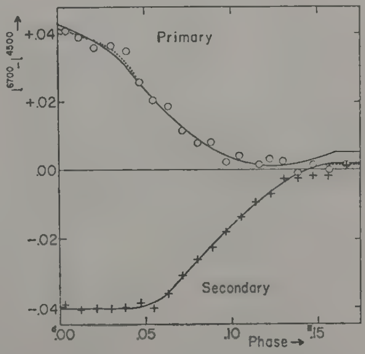

FIG. 3. Color indices of YZ Cassiopeiae according to observations made by Kron. The solid line represents solution I; the dashed line, solution II. Open circles are the observed values for primary eclipse, crosses for secondary eclipse.

the independent solutions made by Kron (1942) for each color separately. The value (57) is larger than the theoretical values of this difference for a star of spectral type A3 which are 0.29 according to Münch and Chandrasekhar (1949), 0.23 according to Hosokawa (1955), and 0.27 according to van't Veer (1960).

The solutions for investigating the differential limb darkening of several other well observed eclipsing binaries will be made by the author with the aid of an electronic computer. The results will be published as the second part of this paper.

ACKNOWLEDGMENTS

The author takes pleasure in thanking Professor Z. Kopal and Professor S. L. Piotrowski for critical reading of the manuscript and helpful suggestions.

REFERENCES

Hosokawa, Y. 1955, *Sci Rept. Tôhoku Univ.* Ser. I, **39**, No. 1 (*Sendai Astron. Rap.* No. 42).
Irwin, J. B. 1947, *Astrophys. J.* **106**, 380.
Kopal, Z. 1946, *Introduction to the Study of Eclipsing Binaries* (Harvard University Press, Cambridge, Massachusetts).
——. 1947, *Harvard Circ.* **450**.
——. 1949, *ibid.* **454**.
——. 1959, *Close Binary Systems* (John Wiley & Sons, Inc., New York).
Kopal, Z. and Shapley, M. B. 1956, *Jodrell Bank Ann.* **1**, 141.
Kron, G. E. 1939, *Lick Bull.* **19**, 59.
——. 1942, *Astrophys. J.* **96**, 173.
Merrill, J. E. 1950, *Contrib. Princeton Univ. Obs.* **23**.
Münch, G. and Chandrasekhar, S. 1949, *Harvard Circ.* **453**.
Piotrowski, S. L. 1948, *Astrophys. J.* **108**, 36.
Russell, H. N. and Merrill, J. E. 1952, *Contrib. Princeton Univ. Obs.* **26**.
Tsesevich, V. P. 1939, *Bull. Astron. Inst. U.S.S.R. Acad. Sci.* No. 45.
——. 1940, *ibid.* No. 50.
Veer, van't F. 1960, *Recherches Astron. Obs. Utrecht* **14**(3).

HE ASTRONOMICAL JOURNAL VOLUME 66, NUMBER 8 OCTOBER, 1961

The Eclipsing System V Tucanae

FRANK BRADSHAW WOOD AND GEORGE E. MCCLUSKEY, JR.
Flower and Cook Observatory, University of Pennsylvania, Philadelphia, Pennsylvania

(Received June 8, 1961)

Photoelectric observations of 171 yellow and 169 blue magnitudes of V Tucanae are presented. The available evidence indicates a constant period. The system was brighter on two nights than on the others. The preliminary elements and their permissible ranges are computed.

I. INTRODUCTION

THE variability of V Tuc (CPD—72°69, 185.1907, HV 3021, HD 5148) was discovered by Miss annon (Pickering 1907, 1908). Further observations ere made in 1917–18 (Dawson 1918) and the period of e variable was found to be 0.8709 day. Dawson also und a length of minimum to be about $0\overset{\mathrm{d}}{.}18$ and the pth 1.8 mag. The arbitrary scale he used did not permit mputation of the physical elements of the system. aposchkin (1947) included the system in his general rvey of eclipsing systems by photographic estimates. Iiss Cannon (Cannon and Pickering 1918) classified e spectrum as A2. Improved light elements and a ery brief description of the light curve, based on the resent observations, have been given by Wood (1959).

II. OBSERVATIONS

The observations were made by the senior author the Mount Stromlo Observatory of the Australian ational University, using the Reynolds 30-inch reector and a 1P21 multiplier photocell refrigerated ith dry ice. The filters have been described by ascoigne and Burr (1956). The spectral ranges corspond closely to the International *P* and *V* system. he linearity of the direct-current amplifier has been arefully checked in the laboratory of the Mount tromlo electronics staff; rougher checks on the stars howed that any variation was less than the error of bservation.

The observations in Table I are expressed in heliontric Julian days, with phases from the elements iven by Wood (1959).

$$\text{Pr. Min.} = \text{JD } 243\,6139.142 + 0\overset{\mathrm{d}}{.}87091649\,E. \qquad (1)$$

he comparison star was BD−72°70. Correction for ifferential extinction is no case exceeded $0\overset{\mathrm{m}}{.}002$. ecause of the rapidity of the light changes during clipse, it was found desirable to take two readings in ach color on the variable star between successive obrvations of the comparison; in order to make the bservations as uniform as possible, the same practice as carried out on all parts of the light curve.

Careful inspection on the best nights showed no ebulosity or faint stars in the region around the varible included in the diaphragm used. However, difficulty as encountered in attempting to take sky readings nearby in that the sky brightness did not repeat from region to region and was consistently brighter than the sky readings near the comparison star. A photograph taken by Dr. A. R. Hogg with the 74-inch Mount Stromlo reflector clearly shows nebulosity in some of the regions where sky readings were attempted. Hence, for purposes of reductions, the sky readings near the comparison star were interpolated to the time of the observations of the variable. Further justification for this treatment will be found in the discussion of the reliability of the solution.

III. EPOCH AND PERIOD

The published times of minimum are listed in Table II, together with residuals from the new light elements given in (1). There is no evidence for change of period but the evidence is so meager that small changes could easily have gone undetected.

IV. DISCUSSION

When the reflected yellow observations between minima were plotted, they fell into two clearly distinct sets, separated by about 0.07 mag. A similar situation existed in the blue, except that the separation was only about 0.04 mag. and the division was not as clearly shown. The observations comprising the upper curve were all taken on two consecutive nights; the system was obviously brighter on these two nights than on the others and the excess brightness continued through secondary.

Obviously, any attempt to make a rectification based on the average of the observations would produce a meaningless solution which would fit neither set satisfactorily. Therefore, four separate rectifications were carried out, i.e., one in each color for both the upper and lower curves. Rectification coefficients were computed for the upper and lower curves separately. Rectification of each followed the standard procedure (Russell and Merrill 1952). In the conventional equation

$$I = A_0 + A_1 \cos B + A_2 \cos 2\theta + B_1 \sin\theta + B_2 \sin\theta, \qquad (2)$$

the following values were found from a least-squares solution:

Upper blue curve, $A_0 = 0.9522 \pm 0.0011$,
$A_1 = -0.0362 \pm 0.0007$,
$A_2 = -0.0286 \pm 0.0022$,

TABLE Ia. Yellow observations of V Tucanae.

JD Hel. 2430000+	Phase	m	JD Hel. 2430000+	Phase	m	JD Hel. 2430000+	Phase	m
6134.9839	0.1965	−0.309	6136.1977	0.5394	−0.297	6165.9871	0.7176	−0.38
.9881	0.2007	0.318	6137.9576	0.5574	0.399	.9984	0.7289	0.38
.9971	0.2097	0.299	.9698	0.5696	0.377	6166.0038	0.7343	0.38
6135.0008	0.2134	0.314	6138.0244	0.6242	0.388	.0306	0.7611	0.39
.0105	0.2231	0.310	.0291	0.6289	0.389	.0349	0.7654	0.38
.0138	0.2264	0.309	.0399	0.6397	0.379	.0465	0.7770	0.40
.0318	0.2444	0.317	.9943	0.7232	0.391	.0515	0.7820	0.39
.0352	0.2478	0.320	.9982	0.7271	0.390	.0636	0.7941	0.45
.0435	0.2561	0.317	6139.0088	0.7377	0.349	.0676	0.7981	0.48
.0481	0.2607	0.308	.0148	0.7437	0.419	.0792	0.8097	0.57
.0588	0.2714	0.308	.0250	0.7539	0.389	.0839	0.8144	0.63
.0642	0.2768	0.357	.0293	0.7582	0.398	.0877	0.8182	0.68
.0741	0.2867	0.304	.0415	0.7704	0.407	.0989	0.8294	0.89
.0805	0.2931	0.300	.0466	0.7755	0.410	.1034	0.8339	1.02
.0924	0.3050	0.319	.0968	0.8257	0.840	.1084	0.8389	1.09
.0976	0.3102	0.328	.1002	0.8291	0.910	.1281	0.8586	1.93
.1092	0.3218	0.289	.1082	0.8371	1.084	.1316	0.8621	2.12
.1145	0.3271	0.292	.1122	0.8411	1.172	.1385	0.8690	2.71
.1396	0.3522	0.328	.1154	0.8443	1.322	.1433	0.0029	2.66
.1435	0.3561	0.330	.1253	0.8542	1.649	.1477	0.0073	2.31
.1552	0.3678	0.360	.1291	0.8580	1.837	.1530	0.0126	1.96
.1594	0.3720	0.374	.1336	0.8625	2.144	.1576	0.0172	1.73
.1703	0.3829	0.367	.1410	0.8699	2.676	.1701	0.0297	1.21
.1760	0.3886	0.380	.1518	0.0098	2.079	.1751	0.0347	1.09
.1888	0.4014	0.395	.1562	0.0142	1.868	.1778	0.0374	1.00
.1937	0.4063	0.405	.1601	0.0181	1.681	.1816	0.0412	0.85
.2055	0.4181	0.411	.1646	0.0226	1.498	.1951	0.0547	0.67
.2107	0.4233	0.410	.1684	0.0264	1.374	.1989	0.0585	0.621
.2255	0.4381	0.412	.1808	0.0388	0.938	.2038	0.0634	0.57
.2297	0.4423	0.418	.1857	0.0437	0.861	6169.0534	0.3002	0.39
.9200	0.2617	0.305	.1900	0.0480	0.775	.0587	0.3055	0.38
.9247	0.2664	0.292	.2035	0.0615	0.580	.0716	0.3184	0.387
.9374	0.2791	0.282	.2079	0.0659	0.554	.0776	0.3244	0.383
.9417	0.2834	0.313	.2119	0.0699	0.545	.0910	0.3378	0.389
.9541	0.2958	0.316	6165.0332	0.6346	0.378	.0965	0.3433	0.384
.9591	0.3008	0.315	.0499	0.6513	0.366	6170.9490	0.4540	0.470
.9691	0.3108	0.335	.0599	0.6613	0.361	.9619	0.4669	0.446
.9744	0.3161	0.324	.0707	0.6721	0.370	.9730	0.4780	0.417
.9872	0.3289	0.322	.0757	0.6771	0.372	.9847	0.4897	0.417
.9930	0.3347	0.312	.0868	0.6882	0.367	.9966	0.5016	0.399
6136.0396	0.3813	0.368	.0912	0.6926	0.353	6171.0077	0.5127	0.379
.0434	0.3851	0.366	.1203	0.7217	0.379	.0201	0.5251	0.375
.0539	0.3956	0.393	.1256	0.7270	0.369	.0385	0.5435	0.367
.0583	0.4000	0.401	.1412	0.7426	0.385	.0515	0.5565	0.370
.0714	0.4131	0.390	.1535	0.7549	0.407	.0666	0.5716	0.384
.0777	0.4194	0.409	.1580	0.7594	0.414	.0808	0.5858	0.365
.0906	0.4323	0.430	.1722	0.7736	0.426	6187.9604	0.0471	0.751
.0949	0.4366	0.434	.1780	0.7794	0.438	.9657	0.0524	0.677
.1061	0.4478	0.427	.1922	0.7936	0.473	.9767	0.0634	0.549
.1110	0.4527	0.426	.1982	0.7996	0.500	.9809	0.0676	0.519
.1238	0.4655	0.390	.2040	0.8054	0.562	.9926	0.0793	0.426
.1300	0.4717	0.378	.9382	0.6687	0.363	.9966	0.0833	0.414
.1585	0.5002	0.324	.9494	0.6799	0.354	6188.0072	0.0939	0.409
.1635	0.5052	0.331	.9540	0.6845	0.363	6221.9803	0.1012	0.440
.1757	0.5174	0.323	.9641	0.6946	0.371	.9890	0.1099	0.400
.1806	0.5223	0.319	.9688	0.6993	0.372	6222.0023	0.1232	0.376
.1920	0.5337	−0.309	.9827	0.7132	−0.386	.0111	0.1320	−0.398

Lower blue curve, $A_0=0.9739\pm0.0003$,
$A_1=-0.0105\pm0.0014$,
$A_2=-0.0274\pm0.0006$,

Lower yellow curve, $A_0=0.9614\pm0.004$,
$A_1=-0.0091\pm0.0029$,
$A_2=-0.026\pm0.0000$,

Upper yellow curve, $A_0=0.9332\pm0.0003$,
$A_1=-0.0455\pm0.0034$,
$A_2=-0.0405\pm0.0006$.

For each of these rectifications, solutions wer attempted, following the procedure of Russell an Merrill (1952) and using the Merrill nomograms an tables (Merrill 1950, 1953). Because of the shallo depth of secondary, the solution was made using th χ function derived from the shape of primary minimu and the usual relationship found from the rectifie depths of the minima.

When the observations were rectified by the coefficients found in the upper curve in each color, no solutio was found. The depth lines and the shape lines did no

Table Ib. Blue observations of V Tucanae.

JD Hel. 430000+	Phase	*m*	JD Hel. 2430000+	Phase	*m*	JD Hel. 2430000+	Phase	*m*
134.9850	0.1976	−0.107	6136.1987	0.5404	−0.094	6165.9850	0.7155	−0.134
.9891	0.2017	0.103	6137.9589	0.5587	0.180	.9887	0.7192	0.146
.9981	0.2107	0.098	.9710	0.5708	0.171	6166.0005	0.7310	0.154
135.0015	0.2141	0.104	6138.0253	0.6251	0.144	.0074	0.7379	0.149
.0113	0.2239	0.107	.0302	0.6300	0.142	.0326	0.7631	0.163
.0145	0.2271	0.103	.0409	0.6407	0.136	.0367	0.7672	0.168
.0326	0.2452	0.097	.9951	0.7240	0.158	.0489	0.7794	0.169
.0359	0.2485	0.110	.9989	0.7278	0.157	.0533	0.7838	0.170
.0443	0.2569	0.093	6139.0099	0.7388	0.140	.0657	0.7962	0.223
.0488	0.2614	0.087	.0161	0.7450	0.180	.0696	0.8001	0.251
.0598	0.2724	0.089	.0258	0.7547	0.158	.0818	0.8123	0.378
.0652	0.2778	0.132	.0306	0.7595	0.167	.0857	0.8162	0.423
.0752	0.2878	0.095	.0428	0.7717	0.173	.0899	0.8204	0.527
.0812	0.2938	0.098	.0476	0.7765	0.160	.1008	0.8313	0.724
.0941	0.3067	0.123	.0976	0.8265	0.639	.1060	0.8365	0.867
.0988	0.3114	0.134	.1009	0.8298	0.687	.1101	0.8406	0.973
.1103	0.3229	0.104	.1090	0.8379	0.879	.1295	0.8600	1.903
.1155	0.3281	0.106	.1127	0.8416	1.023	.1339	0.8644	2.382
.1404	0.3530	0.124	.1167	0.8456	1.221	.1409	0.0005	2.943
.1444	0.3570	0.128	.1260	0.8549	1.539	.1449	0.0045	2.590
.1559	0.3685	0.155	.1298	0.8587	1.797	.1508	0.0104	2.048
.1604	0.3730	0.154	.1346	0.8635	2.187	.1552	0.0148	1.769
.1713	0.3839	0.158	.1416	0.8705	2.940	.1598	0.0194	1.483
.1770	0.3896	0.159	.1527	0.0107	1.981	.1732	0.0328	0.935
.1898	0.4024	0.168	.1568	0.0148	1.709	.1796	0.0392	0.782
.1947	0.4073	0.188	.1610	0.0190	1.483	.1842	0.0438	0.674
.2065	0.4191	0.188	.1655	0.0235	1.293	.1971	0.0567	0.451
.2117	0.4243	0.197	.1693	0.0273	1.109	.2031	0.0609	0.371
.2266	0.4392	0.203	.1818	0.0398	0.736	.2065	0.0661	0.322
.2303	0.4429	0.198	.1868	0.0448	0.668	6169.0561	0.3029	0.148
.9209	0.2626	0.092	.1909	0.0489	0.549	.0610	0.3078	0.154
.9257	0.2674	0.092	.2047	0.0627	0.415	.0745	0.3213	0.141
.9383	0.2800	0.084	.2088	0.0668	0.320	.0800	0.3268	0.158
.9427	0.2844	0.093	.2131	0.0711	0.276	.0936	0.3404	0.142
.9551	0.2968	0.117	6165.0353	0.6367	0.144	.0988	0.3456	0.145
.9599	0.3016	0.107	.0519	0.6533	0.115	6170.9527	0.4577	0.204
.9701	0.3118	0.126	.0625	0.6639	0.108	.9645	0.4695	0.219
.9754	0.3171	0.108	.0737	0.6751	0.128	.9754	0.4804	0.173
.9885	0.3302	0.115	.0774	0.6788	0.126	.9869	0.4919	0.180
.9940	0.3357	0.115	.0890	0.6904	0.120	.9990	0.5040	0.171
6136.0404	0.3821	0.141	.0935	0.6949	0.119	6171.0110	0.5160	0.133
.0442	0.3859	0.159	.1236	0.7250	0.147	.0221	0.5271	0.137
.0548	0.3965	0.175	.1294	0.7308	0.140	.0412	0.5462	0.127
.0593	0.4010	0.167	.1438	0.7452	0.147	.0546	0.5596	0.136
.0726	0.4143	0.174	.1555	0.7569	0.158	.0712	0.5762	0.121
.0791	0.4208	0.180	.1610	0.7624	0.156	.0832	0.5882	0.129
.0914	0.4331	0.194	.1744	0.7758	0.180	6187.9636	0.0503	0.513
.0961	0.4378	0.202	.1811	0.7825	0.178	.9677	0.0544	0.440
.1072	0.4489	0.196	.1952	0.7966	0.228	.9787	0.0654	0.327
.1119	0.4536	0.192	.2011	0.8025	0.280	.9830	0.0697	0.287
.1249	0.4666	0.160	.2063	0.8077	0.325	.9946	0.0813	0.196
.1310	0.4727	0.165	.9410	0.6715	0.129	.9987	0.0854	0.191
.1593	0.5010	0.129	.9519	0.6824	0.126	6221.9857	0.1066	0.159
.1647	0.5064	0.122	.9559	0.6864	0.118	.9916	0.1125	0.157
.1769	0.5186	0.099	.9664	0.6969	0.138	6222.0053	0.1262	0.159
.1818	0.5235	0.112	.9719	0.7024	−0.138	.0081	0.1290	0.176
.1935	0.5352	−0.111						

tersect. Solutions were found using observations ctified by the coefficients found from the lower curves. his suggests that on the nights when the system was nusually bright, factors other than those covered by e conventional theory were present.

If we assume that light was added to the system by temporary shell or stream to form the upper curve, e can then carry through solutions after correcting r this added light. (The fact that the increased light as greater in the yellow than in the blue argues gainst its being a thermal effect connected with intrinsic changes in either component of the variable in the comparison star.) The assumption of added light equal to from 0.06 to 0.07 of the total light in the yellow and 0.02 to 0.04 of the total in the blue permits us to find solutions in which the elements fall well within the range of those given by the observations rectified from the lower curves.

In actual practice, uncertainties in both the depths and shapes of the minima, as given by the scatter and distribution of the observations, were determined and a number of solutions were carried through for assumed

TABLE II. Observed minima.[a]

E	O JD 2400000+	O–C	Reference
−22 363	16662.851	+0.014	Dawson (1918)
−21 851	17108.743	−0.003	Dawson (1918)
−21 480	17431.833	−0.023	Dawson (1918)
−16 784	21521.678	−0.002	Dawson (1918)
−16 783	21522.551	0.000	Dawson (1918)
−16 777	21527.779	+0.003	Dawson (1918)
−16 775	21529.518	0.000	Dawson (1918)
−16 767	21536.483	−0.002	Dawson (1918)
−16 761	21541.712	+0.001	Dawson (1918)
−16 760	21542.582	0.000	Dawson (1918)
−16 752	21549.540	−0.009	Dawson (1918)
−16 690	21603.547	+0.001	Dawson (1918)
−16 684	21608.765	−0.006	Dawson (1918)
−16 644	21643.609	+0.001	Dawson (1918)
−16 629	21656.671	−0.001	Dawson (1918)
−16 628	21657.543	0.000	Dawson (1918)
−16 451	21811.648	−0.047	Dawson (1918)
−16 450	21812.564	−0.002	Dawson (1918)
− 7 828	29321.598	−0.010	Gaposchkin (1947)
0	36139.142	0.000	Wood
+ 31	36166.140	0.000	Wood

[a] The first three minima are as given by Dawson from the times listed by Pickering. The original publication included an error in one date which was corrected by Dawson. The first minimum is the mean of two times on the same night at which the star was listed as "faint."

degrees of limb darkening, $x=0.4$, 0.6, and 0.8. The possibilities were then reduced by considering only those which give common elements (k, i, r_g). Table III lists the elements from the solution we consider the most satisfactory. Table IV is more realistic and lists the permissible ranges.

The weakest part of the whole solution depends on the observations in secondary minimum. Observations at the bottom of secondary were made on three nights; two of these were the two nights when the

TABLE III. $x=0.4$ (assumed). V mag. at max. . . . $10\overset{\text{m}}{.}7$

A_1 (Y)	$2\overset{\text{m}}{.}40$	A_1 (B)	$2\overset{\text{m}}{.}85$
A_2 (Y)	$0\overset{\text{m}}{.}11$	A_2 (B)	$0\overset{\text{m}}{.}10$
$\alpha_0{}^{\text{oc}}$	0.975		
$\alpha_0{}^{\text{tr}}$	0.979		
L_g (Y)	0.941	L_g (B)	0.979
i	$88\overset{\circ}{.}3$		
r_g	0.298		
r_s	0.286		

[a] Using V mag. of the comparison star as measured by A. R. Hog

system was unusually bright and hence the deri depth depends heavily on observations made on night alone. The computed curve thus appears to g a very poor fit in secondary to the observations a whole. Fortunately, two factors make this less seri than it otherwise would be. The first is that the obs vations on the two nights when the star was brigh run consistently above the curve throughout second by the same amount as they do outside eclipse. T additions of an amount of light from the out-of-ecli observations will give a satisfactory fit to these. T second is that if secondary is appreciably shallower th the value used no solution can be found; if it is app ciably deeper, it will move the solution nearer t total eclipse. Since the sharp bottom of primary sho that this is a partial eclipse and since α_0 (ratio of t light lost at the bottom of minimum to that whi would be lost at internal tangency) is 0.98, little furt adjustment in this direction is possible. The same li of argument indicates that little, if any, of the nebulosi in the general region was close enough to the varia to be included in the diaphragm and that the meth of correcting for the sky background was the prop

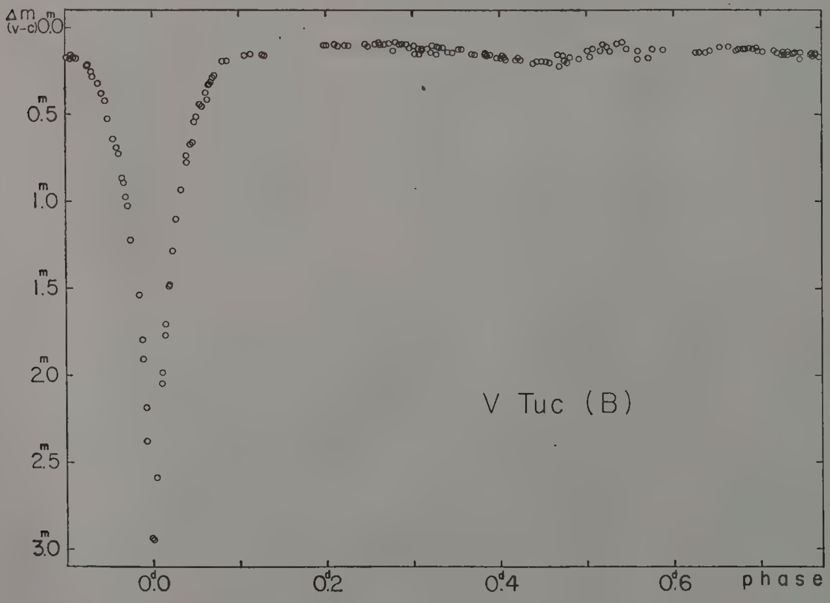

FIG. 1. Blue light curve of V Tuc.

TABLE IV. Limiting solutions.

$x=0.4$	$x=0.6$
0.96 to 0.98	0.95 to 0.97
0.30 to 0.29	0.30 to 0.29
88°.3 to 89°.3	88°.3 to 89°.0
0.0 for lower curves	0.0 for lower curves
0.04 for upper blue curve	0.02 for upper blue curve
0.07 for upper yellow curve	0.06 for upper yellow curve

e. In this case it is the depth of primary which would most seriously affected by systematic errors in eatment of sky background. The result of this would ain be to alter the depth function, and the objections st cited apply to any significant change in this.

In view of the uncertainties of rectification, it seems be unwise to carry the discussion further in detail at resent. This is especially true, since Dr. A. R. Hogg ready has a number of three-color photoelectric obrvations and with J. S. Sommerville is continuing bservation of the system. The large difference of minosity between the components suggests a relavely large mass ratio. This is borne out by the fact hat only a small ellipticity effect is shown by the obervations between eclipse, even though the system is a lose one. This again indicates only minor distortion of he larger component and this in turn requires a large ass ratio. It is possible to estimate this ratio from the ght curve alone (Wood 1960), but we feel that even an approximate numerical value should await a curve obtained when intrinsic variations were not present.

ACKNOWLEDGMENTS

The senior author wishes to express his gratitude to the staff of the Mount Stromlo Observatory of the Australian National University for providing, maintaining, and generously sharing the equipment with which the observations were made. The work was made possible by a sabbatical leave and a Fulbright award. The junior author worked under the Undergraduate Research Participation Program of the National Science Foundation. We are both grateful to Dr. A. R. Hogg for information concerning his most recent observations of the system and especially for measurements indicating the constancy of light of the comparison star used.

REFERENCES

Cannon, A. J. and Pickering, E. C. 1918, *Harvard Ann.* **91**, 67.
Dawson, B. H. 1918, *Astrophys. J*, **48**, 310.
Gaposchkin, S. 1947, *Harvard Ann.* **115**, 117.
Gascoigne, S. C. B. and Burr, E. J. 1956, *Monthly Notices Roy. Astron. Soc.* **116**, 571.
Pickering, E. C., 1907, *Harvard Circ.* 134.
——. 1908, *Astron. Nach.* **177**, 85, (4230).
Merrill, J. E. 1950, *Princeton Contrib.* 23.
——. 1953, *ibid.* 24.
Russell, H. N. and Merrill, J. E. 1952, *ibid.* 26.
Wood, F. B. 1959, *Astron. J.* **64**, 56.
——. 1960, *ibid.* **65**, 23.

THE ASTRONOMICAL JOURNAL VOLUME 66, NUMBER 8 OCTOBER, 1

Mean Densities of Visual Binary Stars

Maria A. Giannuzzi and Lucilla Bianco
Rome Astronomical Observatory, Rome, Italy

(Received February 15, 1960; and in final form, July 10, 1961)

Mean densities of 52 visual binaries and 82 eclipsing variables have been calculated without employing parallax values by using a method originally proposed by Öpik. The visual double stars seem on the average to be 10 times denser than photometric binaries, and their mean density is normally similar to the sun's density. Very likely, however, the difference between densities in the two types of binary systems is the result of observational selection.

INTRODUCTION

THE mean density ρ of a visual binary system can be known even though the parallax is unknown. In fact, in the determination of ρ from the masses and volumes of the binary stars, the parallax is automatically eliminated. This fact was brought out as long ago as 1916 by Öpik, who derived a relation giving the mean densities expressed in terms of the elements of the orbit, of the mass ratio, and of the surface brightness. Öpik obtained this last value, depending on the absolute temperature, from the spectral type; for the mass ratio he adopted some hypothetical values empirically depending on the difference of magnitude of the components. Using these methods he computed the mean density for the principal component of each of 39 binaries. The results were necessarily only rough approximations, because the data were more or less seriously affected by the inadequacy of the above conversions as well as by errors.

Bernewitz (1921) and Thompson (1929) later published similar investigations concerning the density of binary stars. They attempted to derive carefully the relation between surface brightnesses and temperatures and the values of the mass ratios. The agreement between their results is not good. The principal cause of such deviations is to be sought in the uncertainty inherent in the derivation of the temperature scale from the spectral types. Also, for computing the mean density of the principal component, the combined spectral type of the system was considered, which is not always that of the single stars.

DETERMINATION OF THE DENSITY

Giannuzzi (1958) has examined the problem again in order to give a formula that is easier to apply for the mean density ρ of a double star.

From Kepler's third law, taking for units the solar mass and the year, and with the parallax p and semi-axis major a, both in seconds of arc,

$$\mu_1+\mu_2=a^3/p^3P^2. \qquad (1)$$

The volume measured in terms of the sun's volume is

$$V_1+V_2=(R_1/R_\odot)^3+(R_2/R_\odot)^3. \qquad (2)$$

Moreover, the radius R of a star is related to the absolute bolometric magnitude M and to the effective temperature T by the Stefan formula for blackbo
radiation:

$$M_\odot-M=5\log(R/R_\odot)+10\log(T/T_\odot).$$

From the absolute magnitude M and apparent ma
nitude m, in the standard formula,

$$\begin{aligned}-M&=-m-5-5\log p\\ &=5\log(R/R_\odot)+10\log(T/T_\odot)-M_\odot,\end{aligned}$$

from which

$$\frac{R}{R_\odot}=\frac{1}{p}\left(\frac{T}{T_\odot}\right)^{-2}\times10^{-1+0.2M_\odot-0.2m}.$$

Introducing this result in (2) we have

$$V_1+V_2=\frac{10^{-3+0.6M_\odot}}{p^3}\left[\frac{10^{-0.6m_1}}{(T_1/T_\odot)^6}+\frac{10^{-0.6m_2}}{(T_2/T_\odot)^6}\right],$$

whence the mean density ρ is

$$\rho=\frac{\mu_1+\mu_2}{V_1+V_2}=\frac{Ca^3}{P^2}\left[\frac{10^{-0.6m_1}}{(T_1/T_\odot)^6}+\frac{10^{-0.6m_2}}{(T_2/T_\odot)^6}\right]^{-1},$$

where $C=10^{3-0.6M_\odot}=1.45$, if we assume Stebbins an
Kron's (1957) value of $M_\odot=+4.73$. For $T_\odot$ we wi
assume Unsöld's (1955) value of 5780°K.

TEMPERATURES AND ACCURACY OF DATA

In (7), ρ is a function of the sixth power of T
therefore a small error in T greatly affects ρ. But thi
difficulty is not unique to our method, since in the usua
computation of stellar density the radius (indispensabl
in calculating the volume) depends on the second powe
of T; and hence T is present in the calculation of ρ t
the same sixth power. Therefore it is necessary to hav
values of the temperature as exact as possible.

The stellar spectra from which temperatures wer
derived usually refer to the combined light of th
system; colorimetric observations of single component
are very few.

The modern colorimetric measures of visual doubl
stars have been made by Wallenquist (1950) (about 2
systems), by Muller (1952) (51 binaries), and b
Hopmann (1953–1956), who has observed the singl
components of about 700 binaries, but until now ha

ABLE I. Probable errors in effective temperatures and density.

T	p.e. in T	p.e. in ρ
10 000°	±850°	$\pm 0.50\rho$
6000	±340	$\pm 0.34\rho$
3000	±120	$\pm 0.12\rho$

published the data for only 400 of them. Giannuzzi also ook some part in Hopmann's observations at Vienna n 1955. The values for T from Hopmann's list, in view of its homogeneity and much greater size, have been used in the present paper.

Accurate colorimetric observations must be corrected or differential atmospheric extinction, for changes in he color of the photometric lamp from night to night, and for the observer's nightly personal equation. Therefore Hopmann (1953) corrected each measure by an appropriate amount calculated from the theory of atmospheric extinction, and always compared the color of each star with that of many stars of known color, situated in the same region of the sky, and assumed as colorimetric fundamental stars. He then reduced his measures to Becker's scale of radiation temperatures, and gave for each component of each double star a value of c/T_r, where c has the value 14 320° and T_r is the radiation temperature. The average mean error of a c/T_r measure, according to Hopmann, is ± 0.147; accordingly the percentage error in T_r is higher for hotter stars.

From radiation temperatures we have derived effective temperatures T according to Kuiper's (1938) conversions. According to Becker (1952), such a scale introduces an error of about ±1000° for the highest and of about ±100° for the lowest temperatures; that is, the uncertainty of the scale is no more than 5% of its value.

In formula (7), putting $T_1 = T_2$ and taking the logarithmic derivative, we find $d\rho/\rho = 6\,dT/T$. This formula is not quite correct, since the bolometric magnitudes also depend on T, but we think that the discrepancy in temperature is not likely to alter the bolometric corrections appreciably. The probable errors for different values of T are given in Table I.

In order to determine the distribution of double stars according to their mean densities, we take $\log\rho$ in steps of 0.50. Our table of errors suggests that even under the worst conditions any binary system will have been placed in the interval to which it belongs or in that beside it. Moreover, only nine systems of those studied by us have temperatures higher than 9000° and hence the highest probable error; the temperatures of other systems, ranging from 3500° to 9000°, are sensibly more correct. Thus the general distribution of double stars according to their densities should be very nearly correct.

By adopting Unsöld's value for the sun's effective temperature, we have set the zero point of our system such that dwarf stars of type G2 have effective temperatures of 5780°K. Should the zero point change, the T values change accordingly. In particular, again according to Unsöld (1955), if from a system of T values defined on T_b as base value one passes to a system of T' values defined on T_b' as base value, one has the difference

$$(T-T')/T = (T_b - T_b')/T_b.$$

Thus a change of ±100° in the value of the sun's effective temperature would alter all values by little more than 1.5%, so that the densities should vary by $\pm 0.09\rho$.

MAGNITUDES AND ORBITAL ELEMENTS

To determine the apparent bolometric magnitudes we have used Kuiper's (1938) paper, where, for stars hotter than 7000°, tables of bolometric corrections are constructed using theoretical spectral energy curves, and for later types, bolometric corrections are derived from radiometric observations. Our work has pursued the following plan:

(a) Obtain the photovisual magnitude m in the Harvard Photometric System (*Harvard Mimeo.* Ser. III, 1, 2, 1938) which usually gives the combined magnitude of a binary system.

(b) To find the magnitude difference Δm between the separate components, we consulted the following catalogues: Kooreman, *Bull. Astron. Inst. Neth.* **10**, No. 375; Muller, *Ann. Strasborg* **5**, Heft 3; Miczaika, *Veröff. Heidelberg-Königstuhl* **15**, No. 6; Detre, *Astron. Nach.* **273**, No. 253; Hopmann, *Mitt. Wien* **6**, No. 8.

We have not used Wallenquist's (Uppsala) recent photometric measures since his observations show systematic differences with the observations of other catalogues. When several determinations were available for a stellar system, we averaged Δm, since Hopmann has shown that the above sets of measures have no systematic difference between them. For a few stars, for which no magnitude differences are available in these catalogues, we adopted the values of Harvard Photometry or those given in Baize's catalogue of orbits.

(c) Determine m_1 and m_2 by the relations

$$m_1 = m + x, \quad m_2 = m_1 + \Delta m,$$
$$x = 2.5 \log_{10}(1 + 2.512^{-\Delta m}). \tag{8}$$

(d) Reduce m_1 and m_2 expressed on the Harvard Photovisual scale to International Photovisual magnitudes on the system of the North Polar Sequence 1922, by the formula in the *Harvard Mimeograms* referred to above:

$$m_{\mathrm{IPv}} = m_{\mathrm{HPv}} + 0.10 + 0.06C_i,$$

where C_i is the color index, known from the temperature.

(e) Finally, apply the bolometric corrections.

TABLE II. Visual double stars.

Name	Int. pv		T_1	T_2	ρ	logρ	References
	m_1	m_2					
588	7.82	9.66	6160°	4700°	1.00	0.00	Rabe. 1948, *Astron. Nach.* **276**.
755	6.45	6.89	4260	3950	0.014	−1.85	van den Bos. 1938, *Union Obs. Circ.* No. 100.
					0.013	−1.89	Baize. 1946, *Astron. J.* **51**.
					0.015	−1.82	Rabe. 1951, *Astron. Nach.* **280**.
					0.015	−1.82	Rabe. 1955, *I.A.U. Circ.* **6**.
					0.014	−1.85	Muller. 1956, *I.A.U. Circ.* **10**.
1538	6.88	6.93	6430	7200	0.96	−0.02	Volet. 1933, *J. Obs.* **16**.
					1.64	0.21	Palacios. 1954, *Urania* **37**.
1615	4.40	5.35	15 400	10 100	0.47	−0.32	Rabe. 1954, *I.A.U. Circ.* **2**.
2034	8.5	10.1	5450	5150	1.30	0.11	Pensado. 1954, *Bol. Madrid* **4**.
2122	7.37	8.18	6010	4700	0.78	−0.11	Rabe. 1954, *I.A.U. Circ.* **2**.
2416	7.5	7.5	6120	6300	2.44	0.39	Dommanget. 1954, *I.A.U. Circ.* **1**.
3264	5.91	8.44	9200	6080	1.42	0.15	Kuiper. 1937, *Astrophys. J.* **86**.
3711	5.94	6.69	9180	9180	0.66	−0.18	van den Bos. 1933, *Union. Obs. Circ.* No. 90.
					1.16	0.06	Voronov. 1933, *Tashkent. Obs. Circ.* No. 10.
					1.46	0.16	Baize, 1953, *J. Obs.* **36**.
5400AB	5.66	6.20	7270	8500	0.10	−1.00	Broche. 1956, *I.A.U. Circ.* **8**.
5871	7.27	7.32	4470	5250	0.17	−0.77	Van Biesbroeck. 1925, *Monthly Notices Roy. Astron. Soc.* 8
					0.22	−0.66	Karmel. 1940, *Astron. Nach.* **269**.
6650AB	5.62	6.01	6080	5250	0.42	−0.37	Makemson. 1933, *Astron. J.* **42**.
					0.34	−0.47	Gasteyer. 1954, *Astron. J.* **59**.
7307	6.62	6.85	9700	9700	5.51	0.74	Güntzel-Lingner. 1952, *Astron. Nach.* **281**.
					1.97	0.29	Arend. 1954, *Bull. Astron. Belg.* **IV**.
7704	7.26	7.42	9000	7700	0.78	−0.11	Wierzbinski. 1955, *I.A.U. Circ.* **5**.
7724	2.51	3.84	4300	5060	1.5×10^{-4}	−3.82	Güntzel-Lingner. 1956, *I.A.U. Circ.* **8**.
8032	9.36	9.89	5800	4100	4.35	0.64	Baize, 1948, *J. Obs.* **31**.
					2.59	0.41	Baize. 1954, *I.A.U. Circ.* **4**.
8119	4.49	4.96	6580	5130	1.98	0.29	Rakowiecki. 1938, *Wiadom. Matem. Warsaw* **46**.
					1.84	0.26	Rakowiecki. 1938, *Wiadom. Matem. Warsaw* **46**.
8630	3.70	3.72	5000	5590	0.10	−1.00	Strand. 1937, *Leiden. Ann.* **XVIII**.
					0.10	−1.00	Wolf. 1949, *Astron. Nach.* **277**.
					0.10	−1.00	Wolf. 1949, *Astron. Nach.* **277**.
8695	5.15	7.12	3950	7860	1.2×10^{-3}	−2.92	Schmeidler. 1939, *Astron. Nach.* **268**.
					1.4×10^{-3}	−2.85	Rosino. 1944, *Mem. Soc. Astron. Ital.* **15**.
8949	7.60	8.47	3850	3950	0.09	−1.04	Luplau-Janssen. 1931, *Astron. Nach.* **241**.
					0.13	−0.89	Florsch. 1954, *I.A.U. Circ.* **3**.
					0.11	−0.96	Heintz. 1955, *I.A.U. Circ.* **7**.
8974	5.04	7.50	7000	3750	0.017	−1.77	Wierzbinski, 1956, *I.A.U. Circ.* **8**.
9031	7.57	8.03	3550	3120	0.043	−1.37	Rabe. 1927, *Astron. Nach.* **231**.
9182	7.75	7.89	6300	6700	2.39	0.38	Vón Bezold. 1938, *Astron. Nach.* **267**.
					2.49	0.39	Hopmann. 1945, *Veröff. Univ. Sternw. Leipzig* **8**.
9343	4.60	4.80	11 600	12 200	0.13	−0.89	van den Bos. 1937, *Union Obs. Circ.* No. 98.
					0.13	−0.89	Wierzbinski. 1954, *I.A.U. Circ.* **4**.
9380	7.63	7.24	5710	4140	0.12	−0.92	Pensado. 1954, *Univ. Madrid Pub.* **13**.
					0.13	−0.89	Wierzbinski. 1956, *I.A.U. Circ.* **8**.
9413	4.75	6.95	5630	3400	0.39	−0.41	Strand. 1937, *Leiden Ann.* **XVIII**.
					0.40	−0.40	Kümmritz. 1956, *I.A.U. Circ.* **10**.
9578	7.29	7.32	6060	6060	1.21	0.08	Danjon. 1938, *J. Obs.* **21**.
					1.38	0.14	Danjon. 1938, *J. Obs.* **21**.
					1.10	0.04	Aller. 1939, *Astron. Nach.* **268**.
					0.93	−0.03	Muller. 1952, *Bull. Astron.* **16**.
					0.93	−0.03	Van Biesbroeck. 1955, *Yerkes Publs.* **8**.
9617	5.66	6.03	6160	6300	1.42	0.15	Silbernagel. 1927, *Astron. Nach.* **234**.
					1.12	0.05	Danjon. 1938, *Bull. Astron.* **11**.
9626BC	7.03	7.66	4930	6300	0.32	−0.49	Baize. 1952, *J. Obs.* **35**.
9716	7.41	7.49	5120	5080	1.50	0.17	Pitman. 1934, *Publs. Astron. Soc. Pacific* **46**.
					1.86	0.27	Stephens. 1939, *Publs. A. A. S.* **9**.
9979	5.78	6.84	8000	6120	3.40	0.53	Strand. 1937, *Leiden Ann.* **XVIII**.
					3.09	0.49	Giannuzzi. 1951, *Contrib. Sci. Oss. M. Mario* **164**.
					3.42	0.53	Rabe. 1954, *I.A.U. Circ.* **4**.
10075	7.94	7.95	4950	5000	3.27	0.51	Finsen. 1933, *Union Obs. Circ.* No. 90.
					2.90	0.46	Siegrist. 1954, *Univ. Madrid Publ.* **11**.
10157	3.05	5.60	6140	5080	0.26	−0.58	Silbernagel. 1928, *Astron. Nach.* **233**.
					0.26	−0.58	Baize. 1949, *J. Obs.* **32**.
10235	6.84	8.70	6200	4140	0.14	−0.85	Rabe. 1926, *Astron. Nach.* **231**.
11046	4.12	5.93	6500	4000	2.24	0.35	Strand. 1937, *Leiden Ann* **XVIII**.
					2.24	0.35	Geffers. 1954, *Veröff. Bonn* **39**.
11186	8.33	8.63	9550	10 080	4.56	0.66	Luyten. 1934, *Astron. J.* **43**.
					3.75	0.57	Luyten. 1934, *Astron. J.* **43**.
					3.65	0.56	Wilson. 1935, *Astron. J.* **44**.
11635AB	5.12	6.22	8800°	10 540	0.18	−0.74	Güntzel-Lingner. 1956, *I.A.U. Circ.* **8**.
11635CD	5.21	5.51	10 320	10 620	1.21	0.08	Güntzel-Lingner. 1956, *I.A.U. Circ.* **8**.

TABLE II (*continued*)

Name	Int. pv m_1	Int. pv m_2	T_1	T_2	ρ	$\log\rho$	References
371	5.27	7.72	5700	4150°	0.63	−0.20	Rechtenstamm. 1940, *Astron. Nach.* 268.
					0.70	−0.15	Baize. 1943, *J. Obs.* 26.
447	8.22	8.57	6280	5080	0.62	−0.21	Finsen. 1937, *Union Obs. Circ.* No. 98.
889	8.63	8.84	5320	5480	11.4	1.05	Strand. 1937, *Bull. Astron. Inst. Neth.* 8.
					13.0	1.11	Baize. 1945, *l'Astron.* 59.
					12.6	1.10	Rabe. 1948, *Astron. Nach.* 276.
					13.6	1.13	Cester. 1950, *Oss. Trieste P.* 227.
					12.4	1.09	Baize. 1954, *I.A.U. Circ.* 4.
169	9.70	10.24	6310	6280	4.33	0.63	Wierzbinski. 1951, *Acta Astron.* 4.
					3.28	0.51	Baize. 1953, *J. Obs.* 36.
296	4.73	6.11	10 360	11 710	0.038	−1.42	Rabe. 1948, *Astron. Nach.* 276.
360	6.41	7.24	6390	6630	0.21	−0.68	Baize. 1943, *J. Obs.* 26.
499	5.89	6.40	6340	5050	0.073	−1.14	van den Bos. 1933, *Union Obs. Circ.* No. 90.
636	5.41	6.18	3500	3300	0.66	−0.18	Flechter. 1933, *Monthly Notices Roy. Astron. Soc.* 92.
					0.66	−0.18	Zagar. 1934, *Atti R. Inst. Veneto di Sc.*
270	4.81	6.14	6600	6000	0.66	−0.18	Komendantoff. 1936, *Astron. Nach.* 260.
971	4.42	4.63	7000	6050	0.18	−0.75	Strand. 1941, *Astron. J.* 49.
					0.15	−0.82	Giannuzzi. 1954, *Contrib. Sci. Oss. M. Mario* 204.
					0.10	−1.00	Rabe. 1954, *I.A.U. Circ.* 2.
988	5.90	7.29	9080	5890	0.47	−0.33	Van Biesbroeck. 1937, *Yerkes Publs.* 5.
428	6.08	7.43	7400	4150	0.020	−1.69	Güntzel-Lingner. 1956, *I.A.U. Circ.* 9.
665	8.48	9.12	4970	3900	0.46	−0.34	Tannenbaum. 1938, *Union Obs. Circ.* No. 99.
7149	6.36	4.49	5810	6020	0.16	−0.80	Franz. 1955, *I.A.U. Circ.* 6.

There are several sources of uncertainty in the erived apparent photovisual magnitudes. First is the verage probable error ±0.04 in the combined mag-itude taken from Harvard Photometry (1938). econdly, errors affecting the individual magnitudes m_1 nd m_2, according to (8), depend on the amount of Δm nd are largest when $\Delta m=0.00$. In the worst case $m=0.00\pm0.10$ (±0.10 being the highest average p.e. f the photometric catalogues examined), whence $=0.75\pm0.06$ and the resulting errors are $m_1\pm0.07$, $_2\pm0.12$.

Another source of error is introduced with the olometric corrections. According to Kuiper, this should ot exceed about 0^m10 p.e., whence the total probable rror of a bolometric magnitude is not more than ±0.15 (±0.12 for photovisual magnitudes and ±0.10 or bolometric corrections). Since this error has been omputed in the most unfavorable case, we can assume hat on the average the p.e. of a bolometric magnitude sensibly smaller and about ±0.10. In formula (7), utting $T_1=T_2$, $m_1=m_2$, and taking the logarithmic erivative, we find

$$d\rho/\rho=+0.6\,dm/\mathrm{Mod}=1.38\,dm.$$

onsequently as a result of an incorrect knowledge of agnitudes, ρ should be affected on the average by .e.$\pm0.14\rho$ and in any case no more than $\pm0.20\rho$. his considers the accidental errors in m only. But osterhoff (1945) has found evidence of considerable rrors in the zero point for different areas. A good stimate of the systematic p.e. in m may be ±0.13. his affects ρ by $d\rho=\pm0.18\rho$ p.e. The zero point for olometric magnitudes is that value for which $M_\odot$ $=+4.73$. This value has been deduced from the sun's hotovisual magnitude (Stebbins and Kron 1957),

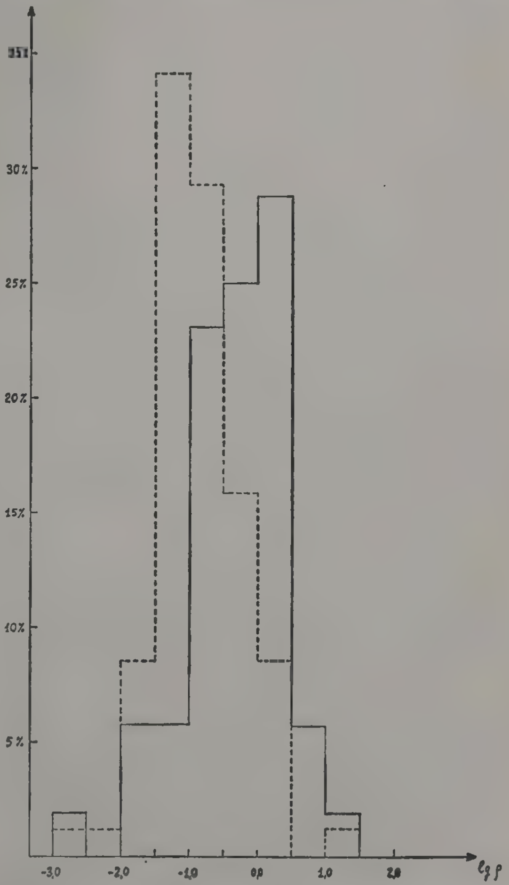

Fig. 1. Comparison of visual (full line) with eclipsing (dotted line) binaries in percentage distribution of logρ.

TABLE III. Eclipsing variables.

Name	logρ	Name	logρ	Name	logρ
		Detached systems			
V 805 Aql	-0.69	σ Aql	-0.95	TT Aur	-0.76
WW Aur	-0.57	AR Aur	-0.39	β Aur	-0.76
SZ Cam	-1.66	GL Car	-0.95	YZ Cas	-0.69
AR Cas	-1.38	SZ Cen	-0.62	AH Cep	-1.12
α CrB	-0.88	AI Cru	-1.09	Y Cyg	-1.07
V 477 Cyg	-0.10	YY Gem	1.43	RX Her	-0.60
TX Her	-0.36	UV Leo	-0.13	U Oph	-0.83
V 451 Oph	-0.69	VV Ori	-1.03	AG Per	-0.71
ξ Phe	-0.73	RS Sgr	-1.33	YY Sgr	-0.65
Y Cam	-1.30	S Cnc	-1.71	RS CVn	-1.56
TV Cas	-1.08	Z Her	-1.00	AR Lac	-1.01
		Semi-detached systems			
RT And	-0.19	TW And	-1.37	ZX And	-1.02
R CMa	-0.57	CV Car	-2.51	RZ Cas	-0.61
U Cep	-1.26	U CrB	-1.39	W Del	-1.53
Z Dra	-0.65	TW Dra	-1.34	RW Gem	-1.40
SZ Her	-0.55	u Her	-1.21	RX Hya	-0.97
T LMi	-1.26	δ Lib	-1.36	RW Mon	-1.04
TY Peg	-1.18	RT Per	-0.41	RY Per	-1.77
β Per	-1.21	V Pup	-1.13	U Sge	-1.42
V 356 Sgr	-2.21	V 505 Sgr	-0.81	μ' Sco	-1.04
RW Tau	-1.02	λ Tau	-1.62	X Tri	-0.63
TX UMa	-1.25	W UMi	-1.28	Z Vul	-1.31
RS Vul	-1.63				
		Contact systems			
AB And	0.03	S Ant	-0.55	i Boo	0.19
TX Cnc	-0.11	VW Cep	0.12	TW Cet	0.08
RZ Com	-0.01	YY Eri	0.07	SW Lac	0.07
V 502 Oph	-0.28	ER Ori	-0.18	U Peg	-0.06
RZ Tau	-0.17	W UMa	0.01	AH Vir	-0.18

$m_\odot=-26.73\pm0.03$. We think the zero point for bolometric magnitudes should change no more than ±0.10. Accordingly, from this cause the densities might vary by an amount $\pm1.33dM_\odot\rho=\pm0.13\rho$.

This discussion shows that the combined effects of different kinds of errors in the magnitudes are as serious as those of the errors in T.

We have neglected interstellar absorption since these stars lie within about 100 parsecs. Also, the selective absorption producing stellar reddening leads to estimate temperatures a little lower than the true value, and this effect should tend to compensate a diminution of m in (7).

To obtain the orbital elements P and a, we have consulted Baize, *Bull. Astron.* 10, 273, 1937 and *J. Obs.* 33, 1, 1950, and for the orbits later computed, the annual reports of the *Monthly Notices Roy. Astron. Soc.* and the Circulaire d'Information of I.A.U. Commission 26.

We have not considered the error in ρ due to an incorrect knowledge of orbital terms, since these affect ρ very slightly, as one can see in Table I, where the values of density are given for each binary and for different orbits.

CONCLUSIONS

In Table II, we have collected the results for 52 double stars having satisfactory data. The columns include: (1) ADS catalogue numbers; (2) photovisu magnitudes m_1 and m_2 on the International scale (3) effective temperatures T_1 and T_2; and (4) mea density in units of solar density.

For comparison, eclipsing binaries are considered fo which the mean density is known by means of photo metric and spectroscopic observations only. Adoptin the data of the Kopal and Shapley catalogue (1956) we have calculated logρ for 82 systems given in Tabl III.

Figure 1 shows the resulting percentage distributio with logρ of the visual binaries (full line) and of th eclipsing binaries (dotted line). For those visua binaries having more than one set of orbital data an hence more than one determination of ρ, we have, o course, counted each system only once, using the mor recent orbit in those three cases where the logρ value were not included in the same interval.

It is clear from the figure that the visual double star of this selection are on the average eight times dense than photometric binaries, also that their mean densit is normally little different from the sun's density However most eclipsing binary stars of Kopal's cata logue have spectral types A and B, while the visua doubles which we have considered are predominentl of spectral type later than dF0.

Unfortunately, not enough systems are available t compare between the two groups of binaries the dis sion in density among stars of the same spectral s. But we would in fact expect that B and A stars uld have about 0.1 the mean density of G and K s (see, e.g., Ledoux and Walraven 1958). Thus it is te probable that the differences between the histo- ms of star density for the present sample of the two es of binary systems are due entirely to the result of ervational selection.

REFERENCES

ker, W. 1952, in Landolt-Börnstein, *Zahlenwerte und Funk- onen* 3, 118.

Bernewitz, E. 1921, *Astron. Nach.* 213, I.

Giannuzzi, M. A. 1958, *Contrib. Sci. Oss. Astron. M. Mario* No. 246.

Hopmann, J. 1953, *Mitt. Wien* **6**, No. 12; 1954, **7**, No. 13, 14; 1956, **9**, No. 2.

Kopal, Z. and Shapley, M. B. 1956, *Jodrell Bank Ann.* **I**, 141.

Kuiper, G. P. 1938, *Astrophys. J.* 88, 429.

Ledoux, P. and Walraven, Th. 1958, *Handbuch Astrophys.* 51.

Muller, P. 1952, *Ann. d. Astrophys.* **15**, 79.

Oosterhoff, P. T. 1945, *Bull. Astron. Inst. Neth.* **10**, 62.

Öpik, E. 1916, *Astrophys. J.* 44, 293.

Stebbins, J. and Kron, G. E. 1957, *ibid.* **126**, 266.

Thompson, A. R. 1929, *J. Brit. Astron. Assoc.* **253**, 247.

Unsöld, A. 1955, *Physik del Sternatmosphären* (Springer-Verlag, Berlin).

Wallenquist, A. 1950, *Medd. Uppsala* 103.

Orbit of Comet 1948 I (Bester)

G. Van Biesbroeck
Yerkes Observatory, Williams Bay, Wisconsin

(Received June 5, 1961)

The computation is based on 243 measures of position covering the period from 141 days before to 356 days after perihelion. Planetary perturbations were taken into account but remained small. The hyperbolic excess comes out 48 times its probable error. The "original" orbit, however, turns out to be a very large ellipse.

COMET 1947 *k* (1948 I) was discovered on September 24 by M. J. Bester at the Boyden Station, Bloemfontein, South Africa on a sky-patrol plate taken with a 3-inch Ross camera. It appeared as a small, diffuse, centrally condensed object of magnitude 11 moving southwestward in Eridanus.

The first accurate positions were obtained September 28 at the Lick Observatory. On October 9 the magnitude was estimated as 9.8 and a broad tail was noted in 350° which extended on October 14 to a distance of 10′ from the well-defined nucleus. By the end of October the comet was out of reach of northern observers and went as far south as −55° on November 22. In December the comet moved far in the western sky, Simonov calling the magnitude 9 on December 22. The last observation before conjunction with the sun was by Johnson at Johannesburg on 1948 January 12, when he estimated the brightness as 7th mag. and noted a tail of one degree in length.

After perihelion passage on 1948 February 16, the comet was first observed in the morning sky by Hirose on March 3, when he called the magnitude 7. By the middle of March it could be seen with the naked eye. It appeared then as large round coma centrally condensed with neither nucleus nor tail. Being conveniently located, the comet was abundantly observed in March and April, when the declination went as far north as 73° (April 23). A minimum distance of 0.74 a.u. from the earth was reached on April 6, at which time the daily geocentric motion was nearly 3°. In May the brightness decreased rapidly. On May 28, although the magnitude had dropped to 11, a tail 20′ long was again visible and there was a sharp nucleus in a coma 1′ in diameter. Observations now become scarce. A last evening measure was obtained at low altitude by Van Biesbroeck on August 1. After the comet reached conjunction with the sun, Jeffers secured a pair of plates on 1948 November 11, when he estimated the magnitude of the nearly stellar object as 17.7. On 1 February 6, Jeffers secured the last observations w the Crossley reflector, the magnitude being estima at 17.5. The measures therefore cover an arc of 2 from 141 days before to 356 days after perihelion. Fr short arcs, preliminary parabolic elements w deduced by Cunningham and Maxwell. A more accur orbit, given in the third column of Table I, was obtain by Cunningham from measures extending to October

The third orbit was used to establish an accura ephemeris for comparison with all the measures. Ta II gives the list of residuals of the individual obs vations. The dates are corrected for aberration ti and reduced from UT to ET. Published parallax fact were corrected when necessary. The references to t original measures are found in the *Astronomisch Jahresbericht* 1947–49. A plot of the residuals again time was useful in illustrating observations showi abnormal discrepancies and also the scattering of t measures by the individual observers. By correspon ence with the observers most discrepancies we eliminated. A few outstanding ones could not be a counted for. These are put in parentheses in the lis meaning that they were not included in making t normal places. Table III gives the list of the observe and the weights from 3 to 1 generally attributed to the from the inspection of the scattering of the measur on the plot mentioned above. One numerous series measures, namely that by Chis (1949) at Cl (Rumania), showed such wide scattering that it w thought better to omit it altogether rather than include it with low weight. The graphical plot of th residuals showed the large uncertainty of the position A well-defined nucleus was mentioned in the ear measures in October 1947; however, when the com reappeared after perihelion it had a large coma 8′ 10′ in diameter (Krumpholz, March 15 and April 1 centrally condensed but without nucleus. Besides, th

TABLE I. Orbits computed.

	Cunningham (1947a)	Maxwell (1947)	Cunningham (1947b)
T	1948 Feb. 17.727 UT	1948 Feb. 17.195 UT	1948 Feb. 16.43302 UT
ω	348°50′ 1947.0	349°24′ 1947.0	350°.24100 1947.0
Ω	270 2 1947.0	270 17 1947.0	270.69135 1947.0
i	140 12 1947.0	140 21 1947.0	140.56326 1947.0
q	0.7677	0.7596	0.7478089

TABLE II. Residuals.

ET	Δα	Δδ	Wt	Obs.
1947				
28.48238	− 0^{s}04	− 0″4	3	SL
28.49693	− 0.01	− 0.8	3	SL
30.51258	− 0.02	+ 0.1	3	JL
2.51680	− 0.03	+ 2.0	3	JL
3.31096	− 0.04	+ 0.5	3	RW
4.08449	− 0.33	+ 1.5	2	JJ
7.90717	− 0.01	+ 0.8	2	JJ
9.35476	− 0.06	+ 2.4	3	VB
10.92977	− 0.25	+ 1.9	2	JJ
14.30930	− 0.06	+ 3.2	3	VB
14.89298	− 0.23	+ 3.7	2	BJ
17.87679	− 0.25	+ 5.9	2	BJ
18.39304	− 0.54	+ 3.3	3	SL
19.04058	− 0.51	+ 1.2	1	D
19.05202	− 0.13	+ 6.2	3	SA
19.47478	− 0.02	+ 6.0	3	G
20.45962	− 0.14	+ 5.3	3	G
21.29532	− 0.17	+ 2.3	3	VB
22.06005	− 0.82	+ 8.0	1	D
23.09170	− 0.99	+ 5.2	1	D
23.34160	− 0.44	+ 4.0	3	VB
23.79649	+ 0.24	+ 4.3	2	BJ
24.01380	+ 0.57	+ 6.8	1	D
27.81526	− 0.63	+ 9.1	2	BJ
29.79989	− 0.60	(− 5.3)	2	JJ
v. 1.02085	− 0.30	+ 12.3	1	D
5.02748	− 0.56	+ 8.4	1	D
5.78934	− 0.37	+ 8.1	2	JJ
8.05261	− 0.21	+ 7.6	1	D
9.80221	− 0.65	+ 8.6	2	JJ
12.02740	− 1.85	+ 7.6	1	D
13.01841	− 0.77	+ 12.9	1	D
13.72427	− 0.40	+ 3.4	2	JJ
15.04078	− 0.97	+ 15.8	1	D
16.05354	− 1.01	+ 13.7	1	D
17.78984	− 0.43	+ 4.5	2	JJ
18.04317	− 1.43	+ 7.2	1	D
22.02018	− 0.89	+ 11.3	1	D
23.73518	− 1.83	+ 9.0	2	JJ
v. 27.72754	− 0.70	+ 9.5	2	JJ
c. 2.08185	− 0.52	+ 9.0	1	D
2.73408	− 0.70	+ 10.6	2	JJ
5.10573	− 0.19	+ 11.8	1	D
6.74373	− 1.25	+ 8.5	2	JJ
13.07210	− 1.05	+ 15.0	1	D
16.76741	− 1.14	+ 13.4	2	JJ
18.03330	− 0.76	+ 13.0	3	BC
c. 22.46467	+ 1.11	+ 14.1	2	SC
1948				
n. 4.75577	− 0.62	+ 14.3	1	JJ
n. 12.75374	− 1.03	+ 17.2	1	JJ
b. 25.10846	− 0.26	+ 5.9	2	JJ
ar. 3.80290	− 0.59	− 15.8	3	HT
3.80915	− 0.44	− 17.9	3	HT
3.81401	− 0.36	− 17.6	3	HT
5.45078	− 0.66	− 25.2	3	VB
5.81267	− 0.95	− 25.1	3	HT
5.82778	− 0.90	− 29.7	3	HT
7.20737	− 0.15	− 34.6	3	PB
7.20983	− 0.21	− 27.0	3	PL
7.21136	− 0.80	− 32.5	3	PL
8.79362	− 0.68	− 40.3	3	HT
8.79779	− 0.64	− 51.6	3	HT
8.80126	− 0.87	− 39.5	3	HT
9.12669	− 0.64	− 44.8	3	AA
9.84436	− 0.62	− 50.0	2	Mi
Mar. 10.20181	− 0^{s}90	− 44″6	3	PB
Mar. 11.52330	− 1.21	− 49.7	3	I
11.52606	− 1.34	− 49.0	3	I
12.14322	− 1.21	− 52.3	3	HP
12.19713	− 1.16	− 54.3	3	PL
12.19892	− 1.13	− 54.7	3	PL
12.20093	− 0.96	− 53.2	3	PB
12.20258	− 1.05	− 52.5	3	BA
14.12826	− 1.68	− 62.8	3	HP
14.18471	− 1.39	− 64.8	3	PL
14.18615	− 1.39	− 65.2	3	PL
14.21363	− 1.54	− 63.8	3	PB
14.76172	− 1.70	− 65.5	3	HT
14.76589	− 1.50	− 68.4	3	HT
14.76936	− 1.60	− 69.3	3	HT
15.13970	− 1.66	− 67.8	3	HS
15.14892	− 1.88	− 73.4	1	SI
15.14995	− 1.78	− 70.5	3	HP
15.17238	− 1.37	− 69.2	3	KV
16.10786	− 1.34	− 78.7	2	O
16.18592	− 1.62	− 77.4	3	BA
17.20419	− 1.61	− 83.7	3	PB
18.79855	− 1.98	− 97.2	2	Mi
19.17668	− 2.08	− 97.5	3	BA
21.20742	− 2.53	−108.4	3	PB
Mar. 22.14241	− 2.79	−122.8	1	SI
Mar. 24.14690	− 2.98	−142.5	3	HS
24.14749	− 2.80	−142.6	3	PT
24.16190	− 3.18	−138.7	3	KV
24.17114	− 3.25	−140.1	3	PB
25.08619	− 3.07	−146.3	3	PL
25.09013	− 2.95	−154.5	3	PL
25.11624	− 2.66	−153.3	3	HS
25.15964	− 3.04	−151.9	3	PT
26.11205	− 3.22	−162.1	3	HS
27.07922	− 3.39	−171.1	3	PL
27.08274	− 3.34	−172.9	3	PL
27.14615	− 3.44	−169.4	3	KV
27.15925	− 3.04	−175.2	3	HS
27.16684	− 3.38	−172.0	3	PT
28.09393	− 3.56	−183.1	3	PL
28.09746	− 3.63	−182.6	3	PL
28.10661	− 3.37	−184.0	3	HS
29.12652	− 3.90	−195.1	3	HS
29.14409	− 3.92	−194.2	3	KV
29.81113	− 4.06	−203.0	3	HT
29.97528	− 3.83	−206.7	2	O
29.98440	− 3.92	−204.8	3	HP
30.03608	− 3.63	−204.6	3	HS
30.72990	− 4.41	−210.4	2	Mi
31.03372	− 4.25	−214.4	3	Ma
31.03574	− 4.07	−214.7	3	HP
31.06988	− 4.00	−219.7	3	HS
Apr. 1.05564	− 4.19	−228.6	2	O
1.14318	− 4.17	−226.4	3	KV
Apr. 1.98891	− 4.02	−236.6	2	Vo
Apr. 2.96208	− 3.97	−247.7	2	KK
2.96258	− 4.45	−248.3	3	HP
3.01784	− 4.18	−247.3	3	Ma
4.90053	− 3.82	−267.3	3	Ma
4.94469	− 4.27	−260.8	3	HP
4.97687	− 4.13	−257.0	2	KK
5.69663	− 5.12	−269.7	2	Mi
5.84196	− 3.80	−273.6	2	O
5.93365	− 4.48	−262.5	3	HP
5.97068	− 4.53	−268.4	3	Ma
6.07096	− 4.23	−267.9	3	PL
6.07483	− 4.00	−270.9	3	PL
7.01540	− 3.52	−281.5	3	Ma
7.11493	− 3.65	−284.5	3	BA
7.97112	− 3.66	−286.9	3	HP

TABLE II (*continued*)

ET	Δα	Δδ	Wt	Obs.
Apr. 8.05960	$-4^{\mathrm{s}}.07$	$-283''.4$	3	KV
8.61894	− 2.91	−284.3	3	HT
8.62310	− 2.16	−289.4	3	HT
8.62538	− 2.57	−288.7	3	HT
8.62866	− 2.24	−285.4	3	HT
8.71561	− 2.67	−293.5	2	Mi
8.91718	− 3.20	−287.2	3	KV
9.69537	− 2.46	−293.8	3	HT
9.85860	− 0.77	−290.0	2	Vs
9.94282	− 0.78	−295.8	3	HP
11.01087	− 0.69	−298.4	3	Ma
11.01101	− 0.44	−297.7	3	HS
11.69330	+ 1.55	−301.8	2	Mi
11.90552	+ 0.50	−312.2	2	Vs
11.99996	+ 0.96	−296.6	3	Ma
12.08619	+ 2.50	−310.2	1	SI
12.11704	+ 1.20	−300.4	3	BA
12.87244	+ 2.61	−284.6	2	Vo
Apr. 12.96975	+ 3.36	−307.4	3	PB
Apr. 13.93649	+ 5.89	−295.2	3	HP
13.95434	+ 4.13	−304.2	2	VS
13.99226	+ 2.87	−292.7	1	SI
14.92505	+ 9.13	−292.9	3	PB
15.04658	+ 9.47	−292.0	3	HP
15.88555	+12.43	−291.6	3	HS
15.95727	+14.39	−298.9	2	Vs
17.04995	+21.23	−278.0	3	HP
17.90949	+25.58	−286.1	3	HS
17.93095	+23.40	−293.7	3	Ma
18.04654	+28.16	−287.8	2	Vo
19.12045	+30.93	−247.4	3	AU
19.90276	+34.77	−241.6	3	KV
20.02321	+37.03	−242.2	2	KK
21.82094	+42.91	−199.3	3	KV
Apr. 21.83647	+45.18	(−263.7)	2	Vo
Apr. 22.82885	+46.60	−182.0	3	KV
22.98851	+49.57	−176.9	3	HS
23.83466	+51.54	−192.5	3	AA
24.78009	+50.09	−142.5	2	Vs
24.80347	+52.14	−136.6	2	Vs
24.82994	+39.06	−137.7	3	KV
Apr. 24.98660	+48.65	−128.5	2	BL
Apr. 27.94068	+48.04	− 88.1	3	AU
27.95193	+48.11	− 85.6	3	AU
28.61441	+46.47	− 79.3	2	Mi
28.87467	+47.45	− 72.3	1	SI
28.93579	+47.17	− 69.9	3	HP
29.78960	+45.42	− 66.6	3	AA
29.79020	+44.84	− 67.8	3	Ma
29.81504	+43.42	− 70.6	3	KV
29.83384	+45.98	− 79.2	2	Vo
30.83680	+47.02	− 77.8	1	KK
30.88221	+42.35	− 75.0	3	Ma
30.93365	+42.66	− 54.4	3	PB
May 1.82438	+46.43	− 49.4	3	Ma

ET	Δα	Δδ	Wt	Ob
May 1.89865	$+41^{\mathrm{s}}.15$	$-48''.5$	3	K
2.92925	+39.90	− 41.6	3	H
3.83143	(+33.44)	− 37.9	3	M
3.92392	+38.08	− 36.4	3	R
3.96547	+37.43	− 39.4	3	H
5.00353	+36.40	− 31.9	3	P
5.02993	+35.94	− 31.2	3	P
5.67480	+34.17	− 25.7	3	H
5.68244	+34.31	− 27.7	3	H
5.83658	+35.55	− 22.5	3	M
5.97035	+35.90	− 22.5	3	H
6.94571	+33.83	− 25.0	3	A
6.95160	+33.80	− 25.5	3	A
7.89433	+33.01	− 21.3	3	R
7.90022	+31.40	− 19.9	3	R
7.96166	+32.53	− 25.1	1	K
8.82807	+31.76	− 23.1	3	M
8.84311	+29.94	− 26.1	2	Vo
8.87626	+31.04	− 22.7	3	K
8.94136	−39.25	− 27.1	3	A
9.80057	+30.75	− 18.6	3	M
10.71341	+29.94	− 17.9	2	K
11.86459	+30.56	− 19.5	2	Vs
May 12.85468	+29.50	− 17.6	2	Vo
May 16.93383	+24.07	− 10.9	2	K
17.97231	+24.13	− 14.5	2	K
19.87922	+23.01	− 15.8	3	BA
25.87103	+21.03	− 14.3	3	M
25.88940	+20.29	− 15.5	3	BA
27.89888	+19.86	− 16.2	3	BA
27.91913	+19.88	− 11.9	3	H
28.15697	+19.91	− 15.4	3	VB
30.86807	+19.35	− 17.0	3	Ma
31.82558	+19.40	− 22.7	3	AA
31.86325	+18.39	− 20.2	3	K
June 1.90298	+19.10	(+ 16.8)	2	Vs
2.50127	+18.18	− 19.6	2	Mi
3.88078	+16.61	− 19.7	1	Vs
4.87060	+17.68	(− 38.0)	1	Vs
6.56530	+17.49	− 27.7	2	Mi
9.16191	+17.25	− 21.0	3	VB
June 11.88322	+16.47	− 22.2	3	BA
June 24.86164	+14.89	− 29.6	3	BA
July 3.17988	+14.23	− 27.5	3	VB
15.18710	+13.49	− 32.6	3	JL
15.19474	+13.46	− 31.7	3	JL
24.12121	+12.69	− 36.6	3	VB
Aug. 1.09880	+12.73	− 29.3	3	VB
Nov. 11.46974	+13.97	− 60.8	3	JL
Nov. 11.50100	+13.92	− 59.3	3	JL
1949				
Feb. 6.42341	+23.08	− 46.0	3	JL
Feb. 6.45258	+23.23	− 46.3	3	JL

fast motion of the comet at that time and its circumpolar position added to the difficulty of the measures, which show a surprisingly large scatter for such a bright object. In May 1948 there appeared a better defined nucleus, but this advantage was soon lost by the rapid decrease in brightness.

The blank lines in Table II indicate how the 243 observations have been grouped in 17 normal places. For each group the mean was obtained by a least-squares solution including a term in t^2. Table IV gives the list of normal places and their weights in colum 2, 3, and 4.

The noninclusion of a few bracketed large residua made slight differences in the weights of the two coo dinates. It was thought best to disregard those min differences.

Next the perturbations by all planets except Mercur and Pluto were computed at 20-day intervals by Encke method, using 1948 February 9.0 as osculation dat The comet did not come near any of the major planet minimum distance to Jupiter was 4.5 a.u. on 1948 ch 9. Minimum distance to Venus was 0.7 a.u. 948 January 8 and to the earth 0.7 a.u. on April 6, these approaches were of short duration. Hence mall corrections for perturbation listed in Table IV lumns 5 and 6. From these we find in columns 7 8 the final residuals from Cunningham's second bolic orbit.

was though that these residuals were small enough se the same parabolic orbit in computing the dif- tial coefficients of the equations. For that purpose cke's (1929; p. 330) form was used. Table V lists 34 equations of condition.

or the least-squares solution of these equations I indebted to the National Bureau of Standards at lder, Colorado. Through the good offices of Dr. F. E. ch and W. B. Jones the work was done on an IBM computer "in less than a minute [sic]." The cor- ions to the elements and their mean errors are n in Table VI. It will be seen that the two elements nd ω were mainly responsible for the deviation of representation.

able VII shows the final representation of the normal es. The mean error of weight 1 comes out as large 1″.94, which corresponds to 1″.12 for a good obser- ion of weight 3. This is not surprising in view of the sical appearance of the comet when the large jority of the measures were obtained. The hyperbolic ess of the eccentricity is small but well established e it is 48 times as large as its mean error.

t is of interest to find out what the "original" nents are and in particular what the initial value of eccentricity was before the comet entered into the er part of the planetary system.

TABLE III. Observers.

Abbreviations	Observer	Location	Weight
AA	Adamopoulos	Athens	3
AU	Arend	Uccle	3
BA	Boyer	Algiers	3
BC	Bobone	Cordoba	3
BJ	Bruwer	Johannesburg	2
BL	Brown	London	2
D	Dujinin	Santiago	1
G	Giclas	Flagstaff	3
HP	Hurnik	Poznan	3
HS	Hoffmeister	Sonneberg	3
HT	Hirose	Tokyo	3
I	Inglis	Lick	3
JJ	Johnson	Johannesburg	2
JL	Jeffers	Lick	3
KK	Konopleva	Kiev	2
KV	Krumpholz	Vienna	3
Ma	Martynov	Kazan	3
Mi	Mitani	Kyoto	2
O	Oterma	Turku	2
PB	Polit	Barcelona	3
PL	Pels	Leiden	3
PT	Prêtre	Toulouse	3
RU	Rigaux	Uccle	3
RW	Reuning	Washington	3
SA	Schmidt	Algiers	3
SC	Simonov	Canberra	2
SI	Schneider	Innsbrück	1
SL	Shane	Lick	3
VB	Van Biesbroeck	Yerkes	3
Vo	Vorsat	Kiev	2
Vs	Vsekhsvyatsky	Kiev	2

was fortunate in securing the interest of B. G. rsden at the Yale Observatory in this question. luding the perturbations by the earth, Jupiter, and urn, he wrote a program and computed the back- rd and forward values of e and $1/a$ for an interval of 12.5 years on an IBM 650 computer "over the weekend." The values, referred to the center of gravity of the solar system, came out as follows:

Elements	e	$1/a$
Osculating (1948 Feb. 9)	1.0003071 ±0.0000064	−0.0004105 ±0.0000085
Original (1935 July 17)	0.999935	+0.000087
Future (1960 Sept. 23)	1.000237	−0.000317

Once more we find that the apparent hyperbolic excess of the eccentricity changes into an original elliptic one corresponding to an orbit of very large size and

TABLE IV. Normal places.

ET	O–C Δα cosδ	Δδ	Wt	Correction for perturb. Δα cosδ	Δδ	Corrected O–C Δα cosδ	Δδ
1947 Oct. 6.0	− 1″.2	+ 1″.4	29	+1″.6	−1″.9	+ 0″.4	− 0″.5
21.0	− 3.9	+ 4.8	26	+1.6	−1.9	− 2.3	+ 2.9
Nov. 12.0	− 6.9	+ 8.8	25	+1.2	−2.2	− 5.7	+ 6.6
Dec. 11.0	− 5.6	+ 11.9	14	+0.1	−0.7	− 5.5	+ 11.2
1948 Jan. 4.756	− 8.2	+ 14.2	1	0.0	0.0	− 8.2	+ 14.2
12.754	− 12.4	+ 17.2	1	0.0	0.0	− 12.4	+ 17.2
Mar. 6.0	− 8.3	− 29.5	46	0.0	+0.1	− 8.3	− 29.4
16.0	− 25.5	− 78.8	69	−0.3	0.0	− 25.8	− 78.8
29.0	− 55.7	−194.1	86	−0.7	−0.1	− 56.4	−194.2
Apr. 7.0	− 40.4	−283.1	91	−1.0	−0.6	− 41.4	−283.7
17.0	+ 43.4	−278.1	41	−1.4	−1.4	+ 42.0	−279.5
24.0	+222.3	−153.6	18	−1.6	−0.7	+220.7	−154.3
May 5.0	+221.1	− 30.7	99	−1.8	+0.6	+219.3	− 30.1
30.0	+175.2	− 17.6	45	−1.7	+1.8	+173.5	− 15.8
July 16.0	+153.6	− 31.5	18	−1.2	+2.4	+152.4	− 29.1
1948 Nov. 11.485	+168.4	− 60.0	6	+2.2	+4.9	+170.6	− 55.1
1949 Feb. 6.438	+219.2	− 46.2	6	+5.0	+6.3	+224.2	− 39.9

TABLE V. Equations of condition.

Date	de	dq	dT	dω	di	dΩ	O–C
			In α				
1947 Oct. 6.0	−0.57096	−0.74970	+ 50.97	+1.18984	−0.40114	−0.81325 =	+ 0.4
21.0	−0.50972	−0.97588	+ 363.71	+1.32937	−0.49702	−0.95880 =	− 2.3
Nov. 12.0	−0.16330	−1.38149	+1744.07	+1.29548	−0.47941	−1.14836 =	− 5.7
Dec. 11.0	+0.16610	−1.03334	+2779.61	+0.57989	−0.05715	−0.77049 =	− 5.5
1948 Jan. 4.756	+0.11862	−0.70947	+2748.85	+0.36716	+0.07224	−0.55178 =	− 8.2
12.754	+0.09826	−0.63584	+2788.16	+0.34666	+0.08823	−0.51457 =	− 12.4
Mar. 6.0	−0.09029	−0.18717	+3090.58	+0.38498	+0.02803	−0.30608 =	− 8.3
16.0	−0.17347	−0.20919	+3201.44	+0.41617	−0.05568	−0.23318 =	− 25.8
29.0	−0.33987	−0.21592	+3532.95	+0.50627	−0.26199	−0.13655 =	− 56.4
Apr. 7.0	−0.43255	+0.03275	+3737.81	+0.68091	−0.48541	−0.20188 =	− 41.4
17.0	−0.26830	+1.03042	+3648.41	+1.17349	−0.73384	−0.78299 =	+ 42.0
24.0	+0.12738	+1.67348	+2413.65	+1.29535	−0.58644	−1.23155 =	+220.7
May 5.0	+0.39924	+1.40924	+ 832.06	+0.90912	−0.20964	−1.11187 =	+219.3
30.0	+0.44106	+0.94567	+ 329.85	+0.63067	−0.03929	−0.87097 =	+173.5
July 16.0	+0.42811	+0.70829	+ 306.34	+0.55966	−0.06586	−0.77047 =	+152.4
Nov. 11.485	+0.45352	+0.67100	+ 351.97	+0.64678	−0.26908	−0.89176 =	+170.6
1949 Feb. 6.438	+0.85692	+0.76173	+ 260.87	+0.83778	−0.10521	−1.18787 =	+224.2
			In δ				
1947 Oct. 6.0	−0.29153	−1.11378	+1026.75	+0.22554	+0.34358	−1.06807 =	− 0.5
21.0	−0.12771	−1.27399	+1590.28	+0.25422	+0.41068	−1.12555 =	+ 2.9
Nov. 12.0	+0.17886	−0.85773	+1897.81	−0.15223	+0.61199	−0.66287 =	+ 6.6
Dec. 11.0	+0.04235	−0.01256	+ 246.30	−0.45071	+0.71900	−0.01114 =	+ 11.2
1948 Jan. 4.756	−0.02694	+0.02727	− 356.05	−0.20515	+0.58466	+0.03802 =	+ 14.2
12.754	−0.02913	+0.02017	− 491.92	−0.13512	+0.53923	+0.05050 =	+ 17.2
Mar. 6.0	+0.04998	−0.47797	−2634.55	+0.07808	+0.06220	+0.42136 =	− 29.4
16.0	+0.09086	−0.90637	−3621.52	−0.05336	−0.09556	+0.68819 =	− 78.8
29.0	+0.10874	−1.85436	−4987.96	−0.57792	−0.21102	+1.28750 =	−194.2
Apr. 7.0	−0.02337	−2.37974	−4493.73	−1.04069	−0.09306	+1.62186 =	−283.7
17.0	−0.37053	−1.94818	−1366.11	−0.78711	−0.18857	+1.34227 =	−279.5
24.0	−0.44454	−0.80454	+ 853.60	+0.06295	−0.64459	+0.57570 =	−154.3
May 5.0	−0.23004	+0.01631	+ 968.41	+0.52697	−0.89051	+0.00497 =	− 30.1
30.0	−0.05586	+0.02888	+ 189.29	+0.35981	−0.84334	−0.01255 =	− 15.8
July 16.0	−0.00592	−0.08865	− 105.20	+0.12492	−0.74783	+0.08400 =	− 29.1
Nov. 11.485	−0.04175	−0.19841	− 155.79	−0.11082	−0.90071	+0.24159 =	− 55.1
1949 Feb. 6.438	−0.19362	−0.05620	+ 27.99	−0.08203	−1.18614	+0.11525 =	− 39.9

TABLE VI. Corrections to elements and their mean errors.

Initial elements (1950.0)	Correction	Mean errors	Final orbit (1950.0)
$e=1$	+0.0003071	±0.0000064	1.0003071
$q=0.7478089$ a.u.	+0.0003268	0.0000075	0.7481357 a.u.
$T=1948$ Feb. 16.43334 ET	−0.01014	0.000009	1948 Feb. 16.42320 ET
Ω=270°73277	+0°00742	0°00069	270°74019
$i=140.56330$	+0.00719	0.00057	140.57049
$\omega=350.24039$	−0.02305	0.00088	350.21734

TABLE VII. Final residuals.

Date	Δα cosδ	Δδ	Weights
1947 Oct. 6.0	−1″3	−0″1	29
21.0	−2.8	+2.1	26
Nov. 12.0	−2.1	+3.5	25
Dec. 11.0	+3.8	+1.9	14
1948 Jan. 4.756	+2.5	+4.0	1
12.754	−1.7	+6.5	1
Mar. 6.0	+3.9	+2.2	46
16.0	+2.7	+0.8	69
29.0	−2.6	+1.1	86
Apr. 7.0	−0.7	−2.5	91
17.0	−0.8	−1.2	41
24.0	+2.6	−0.5	18
May 5.0	−3.1	+1.5	99
30.0	−2.0	−1.1	45
July 16.0	+3.4	−0.8	18
Nov. 11.485	+0.9	+4.6	6
1949 Feb. 6.438	+3.0	−1.1	6

that the future perturbations will eject the comet fro
the solar system.

BRIGHTNESS OF THE COMET

Numerous attempts have been made to represen
the brightness of the comet as a function of its distanc
from the sun. From photovisual observations coverin
the period 1948 March 14 to May 6, Bacchus (1948
finds that the magnitudes reduced to unit distance fo
low 6.75+6.35 log r. This refers to the part of the come
included in a field of 18′ diameter, which therefore ex
cludes part of the tail. Ahnert (1948) has estimated th
total magnitude visually during the interval March 1
to May 1 by extrafocal comparison with stars. He repre
sents his numerous observations by 6.85+10.21 log
and notes a marked bump in the light curve early i

Table VIII. Comparison of results.

	1947 Oct. 4.09	1947 Oct. 9.36	1948 Nov. 11.51	1949 Feb. 6.46
ntric distance	2.375	2.306	3.972	4.889
tric distance	1.776	1.661	4.180	4.083
ed magnitude	Vis. $10\overset{\mathrm{m}}{.}0$ (Johnson)	Vis. $9\overset{\mathrm{m}}{.}8$ (Van Biesbroeck)	Ph. $17\overset{\mathrm{m}}{.}7$ (Jeffers)	Ph. $17\overset{\mathrm{m}}{.}5$ (Jeffers)
ude reduced to unit distance from the earth	8.8	8.7	14.6	14.4
ıs formula	9.1	9.1	10.6	11.1
formula	10.7	10.6	13.0	14.0
and Bertaud formula	13.1	13.0	16.3	17.6

Baldet and Bertaud (1948) represent their photo-
ic magnitudes covering the same period by 7.74
4 log r. Bakharev (1949) computes the photo-
c parameters representing the magnitudes ob-
l by five different observers. The constant term
from 6.29 to 6.76 and the coefficient of log r from
10.5. He also expresses these magnitudes in the
ıative form suggested by Lewin.

we compare what these formulas give for the
st and latest observations (Table VIII) we see that
omet appears to have been brighter before perihelion
after.

single formula represents the whole array of
ıitude observations.

ACKNOWLEDGMENTS

In the laborious discussion of the observations I was assisted by W. Caldwell. Financial support from the National Science Foundation is hereby gratefully acknowledged.

REFERENCES

Ahnert, P. 1948, *Astron. Nach.* **277**, 135.
Bacchus, P. 1948, *Compt. rend.* **227**, 521.
Bakharev, A. M. 1949, *Astron. Circ. U.S.S.R.* No. 86, 5.
Baldet, F. and Bertaud, C. 1948, *Compt. rend.* **227**, 960.
Chis, G. 1949, *J. Obs.* **32**, 39.
Cunningham, L. E. 1947a, *Harvard Ann. Card* No. 848.
——. 1947b, *ibid.* No. 855.
Maxwell, A. D. 1947, *ibid.* No. 850.
Stracke, G. 1929, *Bahnbestimmung der Planeten und Kometen* (Springer-Verlag, Berlin).

The Effect of Solar Radiation Pressure on the Motion of an Artificial Satellite

R. W. Bryant
Theoretical Division, Goddard Space Flight Center, National Aeronautics and Space Administration

(Received April 1, 1961)

The effects of solar radiation pressure on the motion of an artificial satellite are obtained. The results include the effects produced by the intermittant acceleration which results from the eclipsing of the satellite by the earth. Vectorial methods have been utilized to obtain the nonlinear equations describing the motion and the method of Kryloff-Bogoliuboff has been applied in their solution.

INTRODUCTION

Several authors have considered the effects of solar radiation pressure on the motion of an artificial satellite (Parkinson, Jones, and Shapiro 1960; Musen, Bryant, and Bailie 1960; Musen 1960). With the advent of satellites of large area-to-mass ratio such as the Echo I balloon satellite, the magnitude of the radiation pressure effect is substantial and must be taken into account in the analysis of the tracking data. The central objective of this paper is to present the effects, including that of the earth's shadow, which radiation pressure has on the motion of a satellite.

KRYLOFF-BOGOLIUBOFF METHOD

In an article entitled "Low acceleration takeoff from a satellite orbit," Lass and Lorell (1961) have applied the method of Kryloff-Bogoliuboff to low thrust in the following cases: constant radial, constant transverse, and intermittant. The basic reference for the Kryloff-Bogoliuboff method is the book *Introduction To Non-Linear Mechanics* (Kiev, 1937), Chaps. 10–12, by N. M. Kryloff and N. N. Bogoliuboff.

The method may be simply described as follows: Given a nonlinear equation

$$dx/dt=\mu f(x, \sin t),$$

where μ is a small number, one obtains upon integrating

$$\frac{x(t+2\pi)-x(t)}{2\pi}=\frac{\mu}{2\pi}\int_{t}^{t+2\pi} f(x, \sin\tau)d\tau.$$

Since μ is small, x may be considered constant during the integration from $\tau=t$ to $\tau=t+2\pi$. Since $\sin t$ is periodic, the above equation becomes

$$\frac{x(t+2\pi)-x(t)}{2\pi}\approx\frac{\mu}{2\pi}\int_{0}^{2\pi} f(x, \sin\tau)d\tau=\mu F(x).$$

Replacing the left side here by dx/dt, since the slope of the secant line is approximately that of the tangent, gives

$$\frac{dx}{dt}\approx\frac{\mu}{2\pi}\int_{0}^{2\pi} f(x, \sin\tau)d\tau=\mu F(x).$$

This result may be arrived at simply by averaging the original equation over one cycle on the motion w respect to time.

CHANGE IN ENERGY PRODUCED BY RADIATION PRESSURE

Of fundamental importance in the examination atmospheric drag on a satellite is the ability to separ the energy loss (or gain) produced by radiation press from the loss due to drag. The lifetime of the satell will be substantially affected by the changes in ene resulting from radiation pressure.

The effect of radiation pressure, neglecting the eff of the earth's shadow, will produce only short-per terms in the development for the semimajor axis of orbit (Musen 1960). However, the inclusion of shadow results in quite a different phenomenon.

Using the energy integral and Brown's δ/dt opera (see, for example, Musen 1954), we obtain

$$da/dt=2a^2\mathbf{v}\cdot\mathbf{F}/\mu.$$

The velocity vector **v** may be represented in terms o unit vector **P** directed from the center of the earth perigee and a vector **Q** at right angles to **P** such th **P**, **Q**, **R**, with **R** the unit vector in the direction of t angular momentum vector, form a right-handed syste The vector **F** is the disturbing acceleration, a is t semimajor axis, and $\mu=GM$, the gravitational consta multiplied by the mass of the earth. We have

$$\mathbf{v}=\{\mathbf{Q}[\mu a(1-e^2)]^{\frac{1}{2}}\cos E-\mathbf{P}(\mu a)^{\frac{1}{2}}\sin E\}/r,$$
$$\mathbf{F}=-F\mathbf{u}^0,$$

where e is the eccentricity, E the eccentric anoma F the magnitude of disturbing acceleration, $\mathbf{u}^0$ the u vector in direction of the sun, and $r=a(1-e\cos E)$,

$$\mathbf{P}=\begin{Bmatrix}-\cos i\sin\omega\sin\Omega+\cos\omega\cos\Omega\\+\cos i\sin\omega\cos\Omega+\cos\omega\sin\Omega\\+\sin i\sin\omega\end{Bmatrix},$$

$$\mathbf{Q}=\begin{Bmatrix}-\cos i\cos\omega\sin\Omega-\sin\omega\cos\Omega\\+\cos i\cos\omega\cos\Omega-\sin\omega\sin\Omega\\+\sin i\cos\omega\end{Bmatrix},$$

$$\mathbf{R}=\begin{Bmatrix}+\sin i\sin\Omega\\-\sin i\cos\Omega\\+\cos i\end{Bmatrix}.$$

e we obtain for (1)

$$= \frac{-2a^2F}{r(\mu a)^{\frac{1}{2}}}\{\mathbf{Q}\cdot\mathbf{u}^0 a(1-e^2)^{\frac{1}{2}}\cos E - \mathbf{P}\cdot\mathbf{u}^0 a\sin E\}. \quad (2)$$

idering the slowly varying quantities to be constant g one revolution and using

$$d/dE = (r/an)(d/dt),$$

tain

$$-\frac{2a^2F}{n(\mu a)^{\frac{1}{2}}}\left\{\mathbf{Q}\cdot\mathbf{u}^0(1-e^2)^{\frac{1}{2}}\int_{E_1}^{E_2}\cos E dE - \mathbf{P}\cdot\mathbf{u}^0\int_{E_1}^{E_2}\sin E dE\right\}, \quad (3)$$

$$-\frac{2a^3F}{\mu}\left\{\mathbf{Q}\cdot\mathbf{u}^0(1-e^2)^{\frac{1}{2}}\sin E + \mathbf{P}\cdot\mathbf{u}^0\cos E\right\}_{E_1}^{E_2},$$

e E_1 and E_2 are the eccentric anomaly at exit and nce of shadow, respectively, and are obtained from quation

$$\mathbf{r}\cdot\mathbf{u}^0 = -(r^2-\rho^2)^{\frac{1}{2}}, \quad (4)$$

terms of E,

$$(\cos E - e) + \mathbf{Q}\cdot\mathbf{u}^0(1-e^2)^{\frac{1}{2}}\sin E = -[(1-e\cos E)^2 - (\rho/a)^2]^{\frac{1}{2}}, \quad (4')$$

e ρ is the radius of the earth. The solution of this tion is readily obtained by the iterative technique the entrance and exit roots are easily identifiable. e may write the expression for Δa as follows:

$$-(4a^3F/\mu)\sin\tfrac{1}{2}(E_2-E_1) \times[(\mathbf{Q}\cdot\mathbf{u}^0)^2(1-e^2)+(\mathbf{P}\cdot u^0)^2]^{\frac{1}{2}} \times\sin[\tfrac{1}{2}(E_1+E_2)+\phi], \quad (3')$$

arc $\tan[\mathbf{Q}\cdot\mathbf{u}^0(1-e^2)^{\frac{1}{2}}/-\mathbf{P}\cdot\mathbf{u}^0]$.

mination of this expression shows (1) if there is no owing,

$$\sin\tfrac{1}{2}(E_2-E_1)=0,$$

ting in $\Delta a=0$, and (2) if $e=0$, ϕ becomes

$$-\tfrac{1}{2}(E_1+E_2)$$

a consideration of Eq. (4), and again

$$\Delta a = 0.$$

COMPLETE SYSTEM OF EQUATIONS FOR THE OSCULATING ELEMENTS

The equations for the elements may be obtained using (Strömgren 1929)

$$da/dt = 2a^2\mathbf{v}\cdot\mathbf{F}/\mu,$$

$$de/dt = [(a/\mu)(1-e^2)]^{\frac{1}{2}}(T\cos E+N),$$

$$\frac{di}{dt} = \frac{rW}{[\mu a(1-e^2)]^{\frac{1}{2}}}\cos(\omega+f),$$

$$\sin i\frac{d\Omega}{dt} = \frac{rW}{[\mu a(1-e^2)]^{\frac{1}{2}}}\sin(\omega+f),$$

$$\frac{d\omega}{dt}+\cos i\frac{d\Omega}{dt} = \frac{1}{\mu^{\frac{1}{2}}e}\{Ta^{\frac{1}{2}}\sin E - [a(1-e^2)]^{\frac{1}{2}}L\},$$

where $T=\mathbf{F}\cdot\mathbf{R}\times\mathbf{r}^0$, $N=\mathbf{F}\cdot\mathbf{Q}$, $W=\mathbf{F}\cdot\mathbf{R}$, f = true anomaly, $L=\mathbf{F}\cdot\mathbf{P}$, and $\mathbf{r}^0$ = unit vector in direction of $\mathbf{r}$. The complete procedure will be carried out for only one equation. The others are obtained by exactly the same procedure.

$$de/dt = [(a/\mu)(1-e^2)]^{\frac{1}{2}}(T\cos E+N),$$

where

$$T = -F\mathbf{u}^0\cdot\mathbf{R}\times\mathbf{r}^0 = -F\mathbf{u}^0\cdot\mathbf{R}\times\mathbf{r}/r,$$

$$N = -F\mathbf{u}^0\cdot\mathbf{Q} - F\mathbf{Q}\cdot\mathbf{u}^0(a/r)(1-e\cos E).$$

$$= -(Fa/r)[\mathbf{Q}\cdot\mathbf{u}^0(\cos E-e) - \mathbf{P}\cdot\mathbf{u}^0(1-e^2)^{\frac{1}{2}}\sin E],$$

$$\mathbf{r} = \mathbf{P}a(\cos E-e)+\mathbf{Q}a(1-e^2)^{\frac{1}{2}}\sin E.$$

We obtain

$$de/dt = -[(a/\mu)(1-e^2)]^{\frac{1}{2}}F\{\mathbf{Q}\cdot\mathbf{u}^0(a/r) \times(\tfrac{3}{2}-2e\cos E+\tfrac{1}{2}\cos 2E) - \mathbf{P}\cdot\mathbf{u}^0(a/r)(1-e^2)^{\frac{1}{2}}\sin E\cos E\},$$

$$\frac{e(t+\tau)-e(t)}{\tau} = -\frac{F}{\tau}\int_t^{t+\tau}\left[\frac{a}{\mu}(1-e^2)\right]^{\frac{1}{2}} \times\{\mathbf{Q}\cdot\mathbf{u}^0(a/r)(\tfrac{3}{2}-2e\cos E+\tfrac{1}{2}\cos 2E) - \mathbf{P}\cdot\mathbf{u}^0(a/r)(1-e^2)\sin E\cos E\}dt,$$

where τ is the period of the satellite.

Since F is small we may consider slowly varying quantities constant during the integration from t to $t+\tau$. Changing the independent variable for the integration and replacing the secant by the tangent on the left side, we obtain

$$\frac{de}{dt} = -\frac{1}{2\pi}\left[\frac{a}{\mu}(1-e^2)\right]^{\frac{1}{2}} \times F\left\{\mathbf{Q}\cdot\mathbf{u}^0\int_{E_1}^{E_2}(\tfrac{3}{2}-2e\cos E+\tfrac{1}{2}\cos 2E)dE - \mathbf{P}\cdot\mathbf{u}^0(1-e^2)^{\frac{1}{2}}\int_{E_1}^{E_2}\sin E\cos E dE\right\}.$$

The limits are E_1 to E_2 since F is zero outside this range. Hence, the resulting equation is

$$\frac{de}{dt}=-\frac{1}{2\pi}\left[\frac{a}{\mu}(1-e^2)\right]^{\frac{1}{2}}$$

$$\times F\left\{\mathbf{Q}\cdot\mathbf{u}^0\left(\frac{3}{2}E-2e\sin E+\frac{1}{4}E+\frac{1}{4}\sin E\right)\right.$$

$$\left.+\frac{\mathbf{P}\cdot\mathbf{u}^0(1-e^2)^{\frac{1}{2}}}{4}\cos 2E\right\}_{E_1}^{E_2}.$$

The complete set of equations is

$$\frac{da}{dt}=-\frac{a^2F}{\pi(\mu a)^{\frac{1}{2}}}\left\{\mathbf{Q}\cdot\mathbf{u}^0(1-e^2)^{\frac{1}{2}}\sin E+\mathbf{P}\cdot\mathbf{u}^0\cos E\right\}_{E_1}^{E_2},$$

$$\frac{de}{dt}=-\frac{[a(1-e^2)]^{\frac{1}{2}}}{2\pi\mu^{\frac{1}{2}}}F\left\{\mathbf{Q}\cdot\mathbf{u}^0\left(\frac{3E}{2}-2e\sin E+\frac{1}{4}\sin 2E\right)\right.$$

$$\left.+\frac{\mathbf{P}\cdot\mathbf{u}^0(1-e^2)^{\frac{1}{2}}}{4}\cos 2E\right\}_{E_1}^{E_2},$$

$$\frac{di}{dt}=-\frac{aF\mathbf{R}\cdot\mathbf{u}^0}{2\pi[\mu a(1-e^2)]^{\frac{1}{2}}}\left\{\left[-\frac{3e}{2}E+(1+e^2)\sin E\right.\right.$$

$$\left.\left.-\frac{e}{4}\sin 2E\right]\cos\omega+(1-e^2)^{\frac{1}{2}}\left[\cos E-\frac{e}{4}\cos 2E\right]\sin\omega\right\}_{E_1}^{E_2},$$

$$\sin i\frac{d\Omega}{dt}=-\frac{aF\mathbf{R}\cdot\mathbf{u}^0}{2\pi[\mu a(1-e^2)]^{\frac{1}{2}}}\left\{\left[-\frac{3e}{2}E+(1+e^2)\sin E\right.\right.$$

$$\left.-\frac{e}{4}\sin 2E\right]\sin\omega$$

$$-[1-e^2]^{\frac{1}{2}}\left[\cos E-\frac{e}{4}\cos 2E\right]\mathrm{cos}$$

$$\frac{d\omega}{dt}+\cos i\frac{d\Omega}{dt}=-\frac{a^{\frac{1}{2}}F}{2\pi\mu^{\frac{1}{2}}e}\left\{\mathbf{Q}\cdot\mathbf{u}^0\left(e\cos E-\frac{1}{4}\cos 2E\right)\right.$$

$$-\mathbf{P}\cdot\mathbf{u}^0(1-e^2)^{\frac{1}{2}}\left(\frac{3E}{2}-e\sin E-\frac{1}{4}\sin 2E\right)$$

The integration of this system of equations must be carried out using a large-scale computer.

ACKNOWLEDGMENT

The author wishes to express his gratitude to Ann Bailie for her work in verifying the developm

REFERENCES

Lass, H. and Lorell, J. 1961, *ARS J.* **31**, 24.
Musen, P. 1954, *Astron. J.* **59**, 262.
——. 1960, *J. Geophys. Research* **65**, 1391.
Musen, P., Bryant, R., and Bailie, A. 1960, *Science* **131**, 34
Parkinson, R. W., Jones, M., and Shapiro, I. I. 1960, *ibid* 3404.
Strömgren, B. 1929, *Publ. Med. Kobenhavns Obs.* 1929, No.